Silicon Microdosimetry

Anatoly Rosenfeld
Centre for Medical Radiation Physics
University of Wollongong

Lecture Outline

1.Introduction to Solid State microdosimetry

2.Electronic , calibration and sensitivity of Si microdosimeter

2.1. Comparison of TEPC to Si-microdosimeter

3.Concept and design of Silicon on Insulator (SOI) microdosimeters

3.1. Three generation of SOI microdosimeters

3.2.Charge collection in Sensitive Volumes (SV) of SOI microdosimeters

4.Application of SOI microdosimeters

4.1.Radiation protection (Cf-252 and Pu-Be Sources)

4.2.Hadron Therapy

4.2.1.Fast Neutron Therapy (FNT)

4.2.2.Proton Therapy (PT)

4.2.3.Heavy Ion Therapy.(HIT)

4.2.4. LEM vs MKM –SOI microdosimetry experience

5.3D detector technology-future of Si microdosimetry.

5.1.Pecularities of charge collection in 3D Si detectors

5.2.Concept and design of 3D Si microdosimeter.

5.3.GEANT 4 modeling of 3D microdosimeter (avionics environment, isotopic neutron sources)

6.Other Si microdosimetric structures (DRAM , FGMOSFET etc)

7.Conclusion and tips for thinking on new Si microdosimeters design

Microdosimetry and Dose Equivalent

- **Microdosimetry**
  - Assumes the weighting factor is related to the energy deposited in the cell nucleus: ε
  - Measure this for each particle that crosses detector
  - Formulate dose distribution: $d(\varepsilon)$
  - Integrate with weighting factor to give **Dose Equivalent** : $H = \int Q(\varepsilon)d(\varepsilon)\, d\varepsilon$
  - Dose Equivalent can be used to predict biological effect of radiation

- **We require detectors with dimensions commensurate with cell nuclei**

Ionising particle tracks

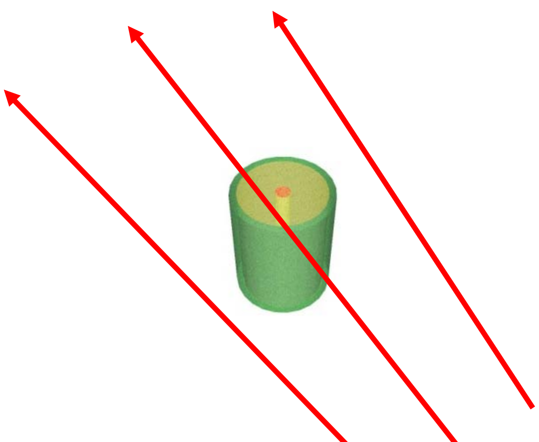

Small Detector (um)

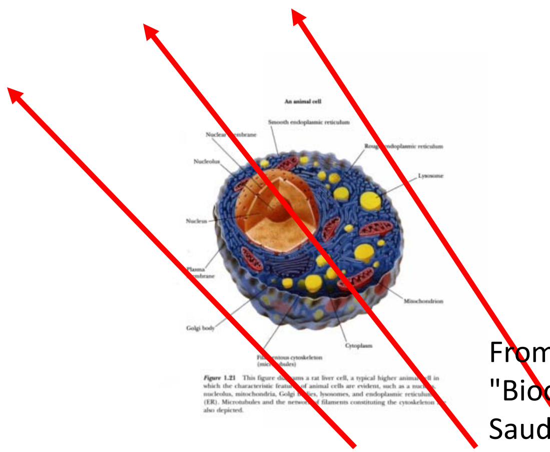

Biological Cell (um)

From Garret and Grisham, "Biochemistry" Copyright 1995 by Sauders College Publishing

Microdosimetry and Fluence approach for stochastic events

Microdosimetry

Measure distribution of ionisation events in microscopic volume

Derive quality factor and equivalent dose estimate

$$H = \int Q(y) d(y) dy$$

Fluence based approach

Measure types and energy distribution of all particles

Integrate product of risk cross section a fluence over energy.

Sum over all particles to directly obtain risk estimate

$$R = \sum_i \int {}_r \sigma_i(E) \phi_i(E) dE$$

Q(y), Q(L) and $\sigma(\mathrm{E})$ were modified recently , ICRU 92 and NCRP 137

Quality coefficient for low doses neutrons is still uncertain

All above characteristics are relevant to Radiation Protection only

Microdosimetry

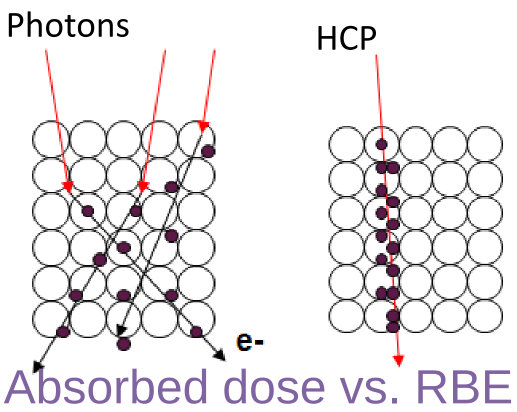

Study of dose deposition in microscopic volumes e.g. Human cells

- Stochastic deposition of energy not correlated with absorbed dose
- Important for radiation protection in radiotherapy and space radiation environments

Microdosimeter measures energy deposition events in small (cell-sized) volumes

- Lineal energy, y = E/ <l> where <l> is mean chord length
- Most common representation in yd(y) vs. y. yd(y) indicates the dose delivered in the range y to y+dy
- Average Quality factor, Q can be calculated from y

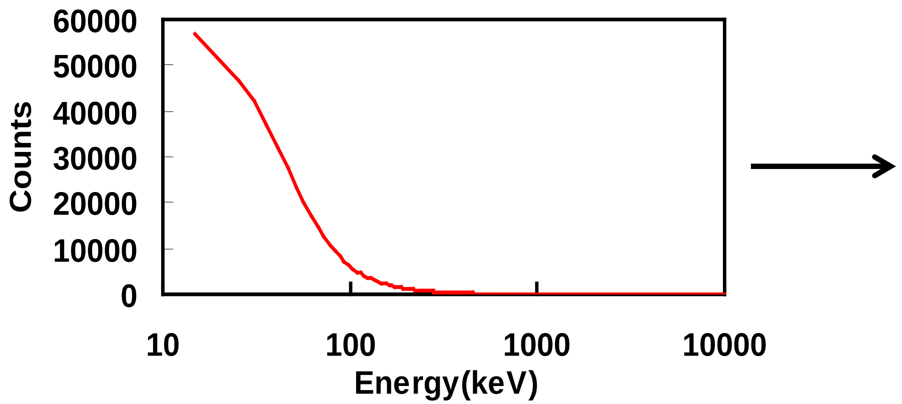

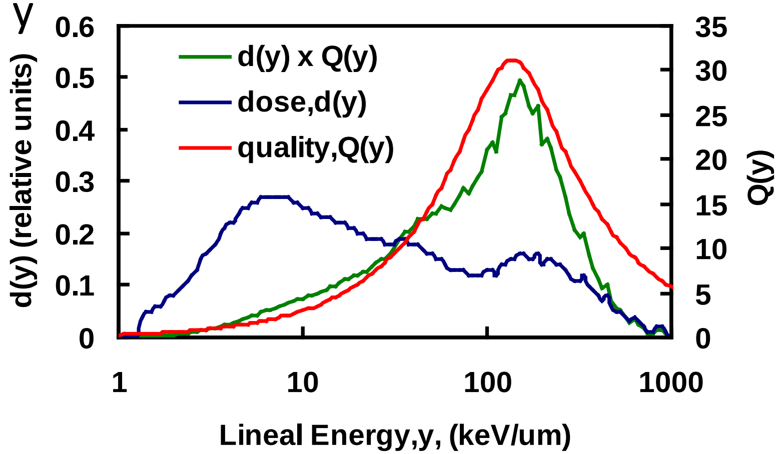

CENTRE FOR MEDICAL RADIATION PHYSICS
UNIVERSITY OF WOLLONGONG

New Approach: Silicon Microdosimetry

Radiation Effect on a Biological Cell

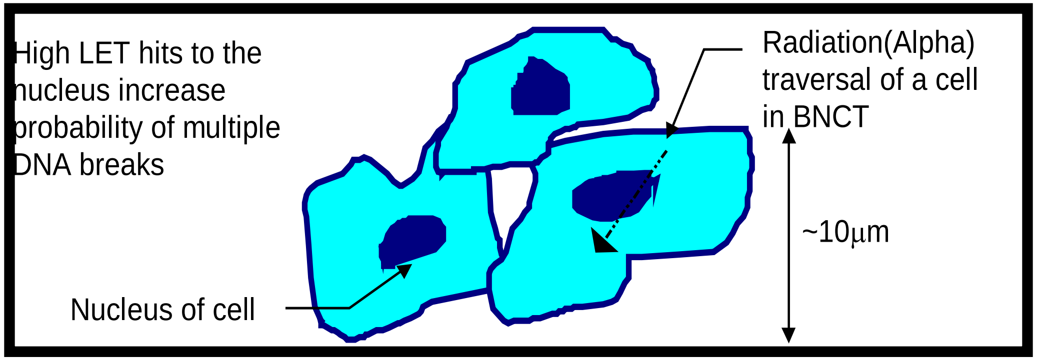

Radiation Effect on a Silicon Cell

(Cross-Section of a Single Diode, 4800 diodes connected in parallel)

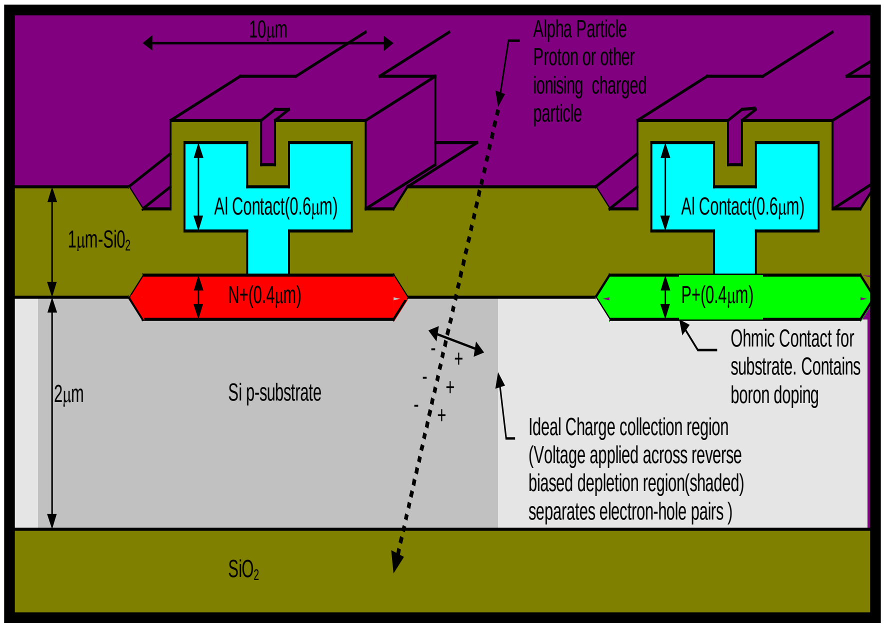

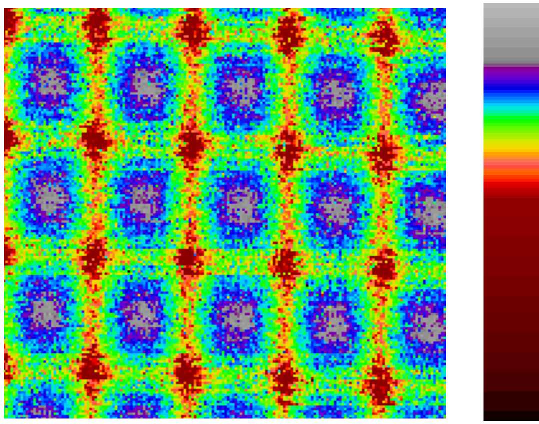

2 MeV alpha particle Microbeam
10x10x2 μm cells

CENTRE FOR MEDICAL RADIATION PHYSICS
UNIVERSITY OF WOLLONGONG

Silicon Microdosimetry at CMRP

1st Generation

- Fabricated on bonded silicon-on-insulator (SOI) wafer
- As and B ions diffused to create p-i-n junctions
- Elongated Rectangular Parallelepiped Structure
- Array of 4800 cells
- Disadvantage: cross-talk between neighboring cells

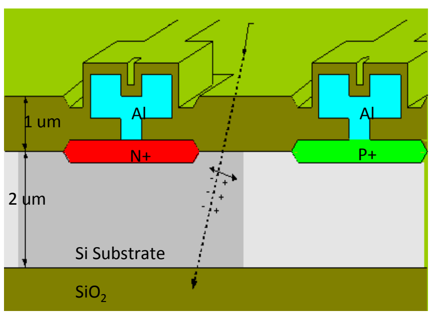

2nd Generation: MESA

- Fabricated on p-type SOI wafer
- Phosphorus and boron diffused to produce p-i-n diodes
- Array of 900 cylindrical cells
- Array of 3D raised mesa structures to reduce lateral diffusion and cross talk
- Cylindrical sensitive volume is a better approximation of spherical site
- Disadvantage: low yield due to difficulty evaporating Al track on raised mesa structure

2nd Generation: PLANAR

- Fabricated on p-type SOI wafer
- Phosphorus and boron diffused to produce p-i-n diodes
- Planar topology incorporating guard ring structure
- Array of 3600 cells

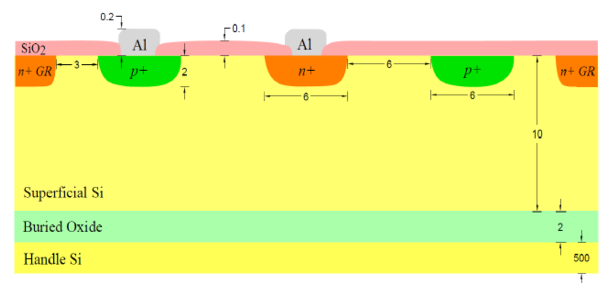

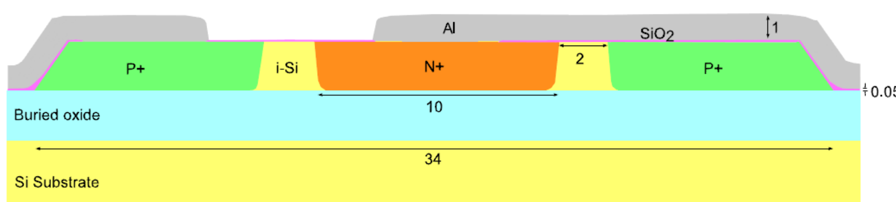

Comparison of proportional counter to silicon microdosimete

Category	Parameter	Proportional Counter	Silicon microdosimeter
Detector performance	Energy Resolution (Note ii)	Moderate	Moderate,
	Low energy sensitivity (Note iii)	Excellent, Single Ionizations, Minimum y = 0.05 keV/μm	Moderate, Minimum y = 0.4 keV/μm
	Sensitive volume definition	Good	Moderate
	Tissue Equivalence	Good	Moderate
	Radiation Hardness	Excellent	Moderate
	Spatial Resolution	Poor, 2.5 cm. 0.5 mm best case [20]	Excellent, 1 μm.
	Wall effect Immunity	Poor	Excellent
	Model cell array	No	Yes
	Shape design flexibility	Moderate	Moderate
Ease of Use	Calibration	Simple	Simple
	Cost	High	Low
	Portability	Moderate	Excellent
	System Complexity	Poor: Requires HV supply and gas supply.	Good: only requires low voltage supply.
	In-vivo use	No	Yes
	Integration	Poor	Excellent

The shaded areas identify the best performance of the two devices for each parameter. SOI microdosimeter is potentially better than TEPC energy resolution (lower *W*=3.62 eVc.f. 30 eV, better Fano factor and no gas multiplication but needs low preamplifier noise. 1 1 μm^3 cubic silicon microdosimeter with ultra low preamplifier noise ~15 erms can better perform that 2.5cm TEPCsimulated diameter d = 1μm

P.Bradley, A.Rosenfeld, M.Zaider, NIM,

Table 3.

Comparison of minimum detectable energy and resolution between TEPC and silicon microdosimeter

Parameter	Symbol	TEPC	Silicon Microdosimeter
Minimum Detectable Energy	E_{min}	$E_m \approx 5\frac{e_{rms}W}{g}$	$E_m \approx 5e_{rms}W$
Theoretical Resolution	R_{th} (%)	$2.35\sqrt{\frac{W}{T}[F+m]}100$	$2.35\sqrt{\frac{W}{T}F}100$
Instrumentation Resolution	R_{inst} (%)	$2.35\sqrt{\left(\frac{W}{T}\frac{e_{rms}}{g}\right)^2 + R_{rest}^2}100$	$2.35\frac{W}{T}e_{rms}100$
Total Resolution	R_T (%)	$2.35\sqrt{\frac{W}{T}[F+m]+\left(\frac{W}{T}\frac{e_{rms}}{g}\right)^2 + R_{rest}^2}100$	$2.35\sqrt{\frac{W}{T}F+\left(\frac{W}{T}e_{rms}\right)^2}100$

Note: W = mean energy per ion pair = 30 eV (TEPC), 3.62 eV (Si)
g = gas gain
e_{rms} = system electronic noise (rms electrons) referred to the preamplifier input
F = Fano factor ~ 0.3 (TEPC), ~ 0.1 (Si)
T = energy absorbed
R_{rest} = non-preamplifier instrument resolution

CENTRE FOR MEDICAL RADIATION PHYSICS
UNIVERSITY OF WOLLONGONG

Design of 2nd Generation Microdosimeter

SV Design

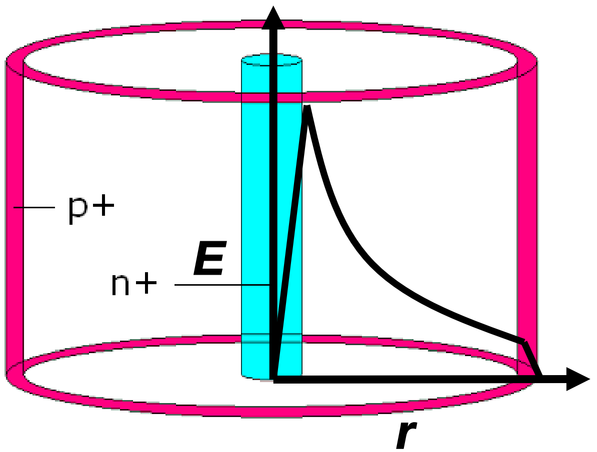

Design Features

- Isolated SV with well defined CC boundary
  - 100% CCE
  - Gaussian peak for monoenergetic ions
- 3D Cylindrical SV
  - better approx. ideal sphere
  - ~~~~uniform response to isotropic field
- Radial E- Field
  - amplification = increased dynamic range
- Alternating odd / even array design
  - track structure measurement

CENTRE FOR MEDICAL RADIATION PHYSICS
UNIVERSITY OF WOLLONGONG

Fabrication Steps

1. SOI Wafer

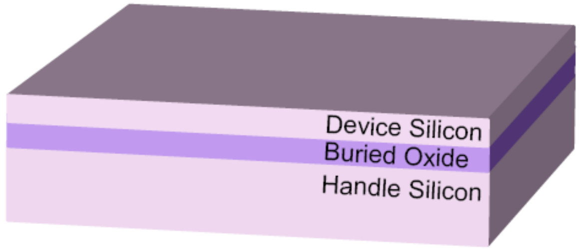

2. Phosphorus Diffusion

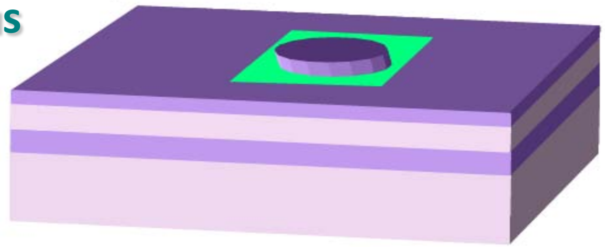

3. Boron Diffusion

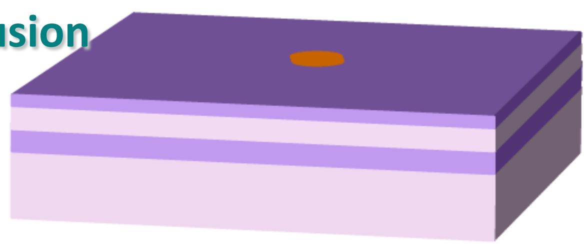

4. TMAH Etching

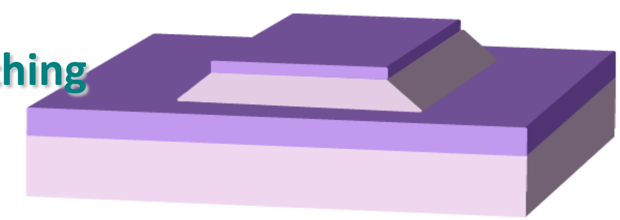

5. Metallisation

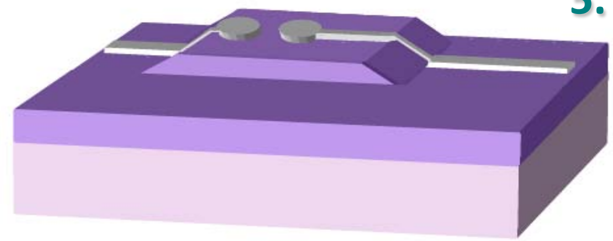

6. Bond Pads Metallisation

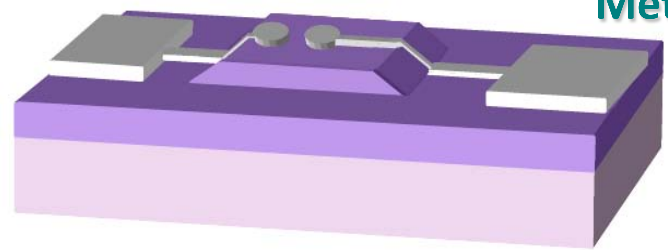

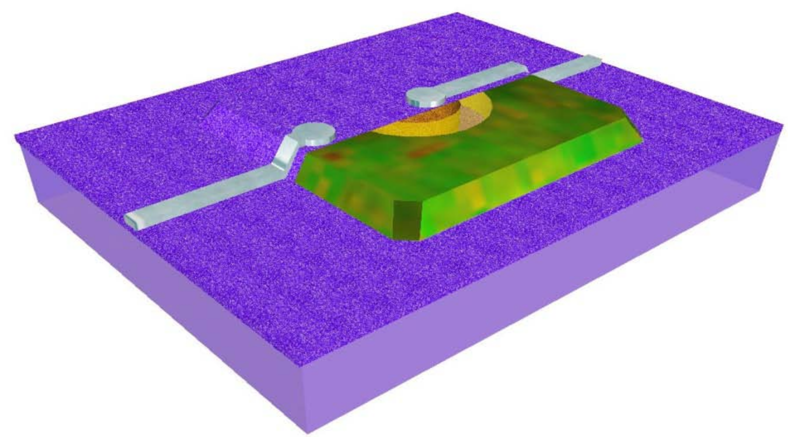

Final Device Structure

W.H. Lim et al. IEEE Trans on Nucl. Sci., NS-56, issue 2, 424-428, 2009

CENTRE FOR MEDICAL RADIATION PHYSICS
UNIVERSITY OF WOLLONGONG

Experimental Results

TMAH Etching

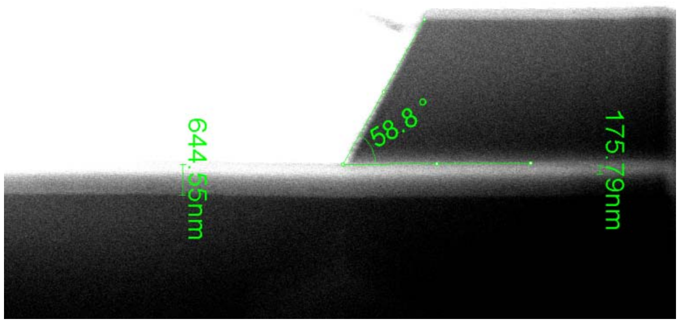

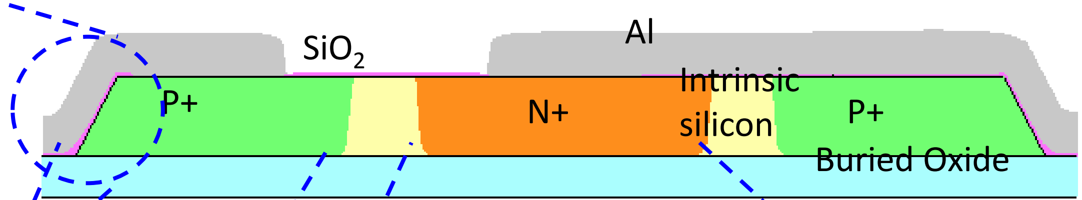

Boron Diffusion

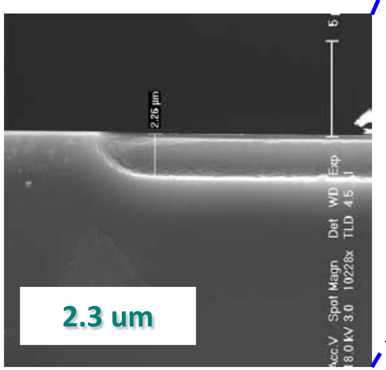

Diffusion Time: 75 mins

Phosphorus Diffusion

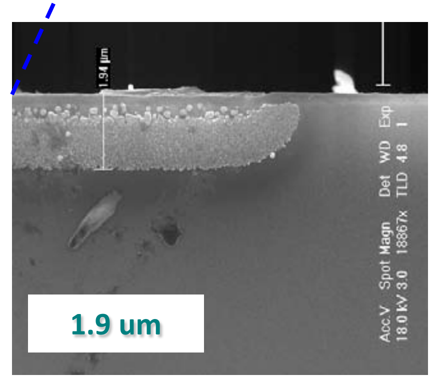

Diffusion Time: 60 mins

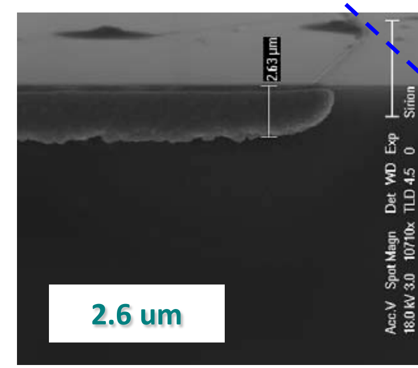

Diffusion Time: 90 mins

Detector or … ?

Has fabrication the fabrication process produced a microdosimeter?

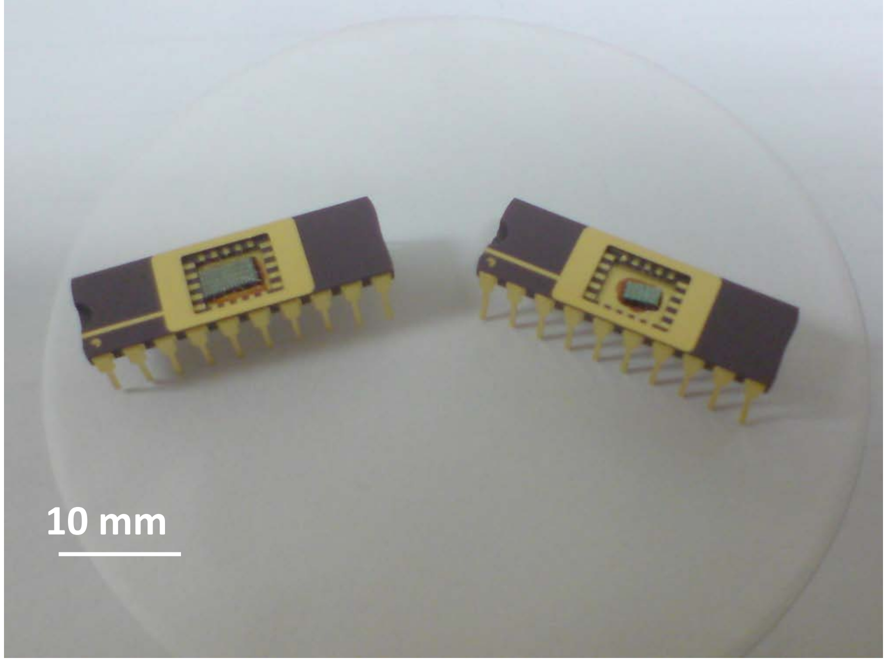

IBICC has the answers….

Single Detector Designs

2 micron thick SOI devices

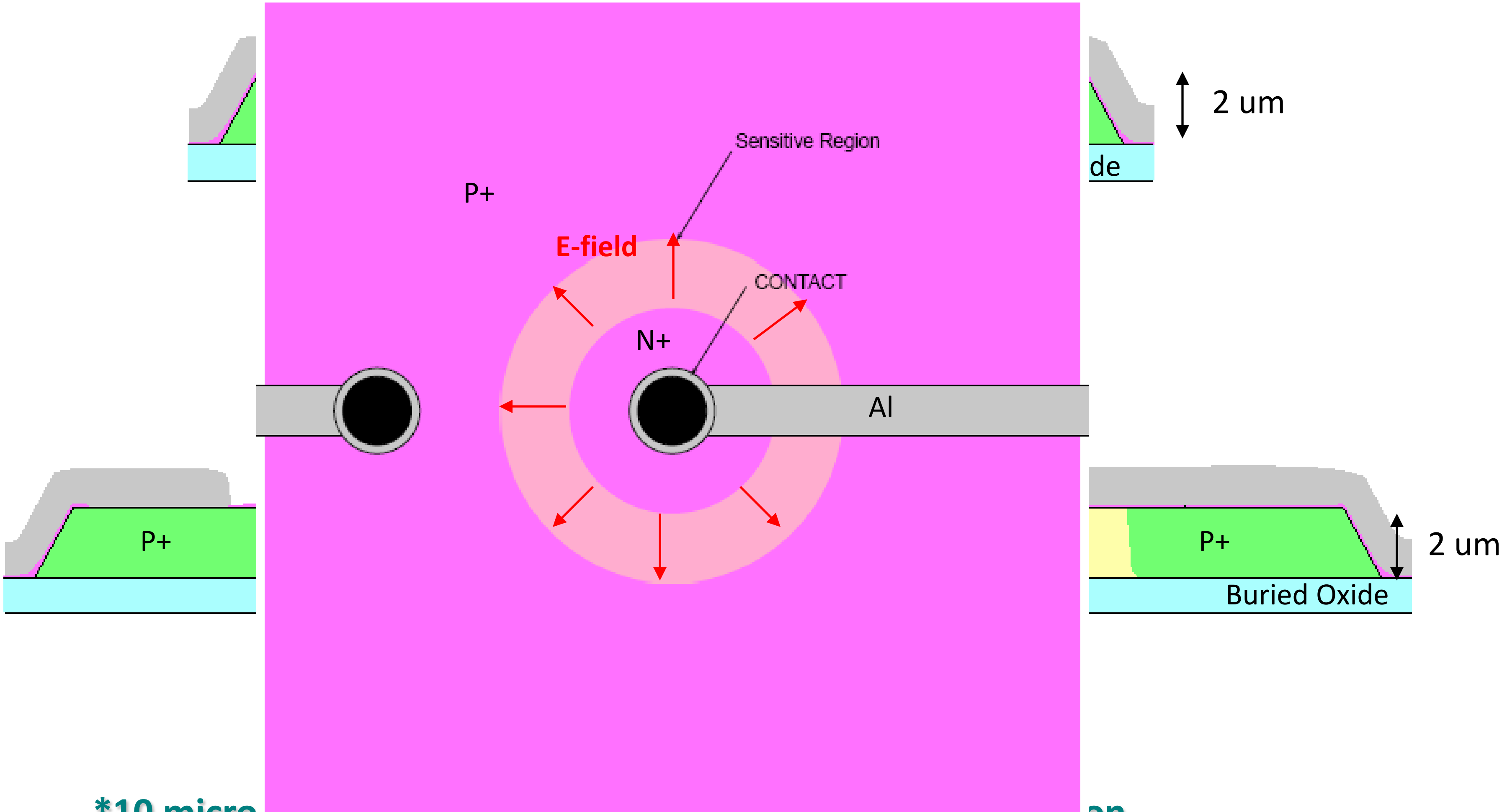

*10 micro

on

SOI planar silicon microdosimeter:generation 3/2

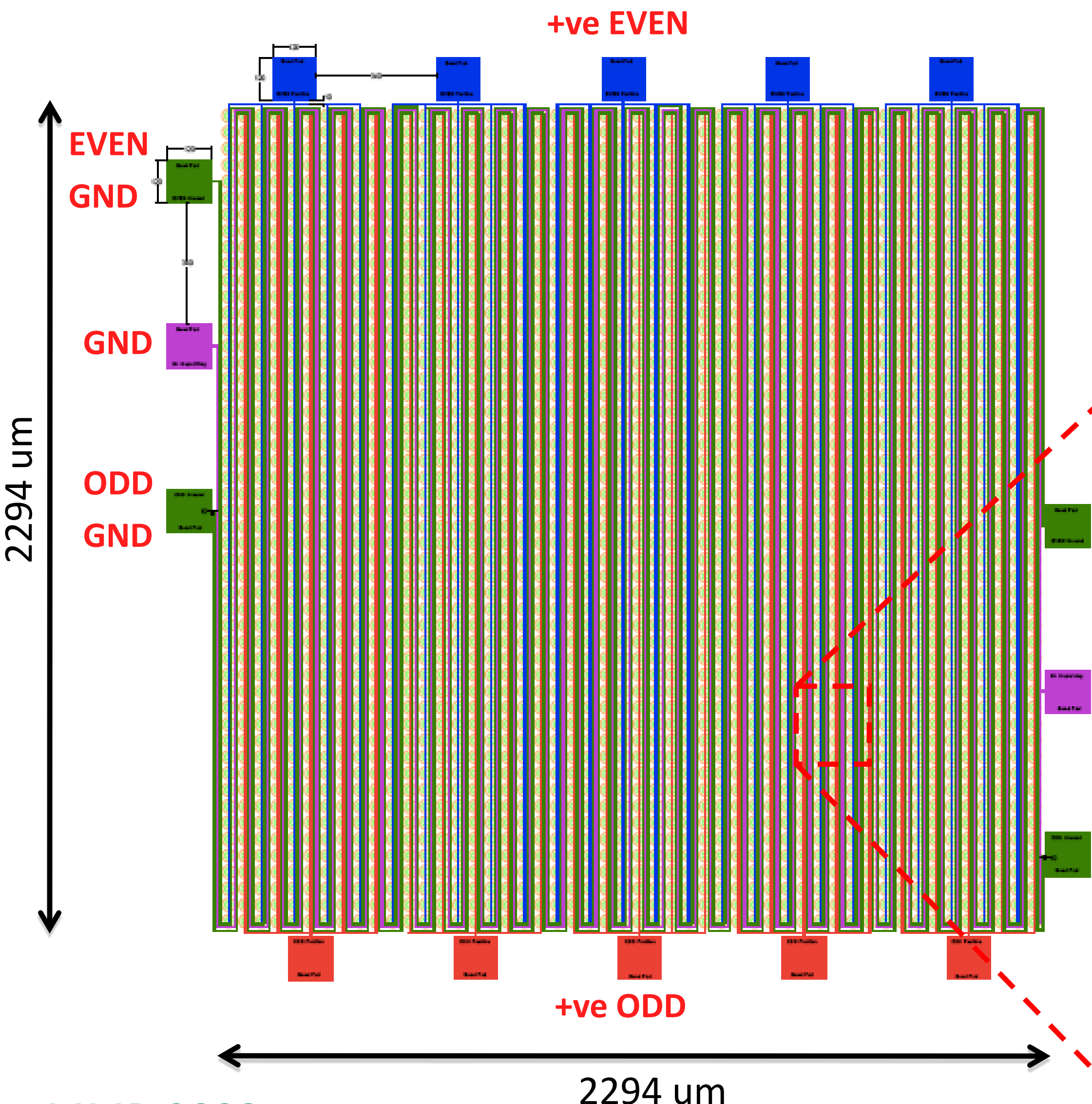

- Increase from 900 to 2500 detectors
- Improve signal to noise ratio
- Maintain observation of Delta Ray effects

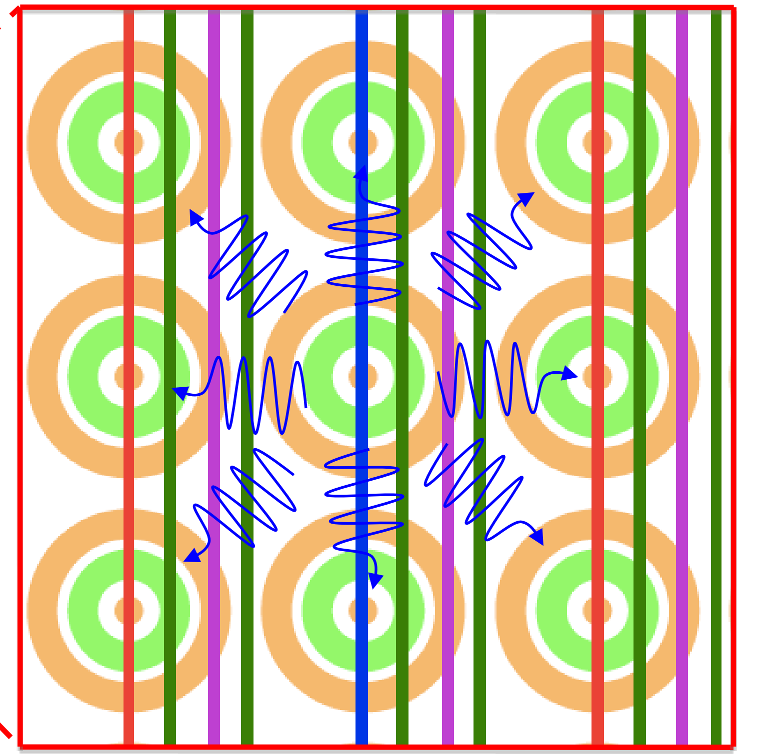

- MMD 2008 -

Defined Annulus N+ Guard Ring:generation 3/2

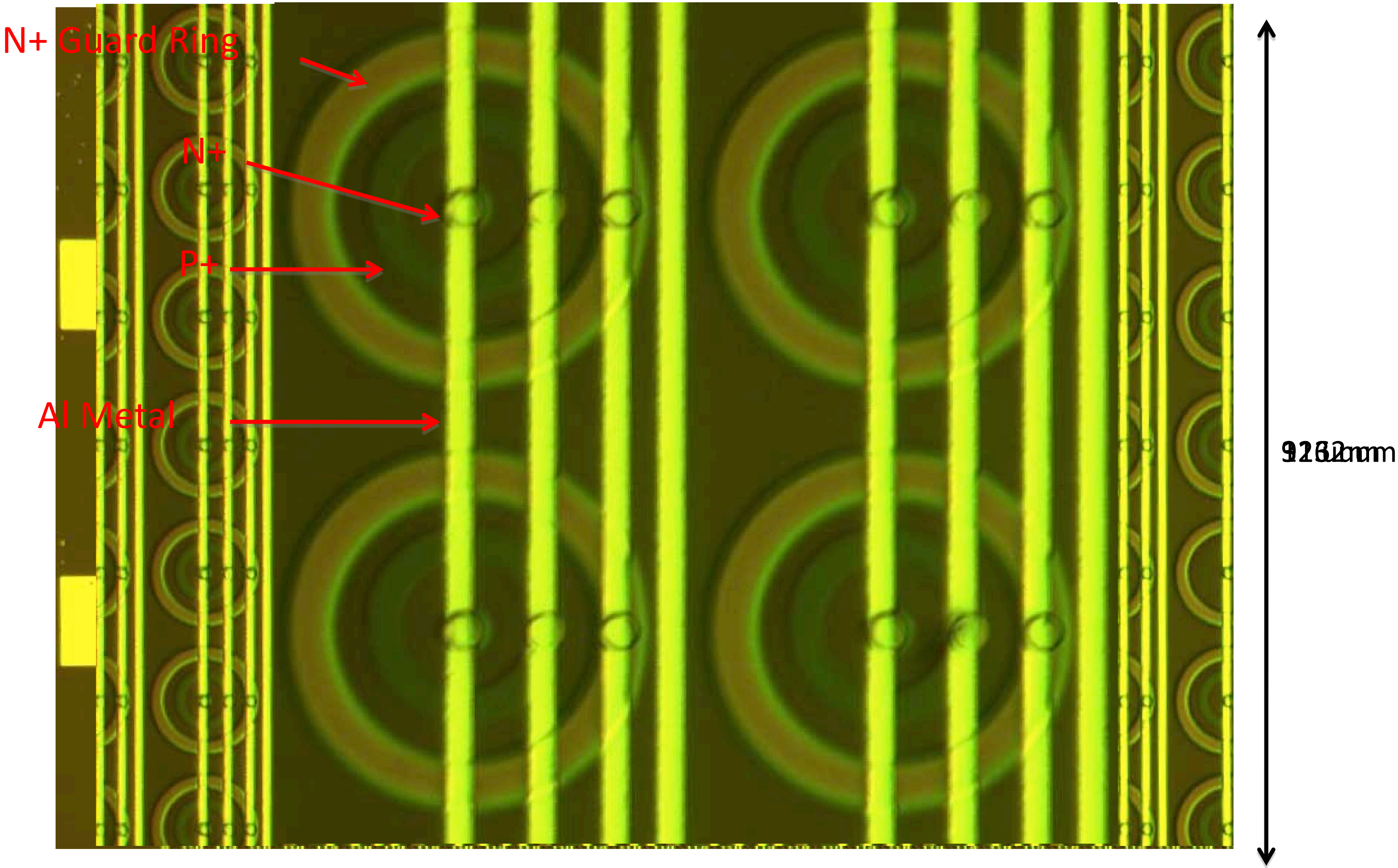

IBICC and the ANSTO Heavy Ion Microprobe

- 3 MeV He^{2+} ion beam
- Beam spot size ≈ 1 μm
- Beam raster scanned across device
- Deposited energy, *ΔE*, measured in coincidence with beam position, *x* and *y*
- Resolution makes microprobe ideal for studying microdosimeter features

Tested 2nd Generation Microdosimeters

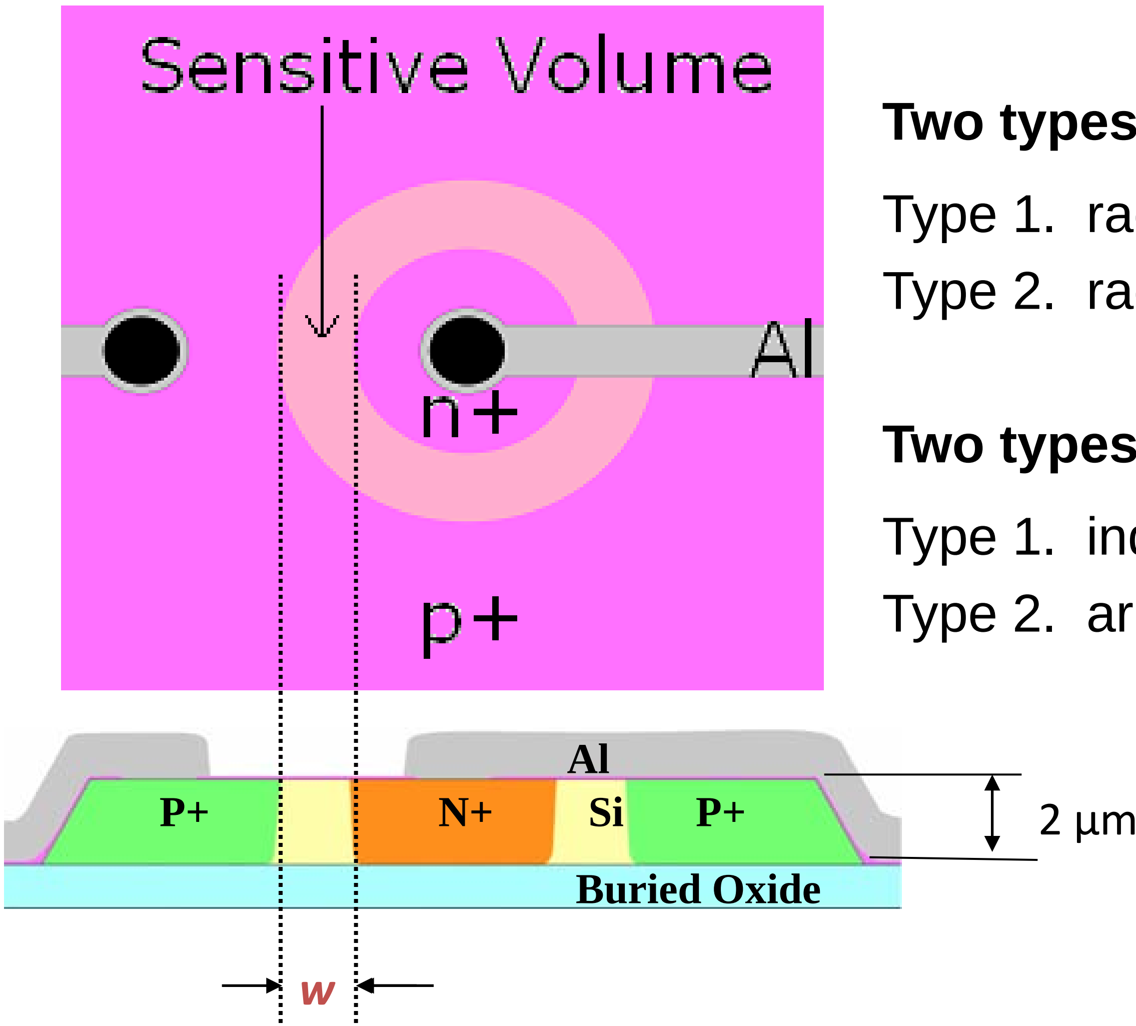

Two types of SV produced

Type 1. radial width (*w*) = 2 μm

Type 2. radial width (*w*) = 10 μm

Two types SV readout

Type 1. individual SV (*w* = 2 or 10 μm)

Type 2. array of SVs in // (*w* = 2 μm)

IBICC for 2 μm device (single cell)

- 3 MeV He^+ ions; $\frac{dE_{(Si)}}{dx} = 196.2\ \mathrm{keV{\cdot}\mu m^{-1}}$
- Scan of 2 μm device; single cell readout

Spectrum of energy deposition events

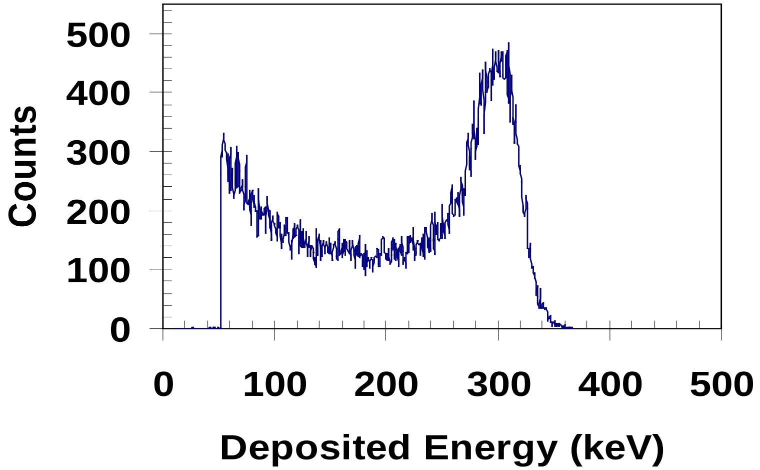

- Device 1.6 um thick

Median energy map

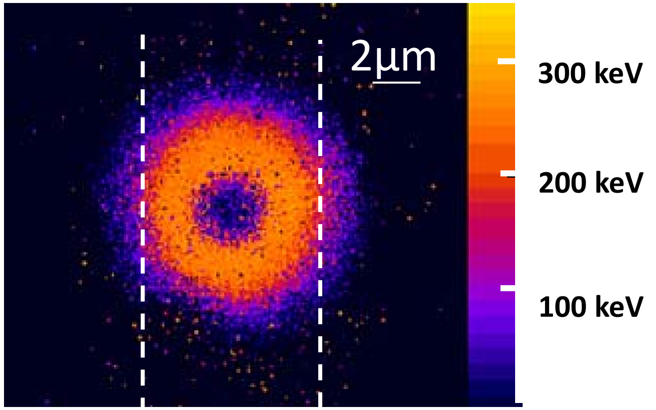

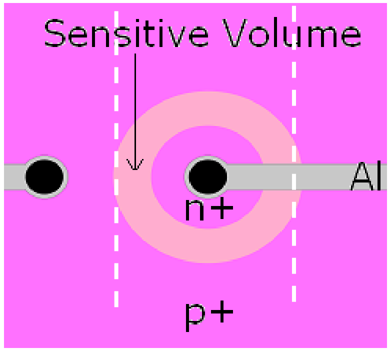

- Isolated SV as per design

A.L.Ziebell et al. *IEEE Trans on Nucl Sci.*, NS- 55, 3414 – 3420, Dec 2008

Response to 5.5 MeV Alphas

LET Response

- 3 MeV He: $\frac{dE_{(Si)}}{dx} = 196\ \text{keV}\ \mu\text{m}^{-1}$
- 5.5 MeV He: $\frac{dE_{(Si)}}{dx} = 135\ \text{keV}\ \mu\text{m}^{-1}$

Deposited Energy in 1.6 µm

$1.6\ \mu\text{m} \times (196 - 135)\ \text{keV}\ \mu\text{m}^{-1} = 96\ \text{keV}$!

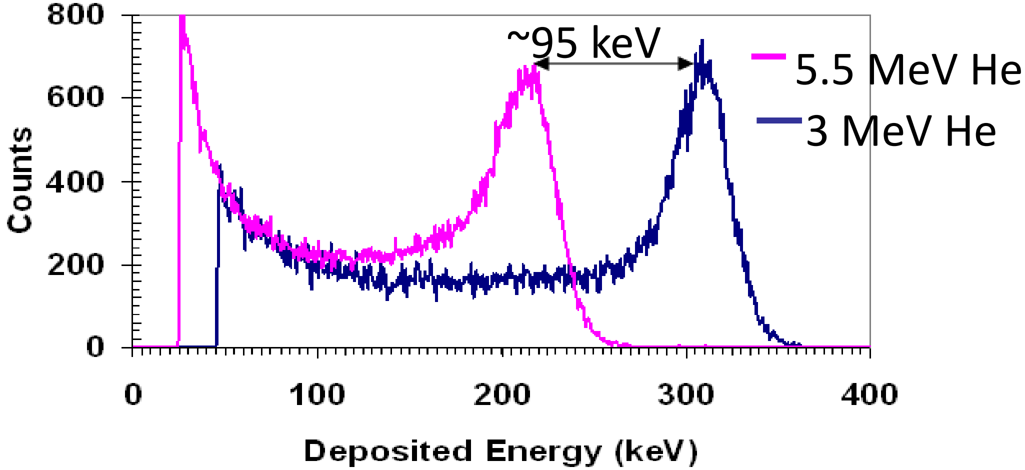

3 MeV He Deposited Energy vs…

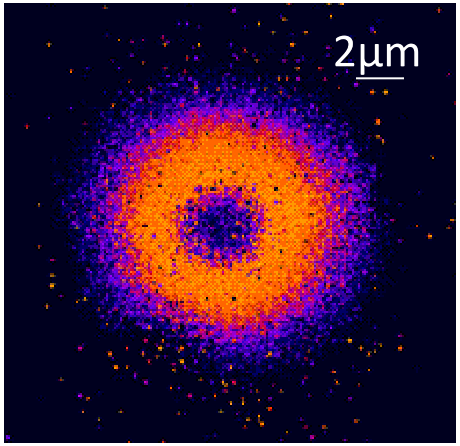

5.5 MeV He MeV Deposited Energy

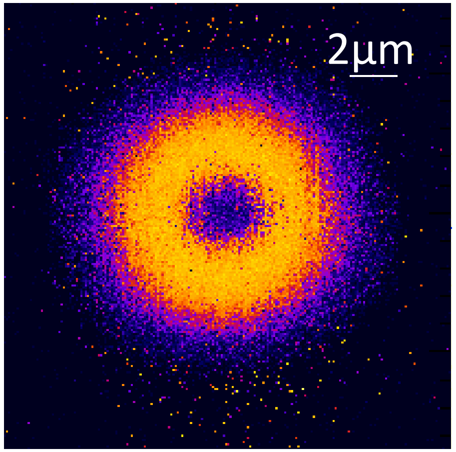

IBICC for 10 µm device (single cell)

- Scan of 10 µm device; single cell readout

Spectrum of energy deposition events

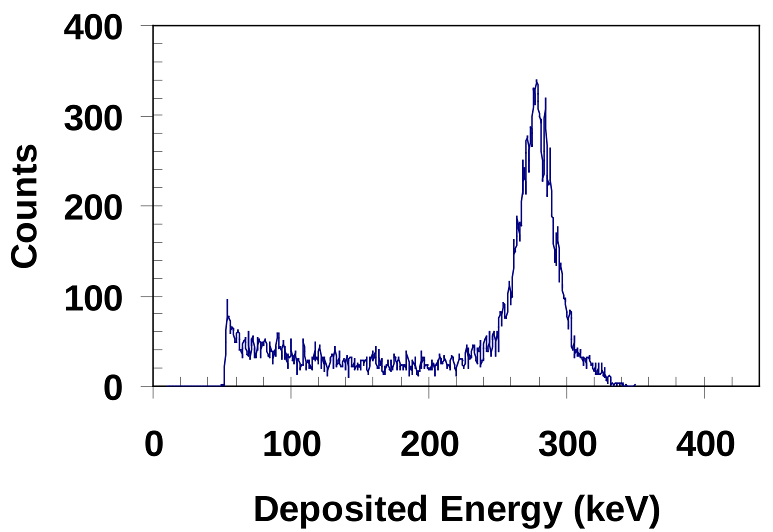

Event frequency map

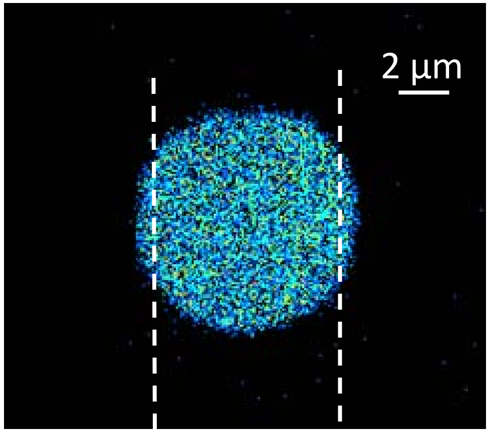

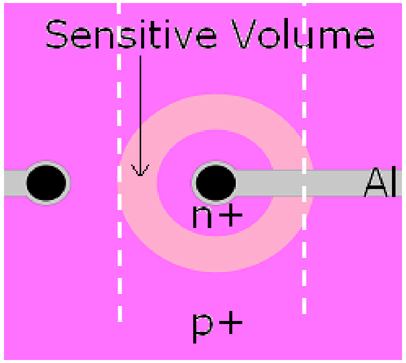

- All events occur within the defined SV
- Spurious events observed outside SV result of beam scatter

IBICC for 10 μm device (single cell)

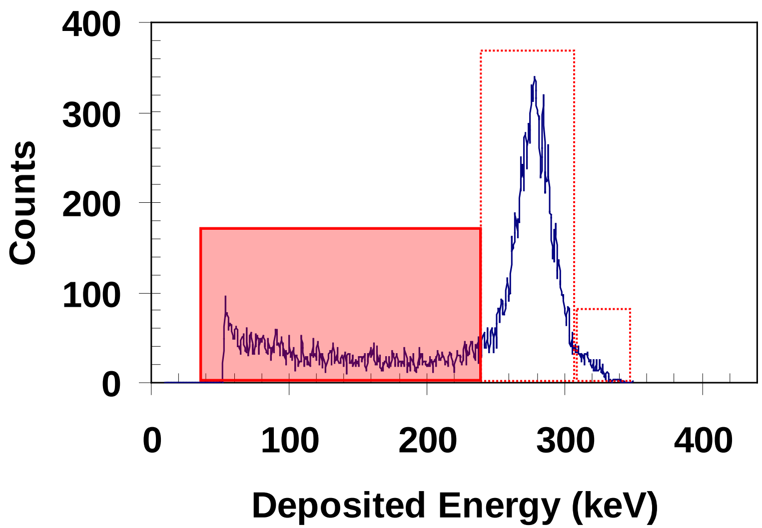

Event frequency distribution (x.y) for selected energy regions of interest

Low energy deposition events

- Attributed to charge recombination within p^+ and n^+ regions

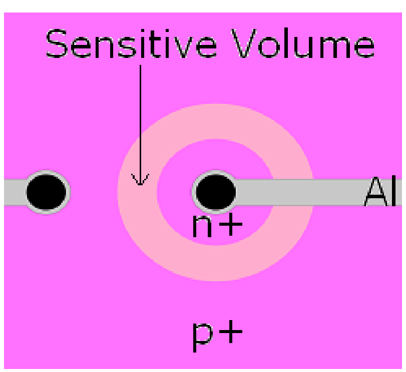

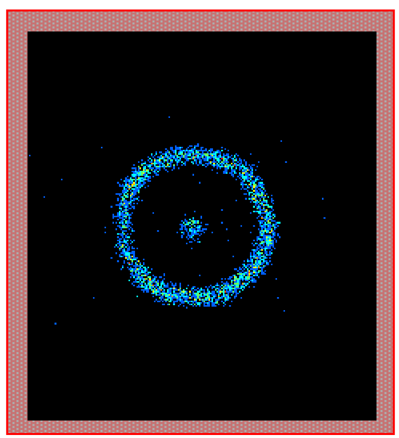

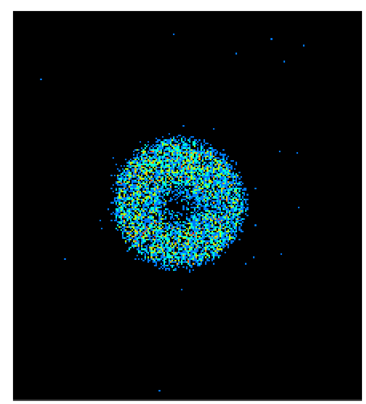

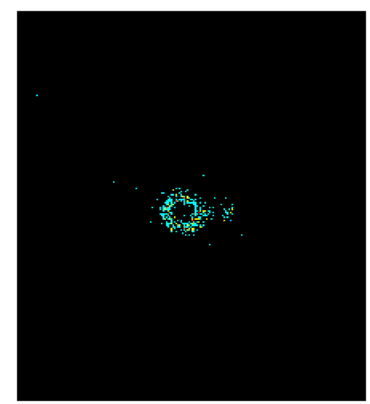

IBICC for 10 μm device (single cell)

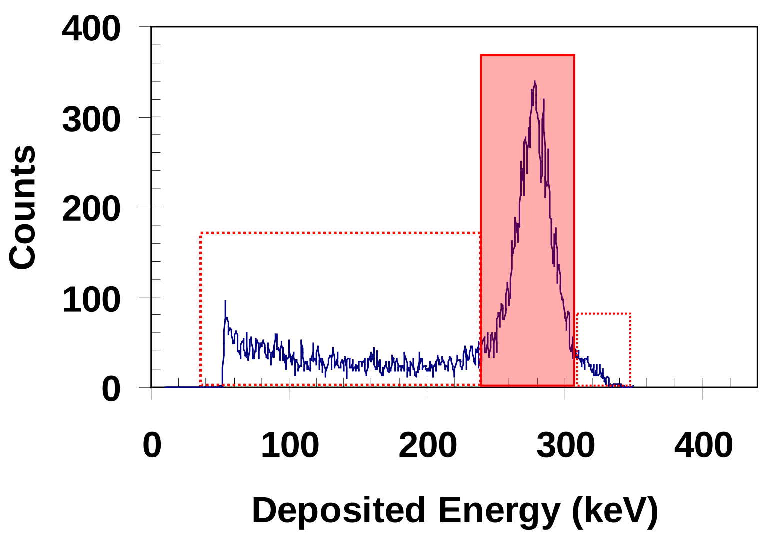

Event frequency distribution (x.y) for selected energy regions of interest

Peak energy deposition events

- Full energy collection associated with drift of charge under applied E-field.

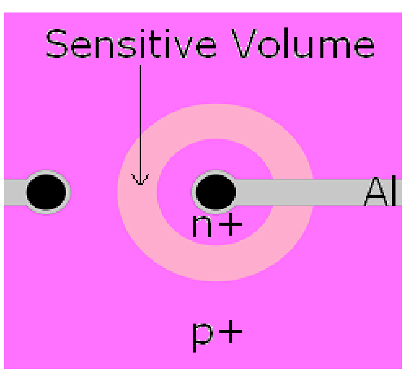

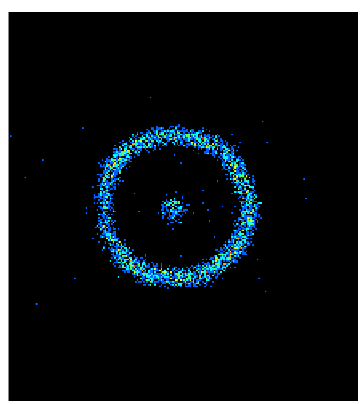

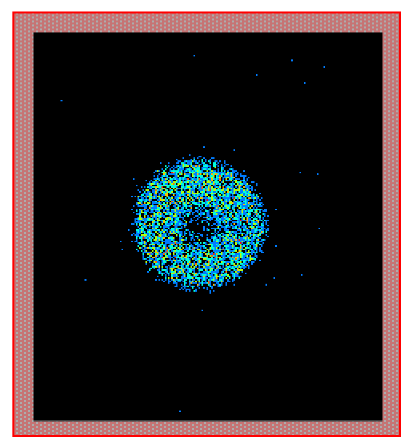

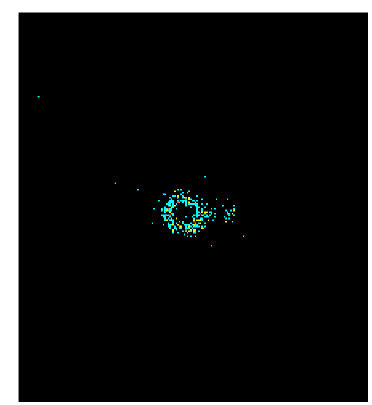

IBICC for 10 μm device (single cell)

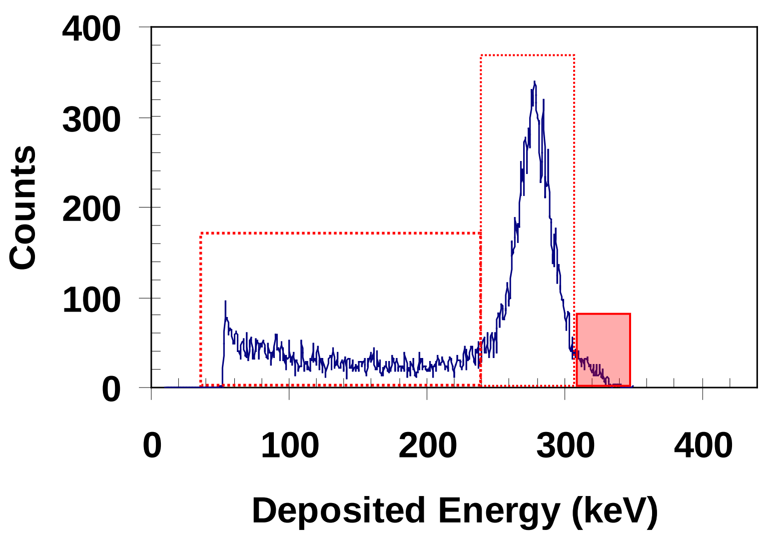

Event frequency distribution (x.y) for selected energy regions of interest

High energy deposition events

- Enhanced CC correlates with Al contact
- Attenuation by overlaying Al contact increases $\frac{dE_{(Si)}}{dx}$?
- Thicker Si under Al contact?

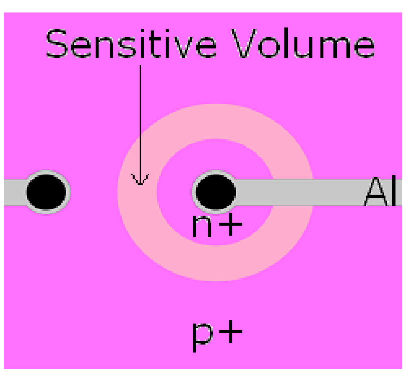

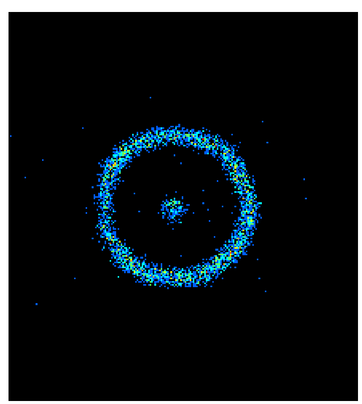

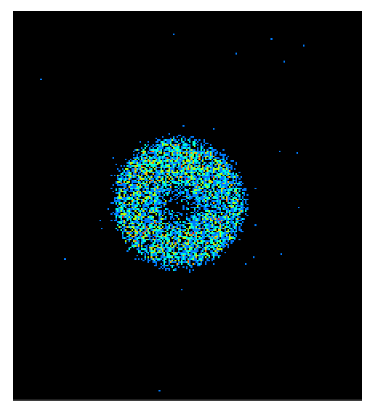

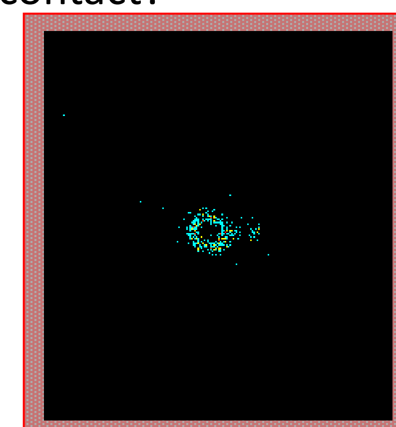

3D SOI silicon microdosimetry: generation 2/1

3D silicon mesa p-n junction array with internal charge amplification produced at UNSW SNF

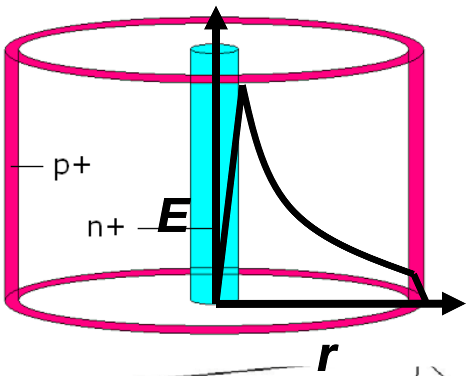

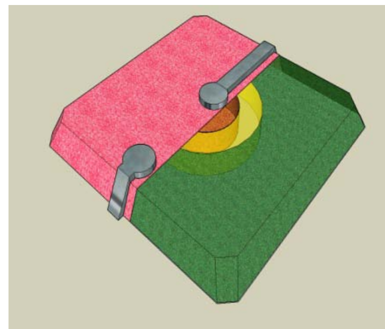

Single mesa 3D SV

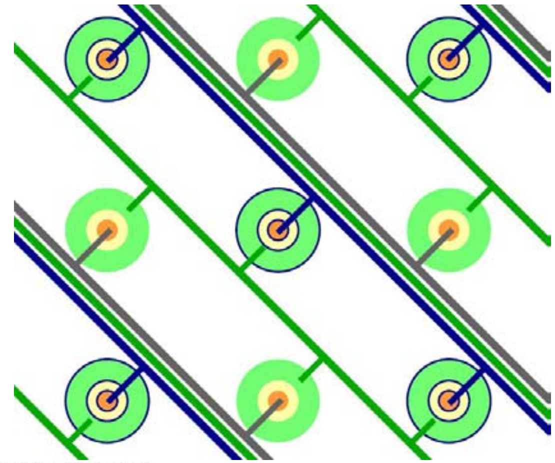

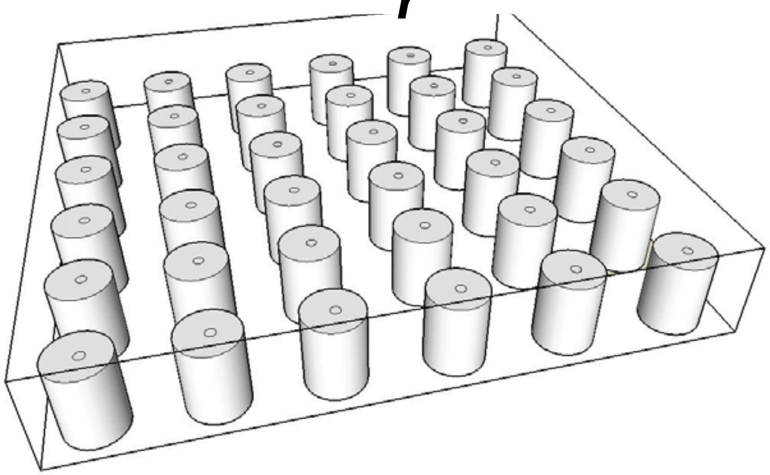

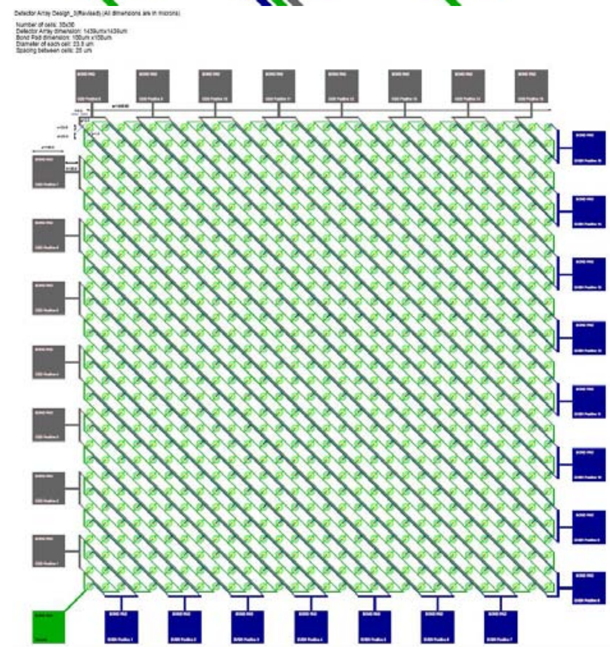

CENTRE FOR MEDICAL RADIATION PHYSICS

UNIVERSITY OF WOLLONGONG

Array Device Signal Readout

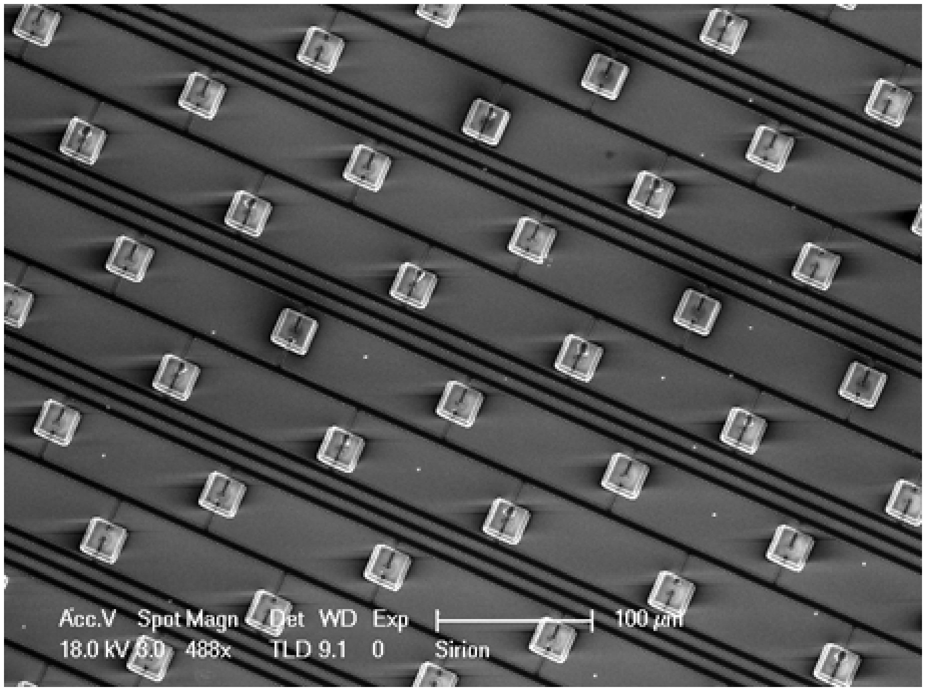

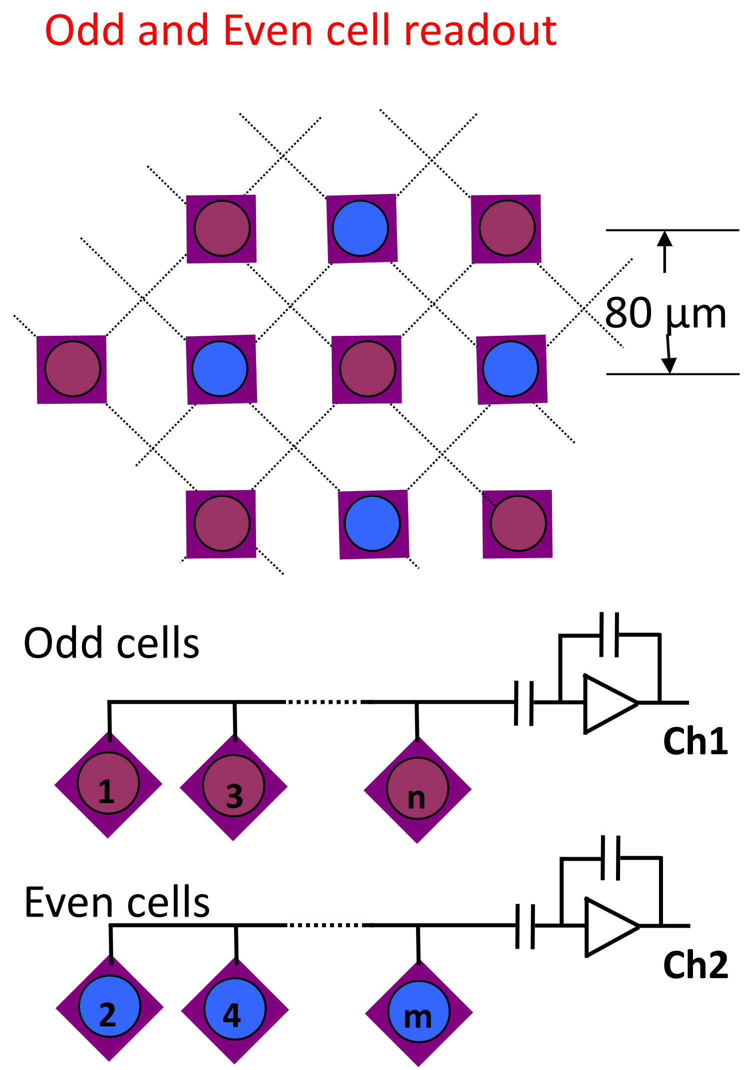

- Separate odd / even array readout could allow track structure information to be measured

SOI microdosimetry: generation 3/1

Measurement Conditions

- 3 MeV He^+ ions;
- Beam scanning area (230μm x 230μm)
- Only even array connected to preamplifier

Median energy map

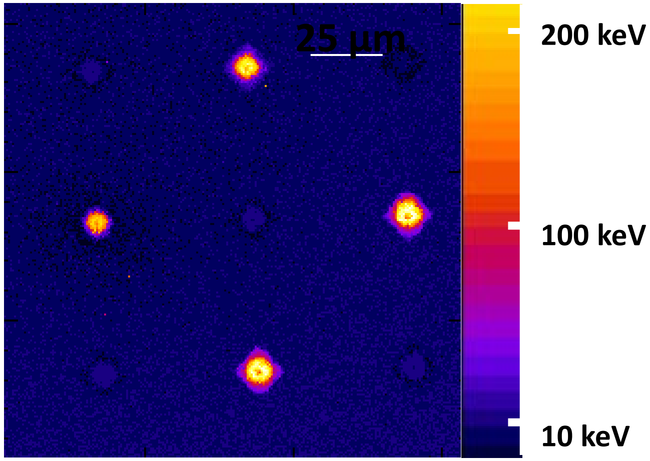

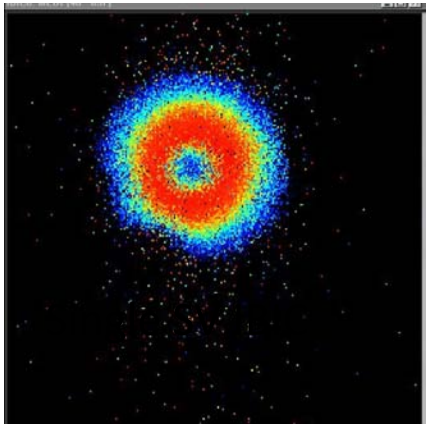

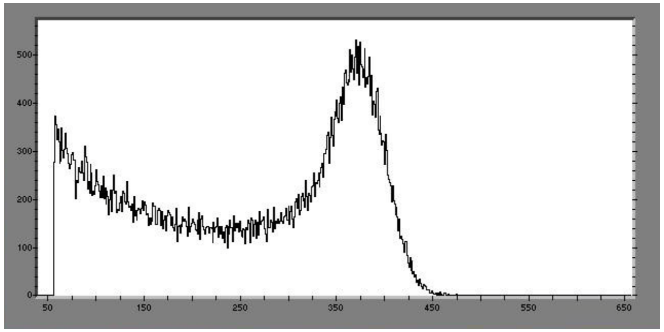

5MeV alpha particle IBIC

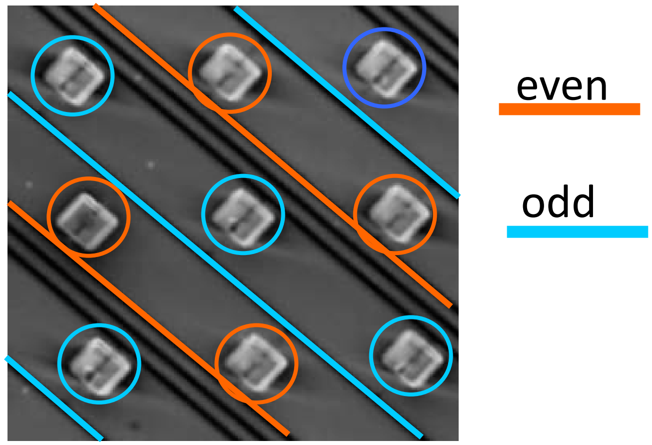

- Excellent charge collection efficiency in SV
- Excellent separation between even and odd array
- Low energy event from ions strike in a passive region

SOI silicon microdosimetry:generation 3/2

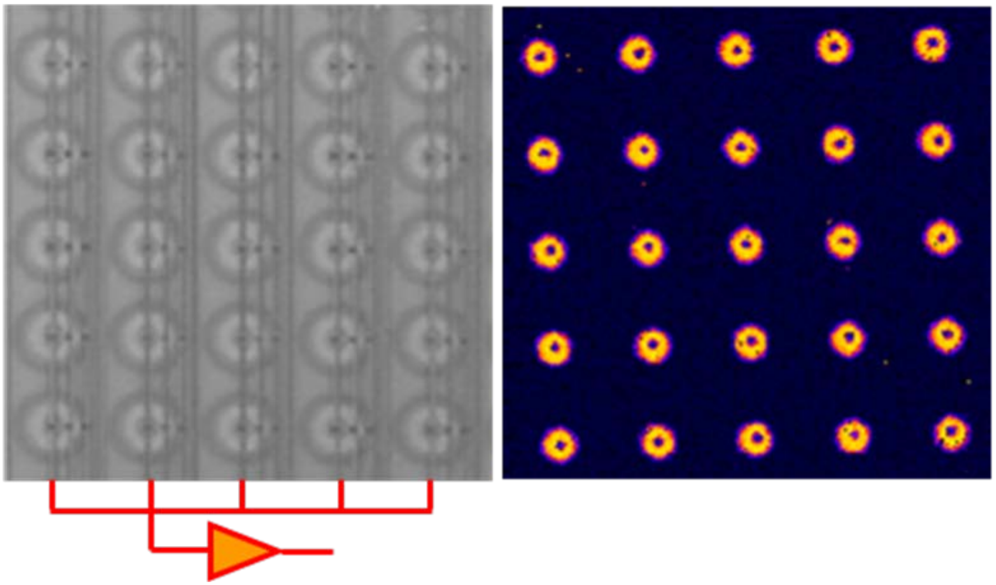

CMRP PhD students
Amy Ziebell and Nai Shian Lai

Response of new 3D SOI microdosimeter on 1 μm diameter 3 MeV alpha particles scanning microbeam

Each cell has sensitive volume with a radius of 6 μm and pitch about 20 μm

via Dopant Diffusion

Note: – All Dimensions in Microns

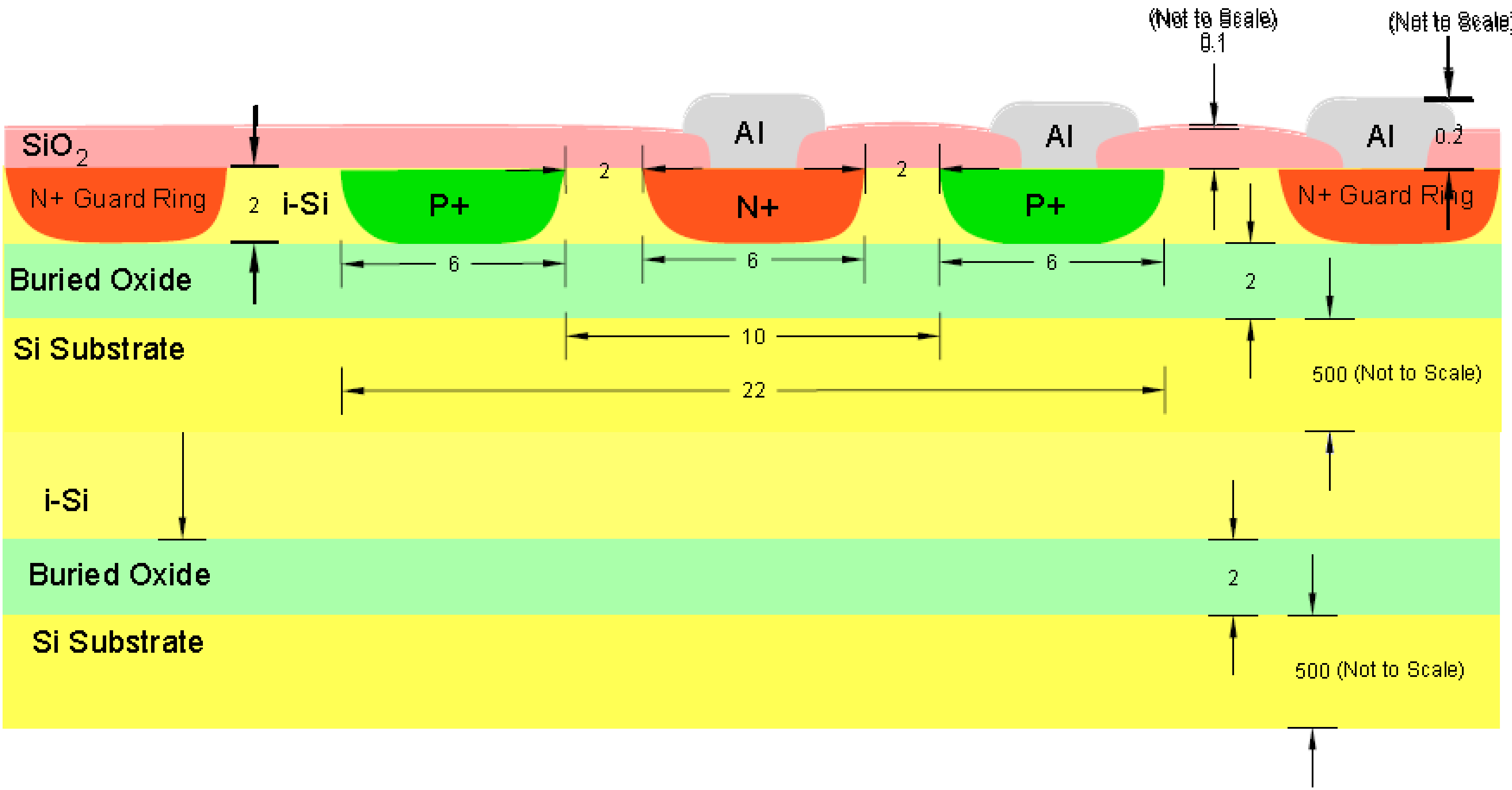

A. Cross-sectional Schemetic of the Microdosimeter

- MMD 2008 - N.S. Lai et al IEEE Trans on Nucl. Sci. ,NS-56 , 1637-1641, 2009

via Dopant Diffusion

Note: – All Dimensions in Microns
– N+ Guard Ring Not Shown

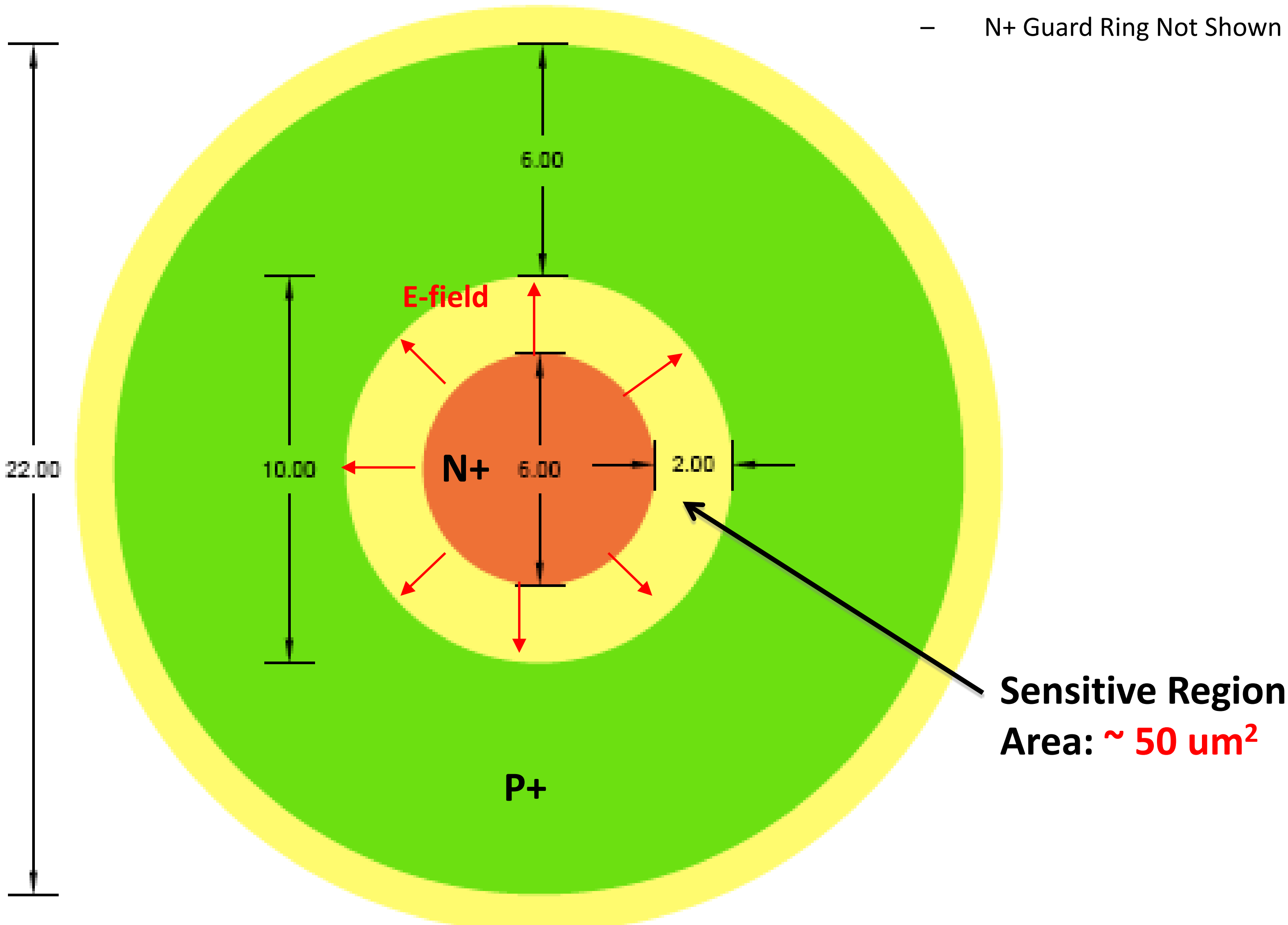

B. Top View of the Microdosimeter before Oxidation and Metallization

via Ion Implantaion

Note: – All Dimensions in Microns

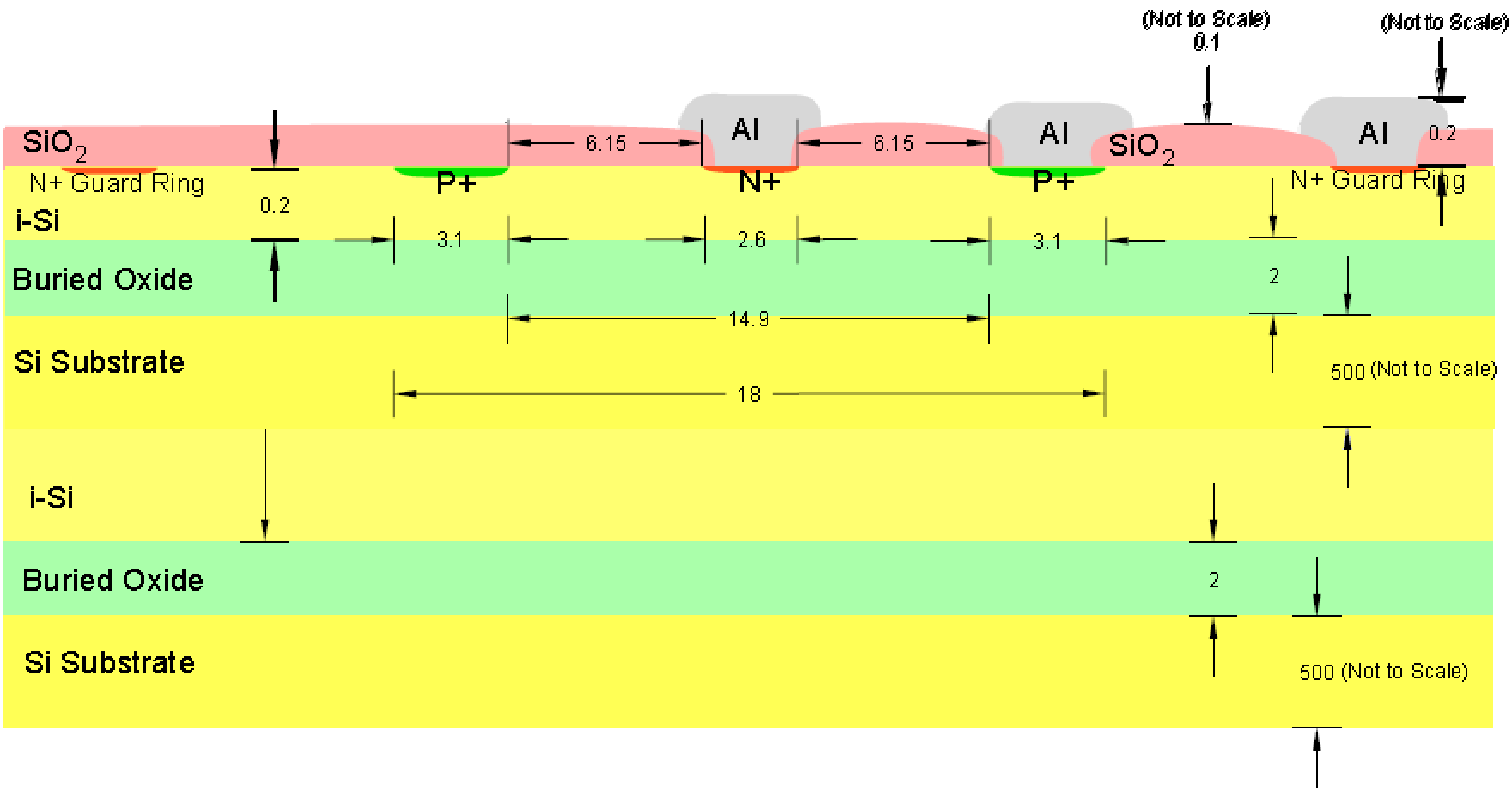

A. Cross-sectional Schemetic of the Microdosimeter

- MMD 2008 -

2nd Generation vs 3rd Generation

2nd Generation

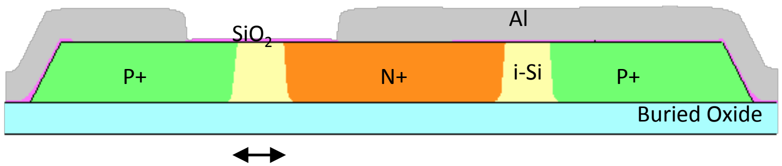

Sensitive region = 2 um

3rd Generation

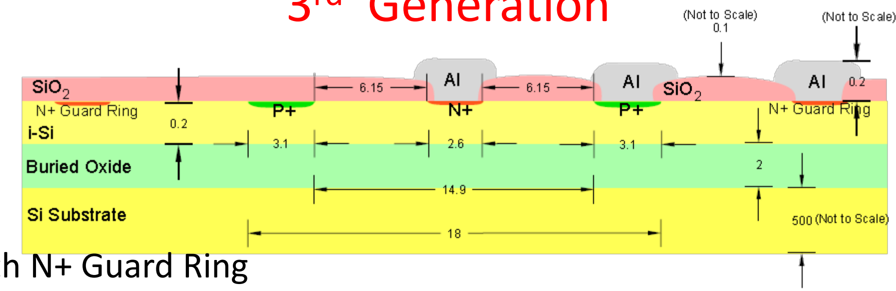

No N+ Guard Ring → With N+ Guard Ring

Mesa Structure via dopant diffusion → Planar Structure via ion implant

No Avalanche Signal Multiplication → Possible Avalanche Signal Multiplication

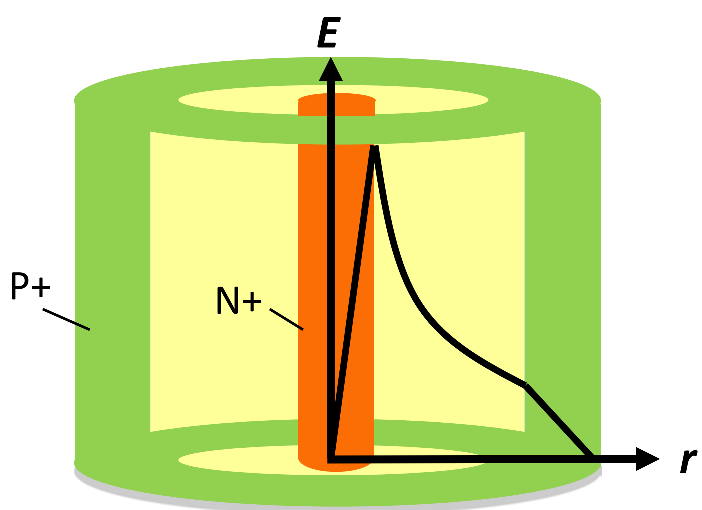

Design of SV - 2um Thick SOI

→

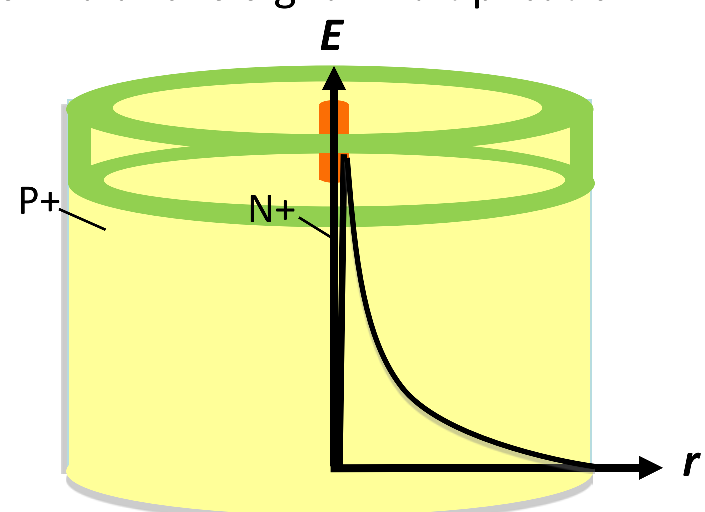

Design of SV - 2um Thick SOI

via Ion Implantation

Note: – All Dimensions in Microns
– N+ Guard Ring Not Shown

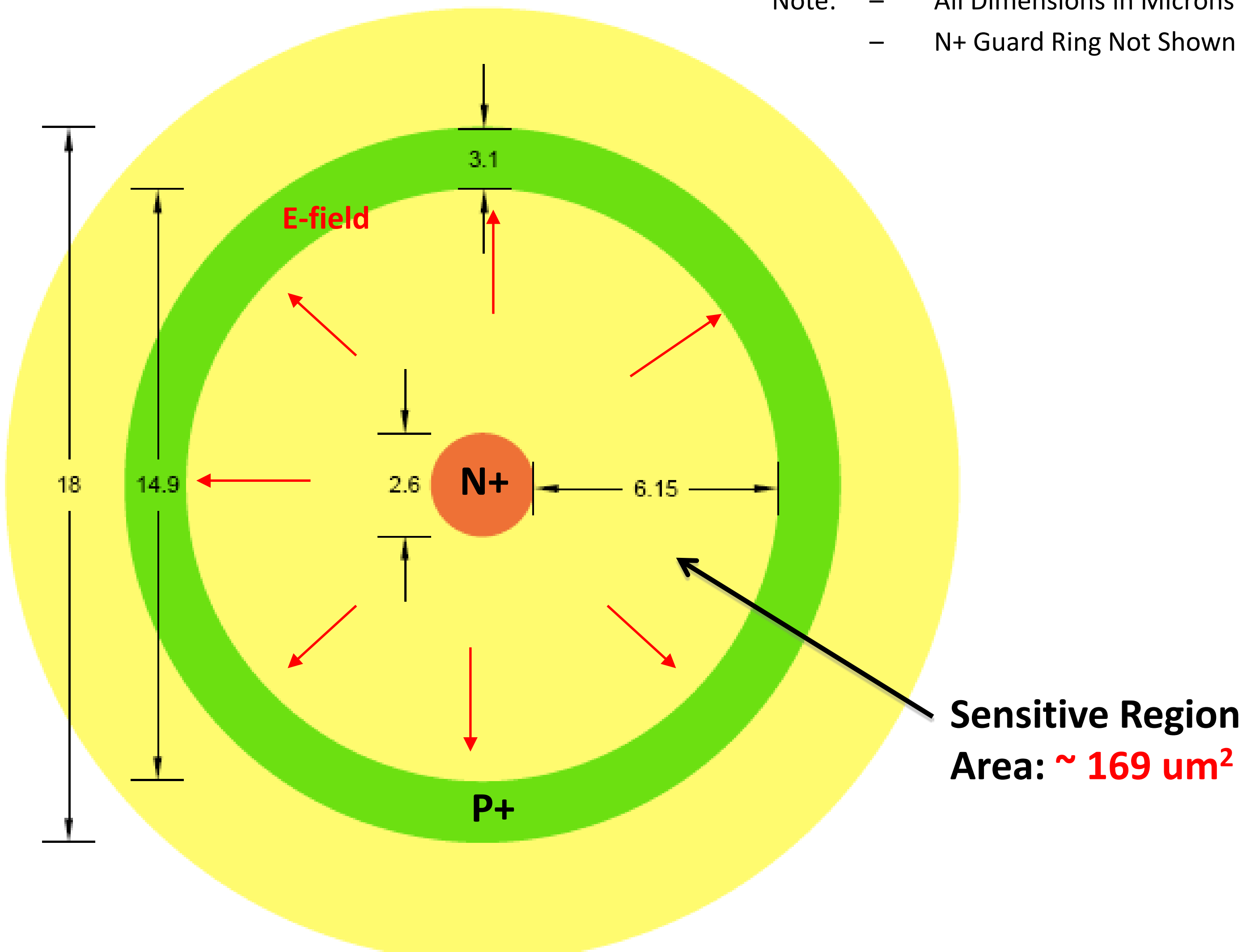

B. Top View of the Microdosimeter before Oxidation and Metallization

TCAD Modeling: Voltage & Electric Field

Modeling of Voltage

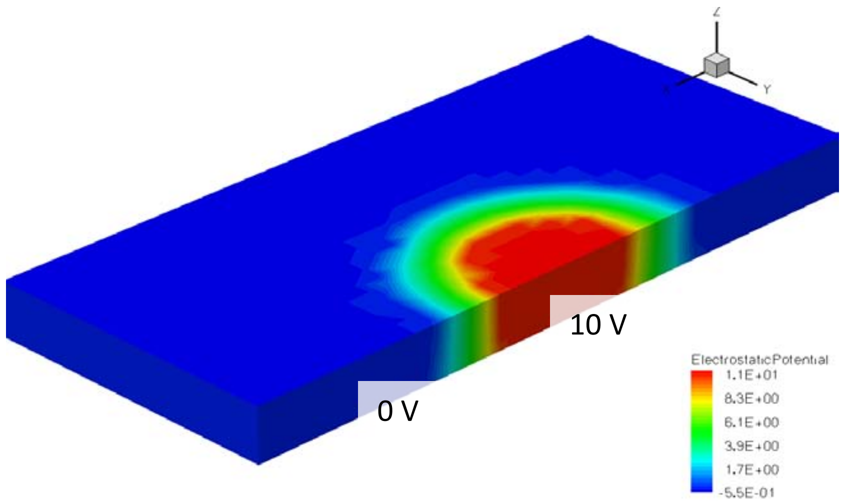

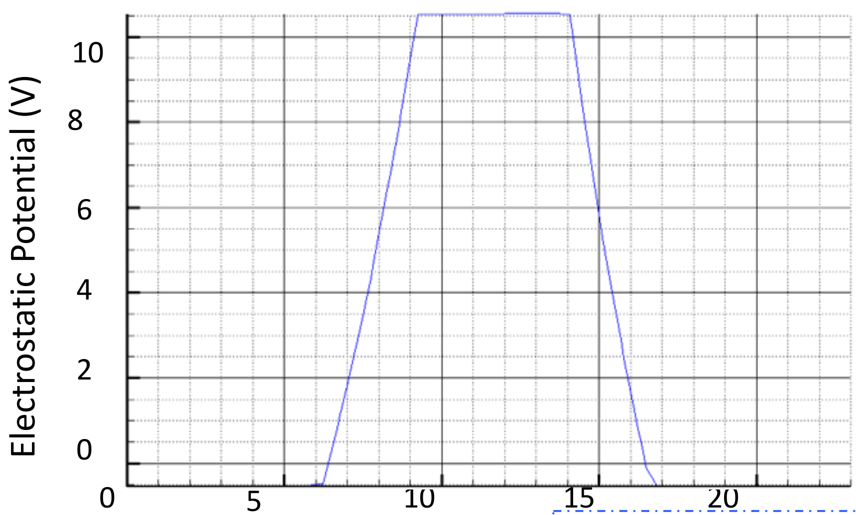

Modeling of Electric Field

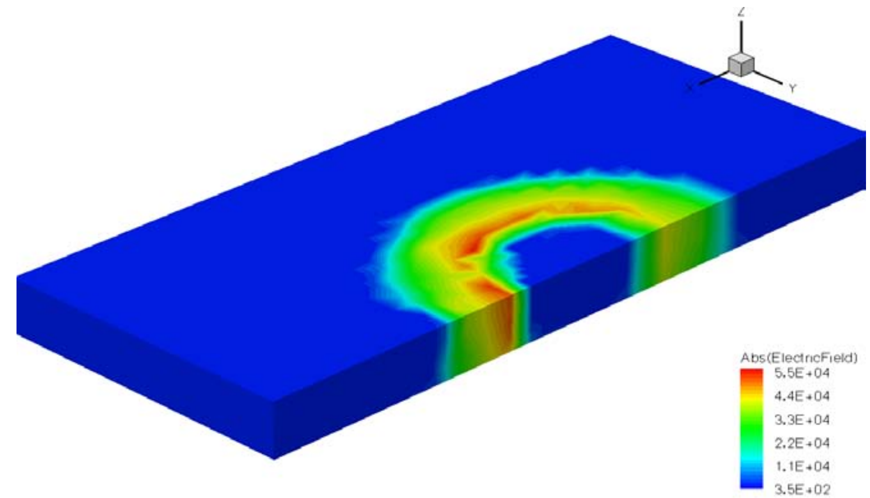

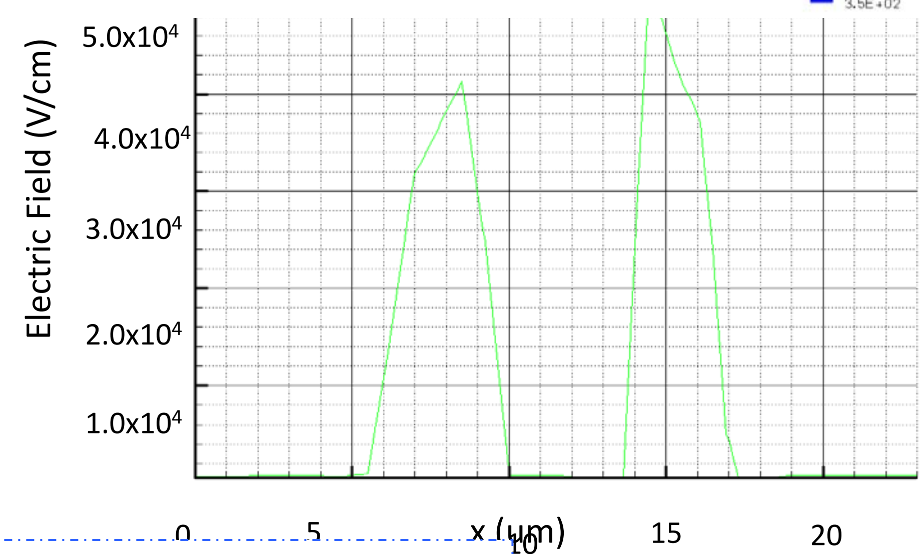

★Threshold for avalanche = 1×10^6 V/cm

- MMD 2008 -

TCAD Modeling: Charge Transient

Energy of He ion = 1 MeV

Bias Voltage = -10 V

Sensitive width = 2 um

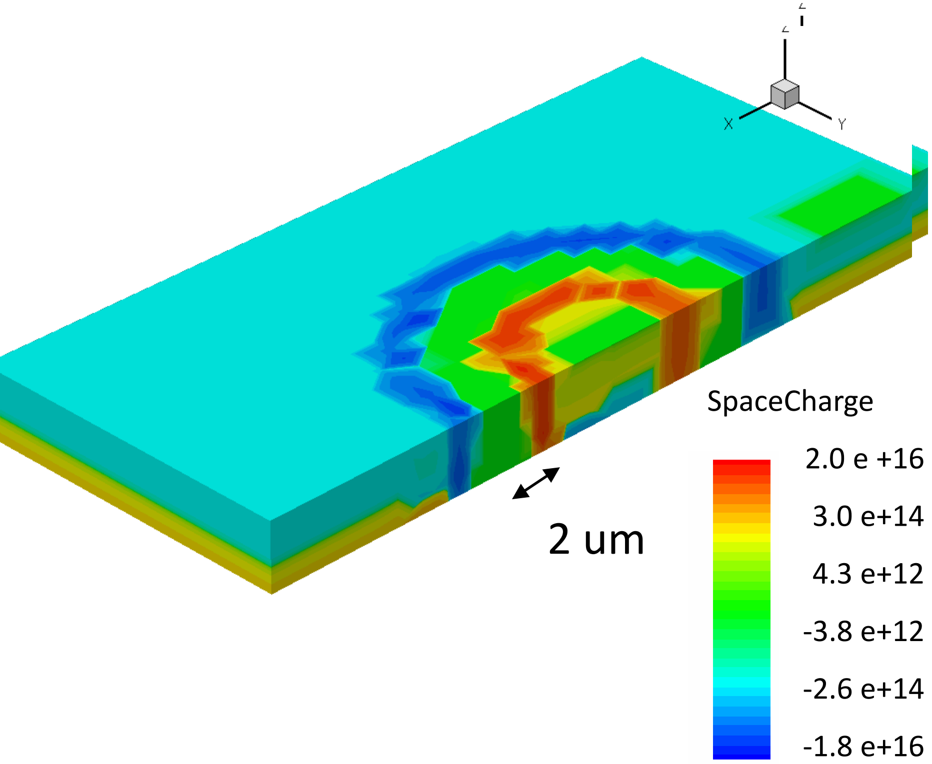

Time scale

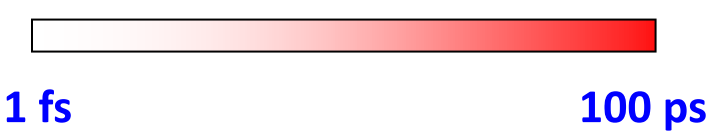

Sensitive width = 10 um

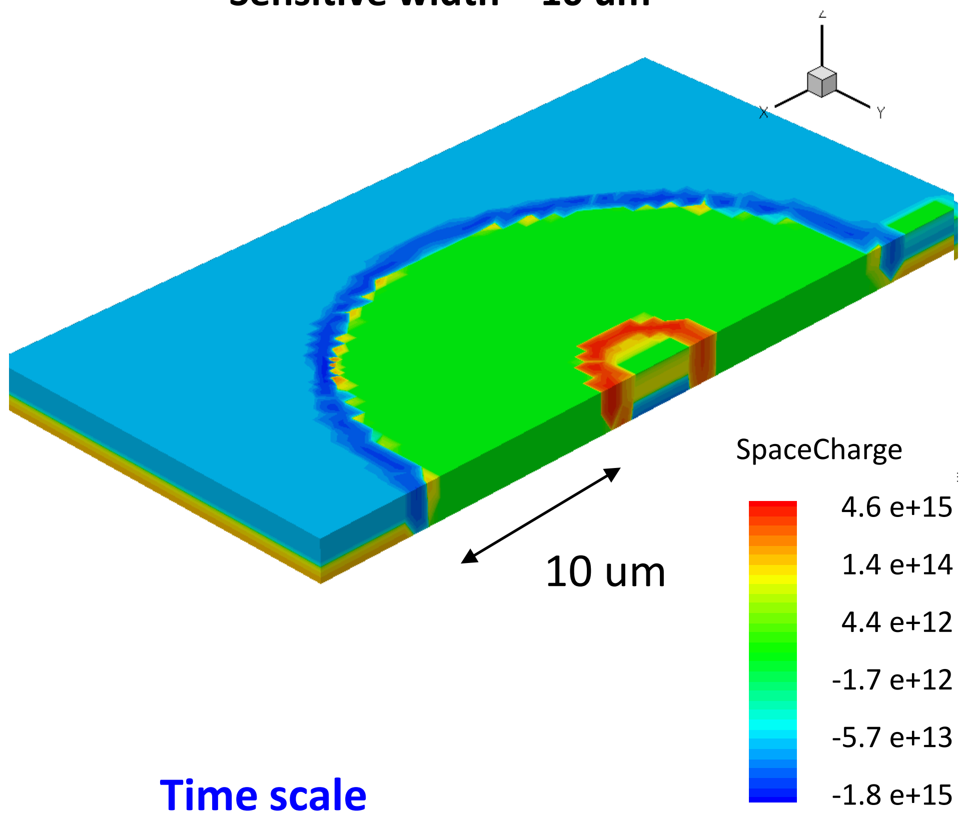

Time scale

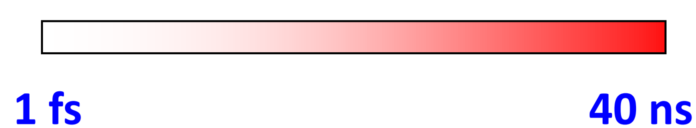

TCAD Modeling

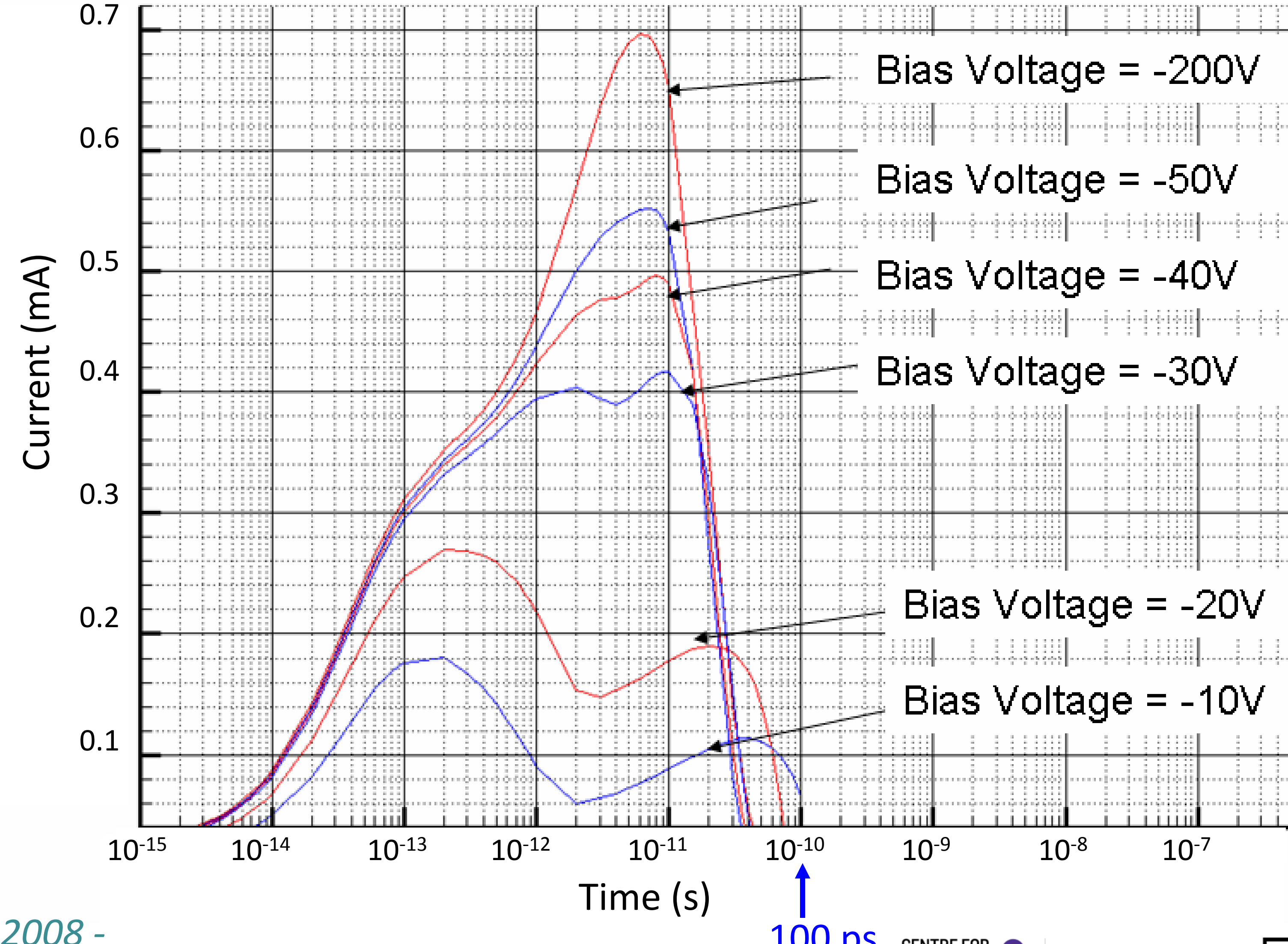

- MMD 2008 -

Chord Length Distribution study

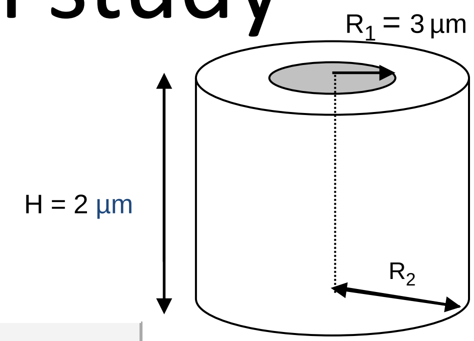

The detector concept is exposed to a uniform isotropic field of infinite straight lines

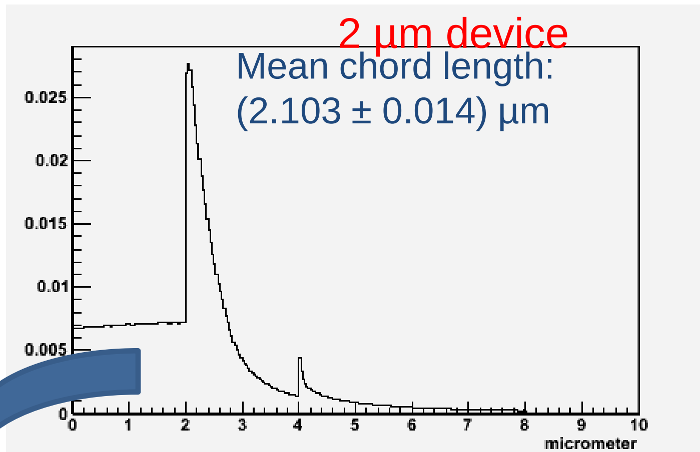

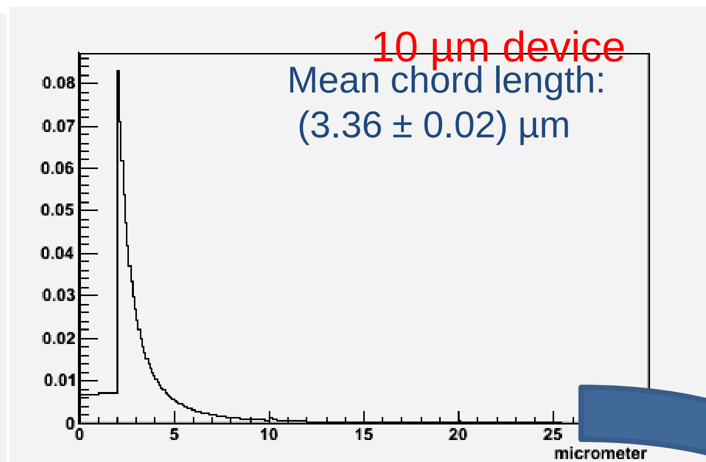

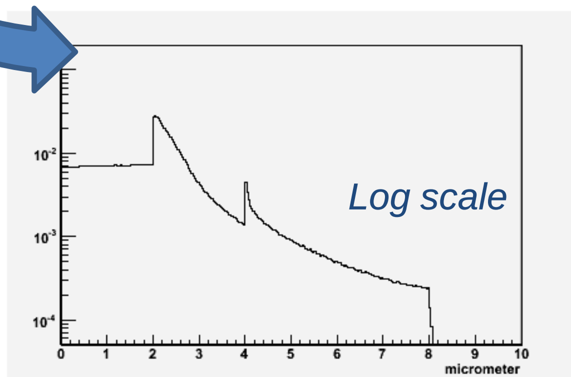

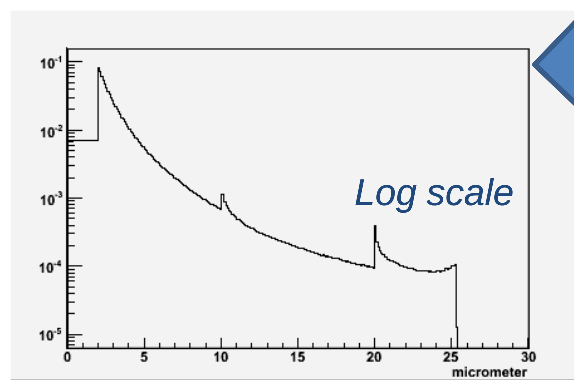

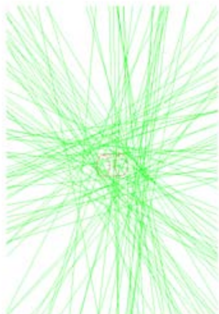

Geant4

Results

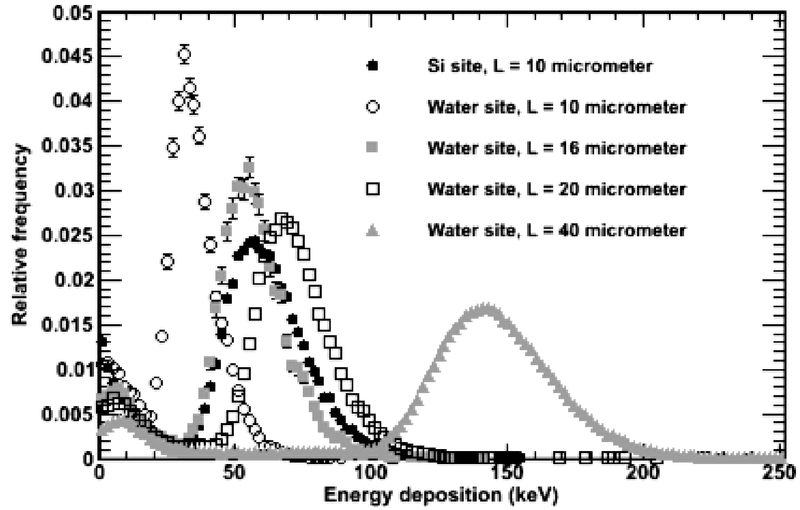

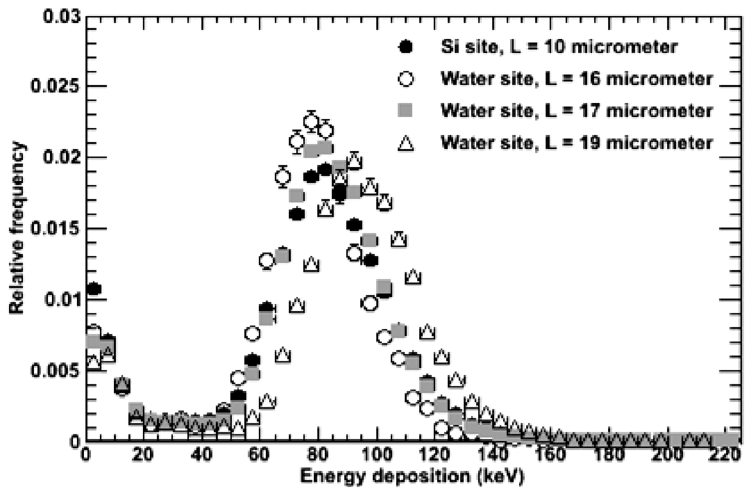

Energy deposition spectra resulting from a 50 MeV proton beam at 2.1 cm depth in the water phantom. (Bragg peak)

Conversion Si to Tissue

- Statistical analysis by means of Kolmogorov-Smirnov test

	Water microdosimeter site	Left branch *p*-value	Right branch *p*-value
Position I	$L = 17$ μm	0.8730	0.9955
Position II	$L = 17$ μm	0.9897	0.8384
Position III	$L = 17$ μm	0.6172	0.9996
Position IV	$L = 17$ μm	0.8580	1.0000

- Linear coefficient ***C* = (0.56 ± 0.03)*** was determined to convert microdosimetric spectra from silicon to water for incident proton energies between a few MeV and 250 MeV.
- For a water cylinder with height *h* and diameter *d*, the required scaling is *C*·h*, *C*·d* of silicon.

Conversion Si to Tissue

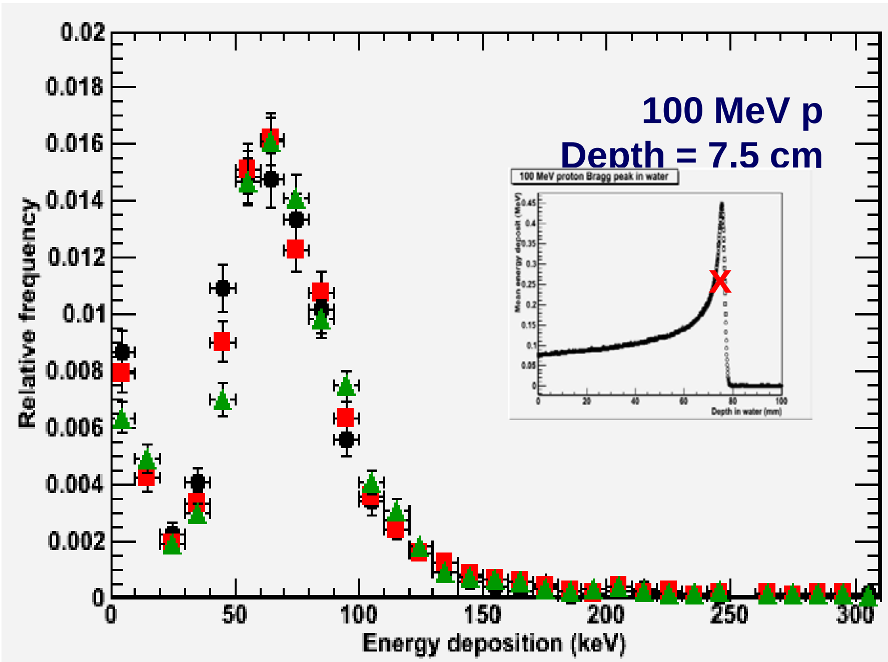

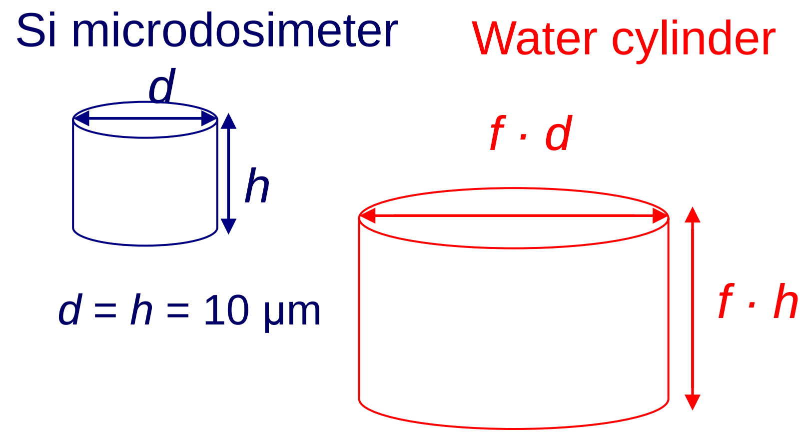

10 μm silicon detector
17 μm water detector
18 μm water detector

- Comprehensive MC simulations were carried out for alpha , Li ions , N ions and protons for cylindrical and RPP SV
- Comparison between **equivalent energy deposition spectra** Si/W SVs and ratio of stopping powers Si/Water allow introduce average scaling coefficient 0.63 for RPP and 0.60 for cylinder for most applications

P.Bradley et al. *Med.Phys*., 25(11), 2220-2225,1998
S.Guatelli et al., *IEEE Trans. On Nucl.Sci.*, Dec , 2008

Experimental Setup

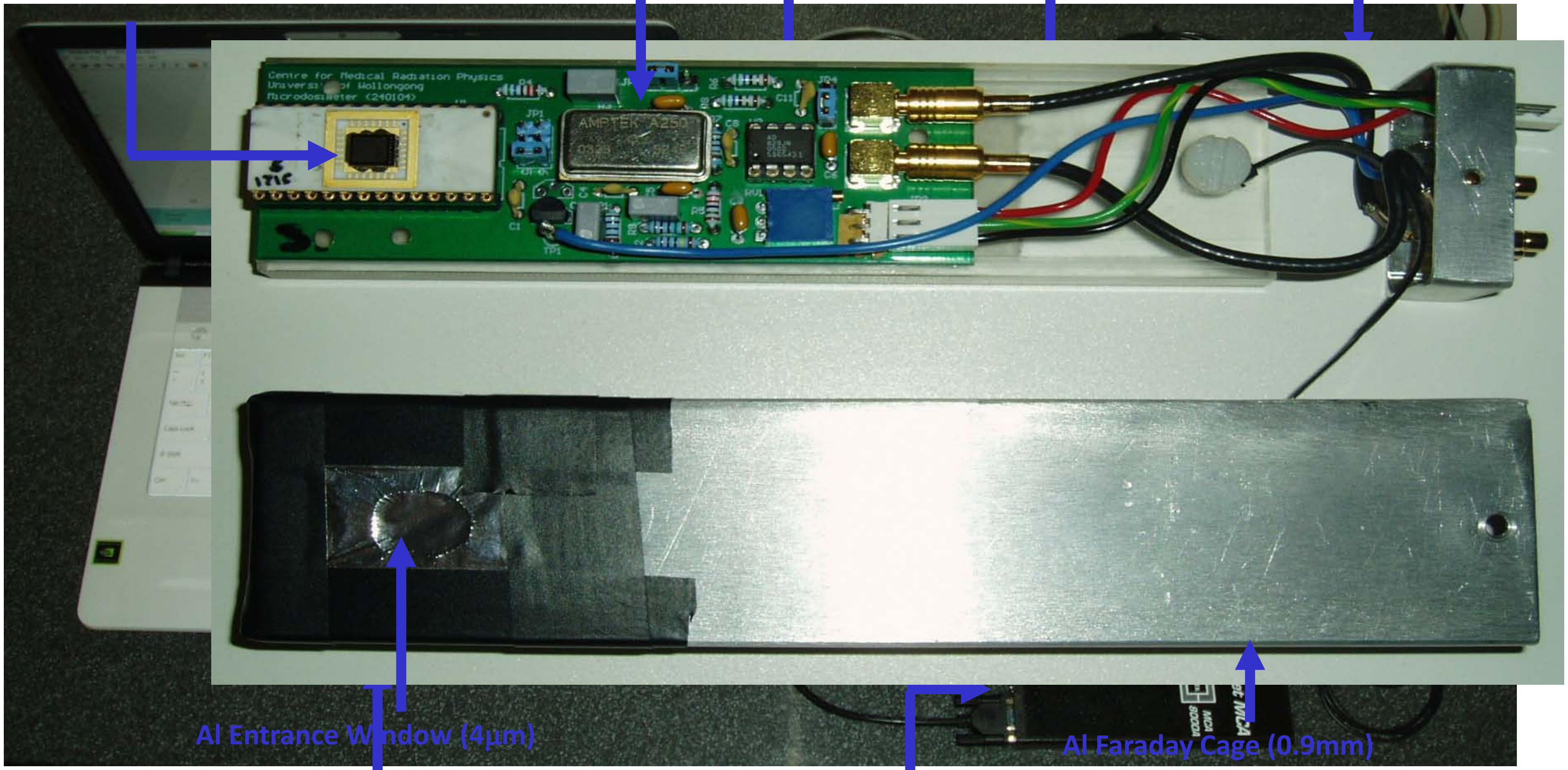

Dose Equivalent Determination

- Dose is determined from the f(E)/E Spectra in the following method:

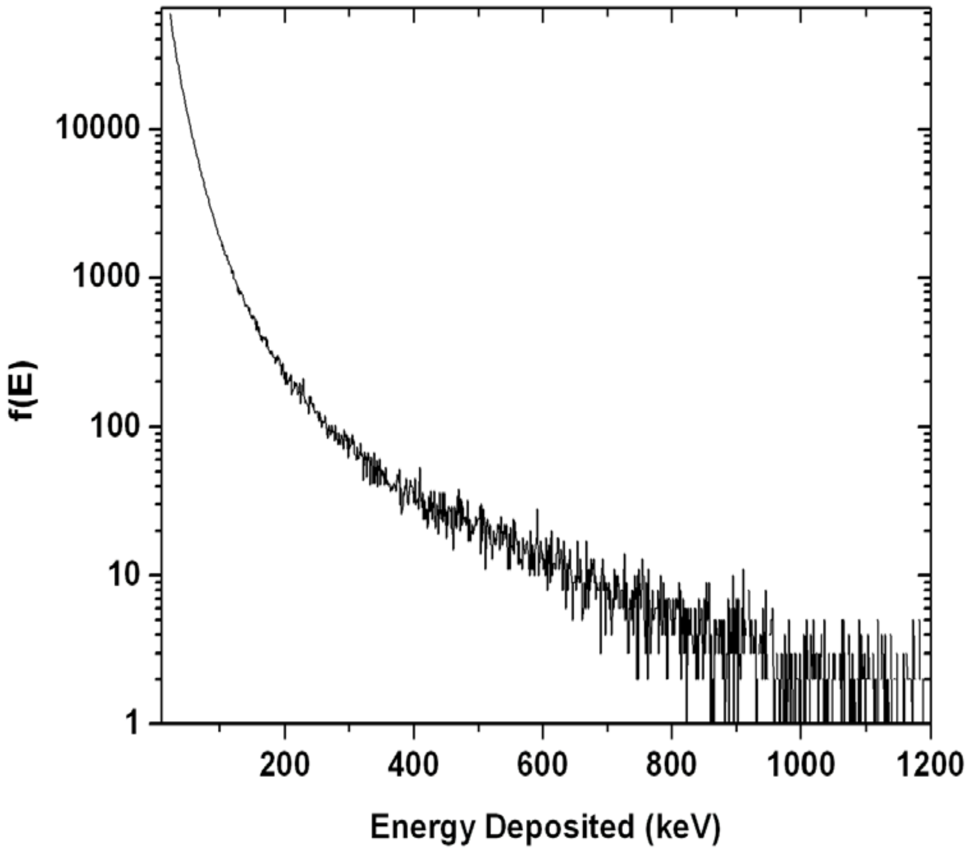

$$D_{Si} = \frac{\int_0^\infty f(E).E.dE}{M} = \frac{\int_0^\infty f(E).E.dE}{\rho_{Si} V n_{cells}}$$

$$\therefore D_{Si} = D_{TE} \frac{S_{Si}}{S_{TE}}$$

Dose Equivalent Determination

- The lineal Energy Spectra is determined by dividing the energy by the mean chord length <l>:

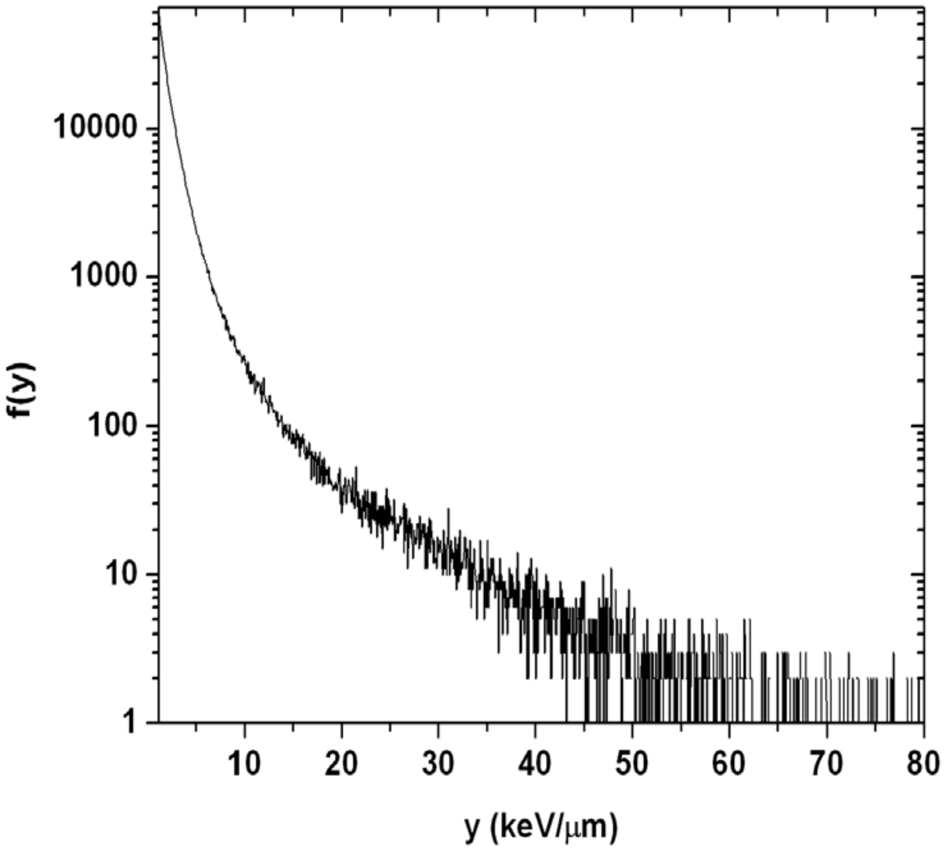

$$< l >= \frac{4V}{S\zeta}$$

$$y = \frac{E}{< l >}$$

- Where <l> in this case is 19.05µm and ζ=0.63 is the TE conversion factor

Dose Equivalent Determination

- A normalised dose weighted lineal energy spectra can be obtained using the following relationship:

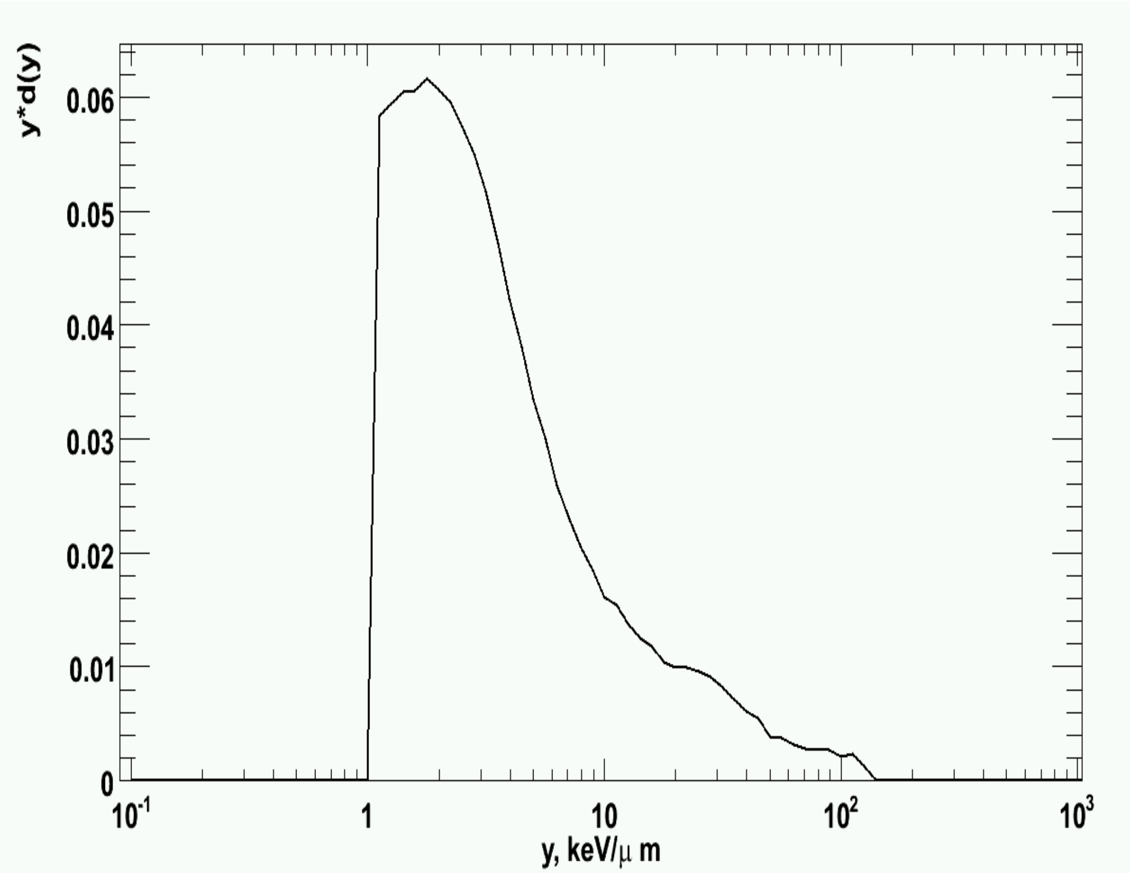

$$d(y) = \frac{yf(y)}{y_f}$$

$$y_f = \int_0^\infty yf(y)dy$$

$$\int_0^\infty d(y)dy = 1$$

Dose Equivalent Determination

- The final step in determining dose equivalent (Sv) is to convolve the dy spectra with a quality spectra Q(y).

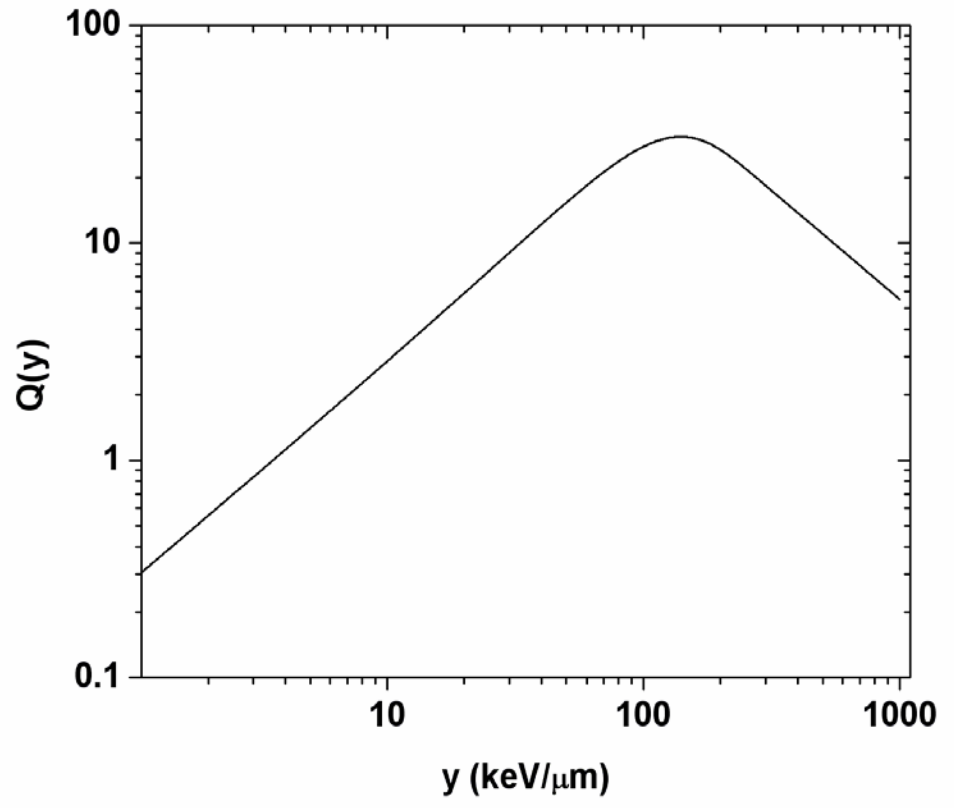

$$H = \int_0^\infty Q(y)D(y)dy$$

$$\therefore H = \int_0^\infty Q(y)D_{TE}d(y)dy$$

SOI Microdosimetry for Personal Radiation Protection: n-γ Sources and Fluence

- ^{252}Cf source mounted in a lead container, ANSTO
- Source activity at time of irradiation = 4.49×10^6 n/s in 4π
- Distance of microdosimeter from source = 130mm
- Total neutron flux on microdosimeter array = 25n/s for array A1(about 1.5 mm2)
- Total neutron fluence ~4.25×10^6 incident on array A1

SOI Microdosimetry in Personal Radiation Protection

SOI Microdosimetry of ^{252}Cf and PuBe neutron sources, ANSTO

Neutron spectra from IAEA TRS 403

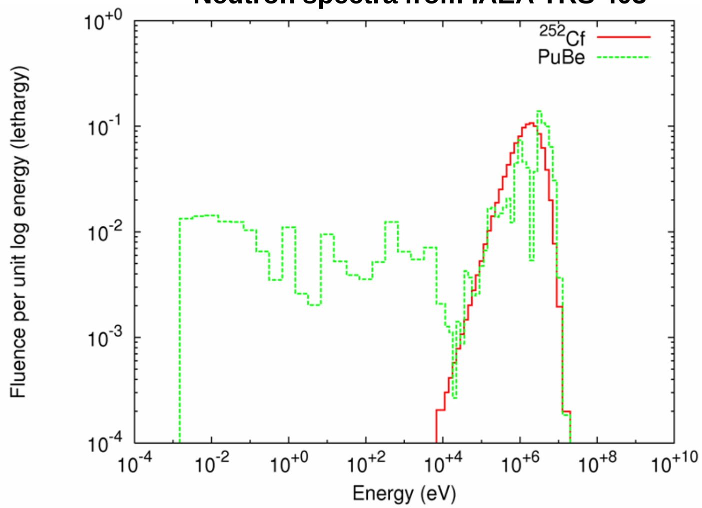

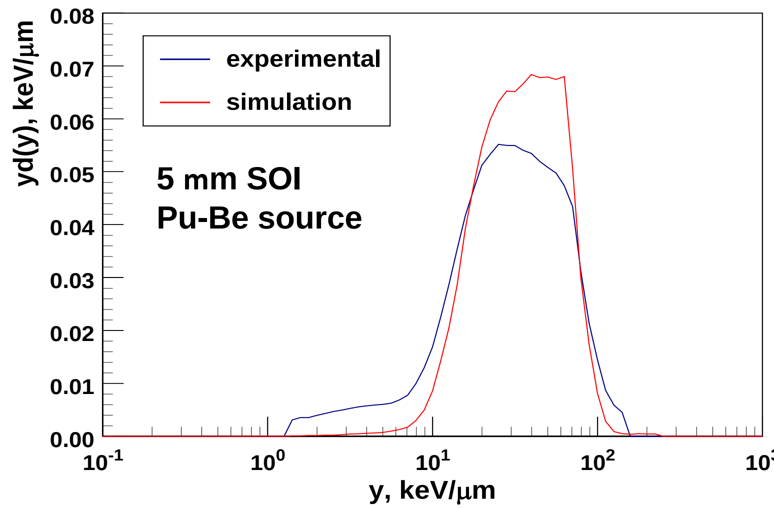

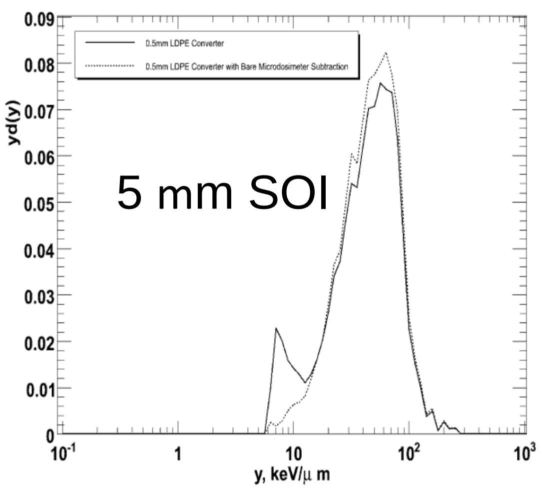

Cf-252 microdosimetry

Measurements in free air
LDP converter 0.5mm

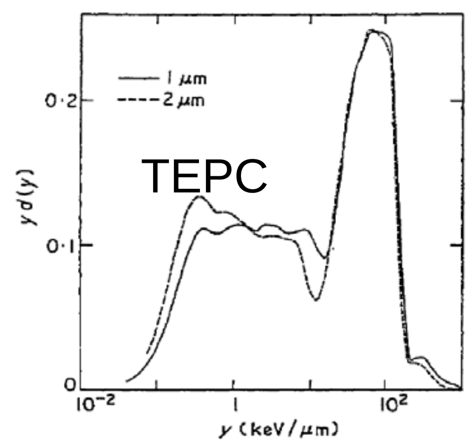

J. F. Dicello et al. Phys. Med. Biol., 1972, Vol. 17, No. 3, 345-355

M.Reinhard et al, IEEE Trans NSS track record, 2008

Results: Zero Crossing Time Maps

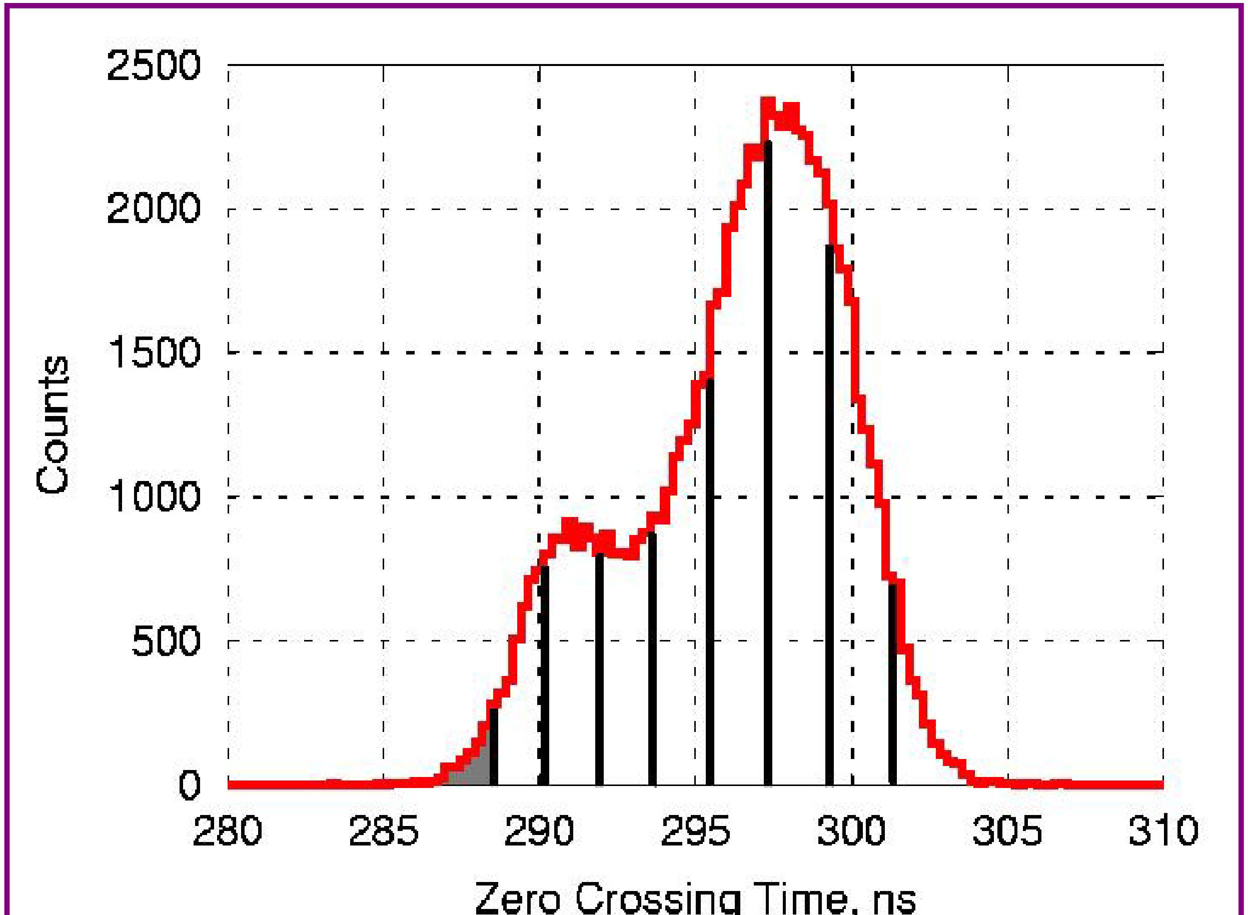

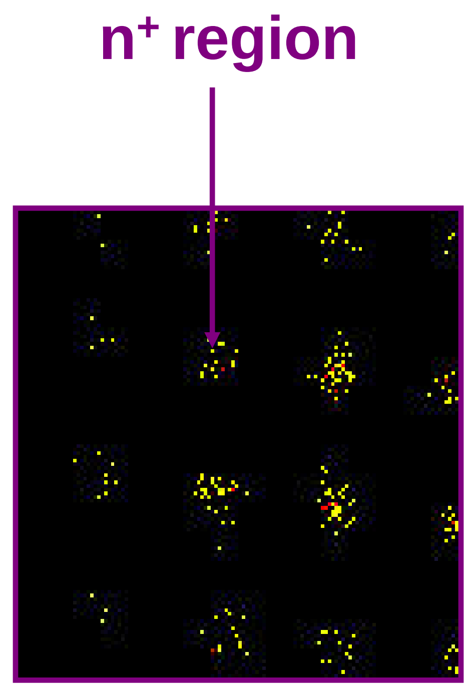

I.Cornelius et al. *IEEE Trans. Nucl. Sci* , **49**,N6, 2805-2809, 2002

Results: Zero Crossing Time Maps

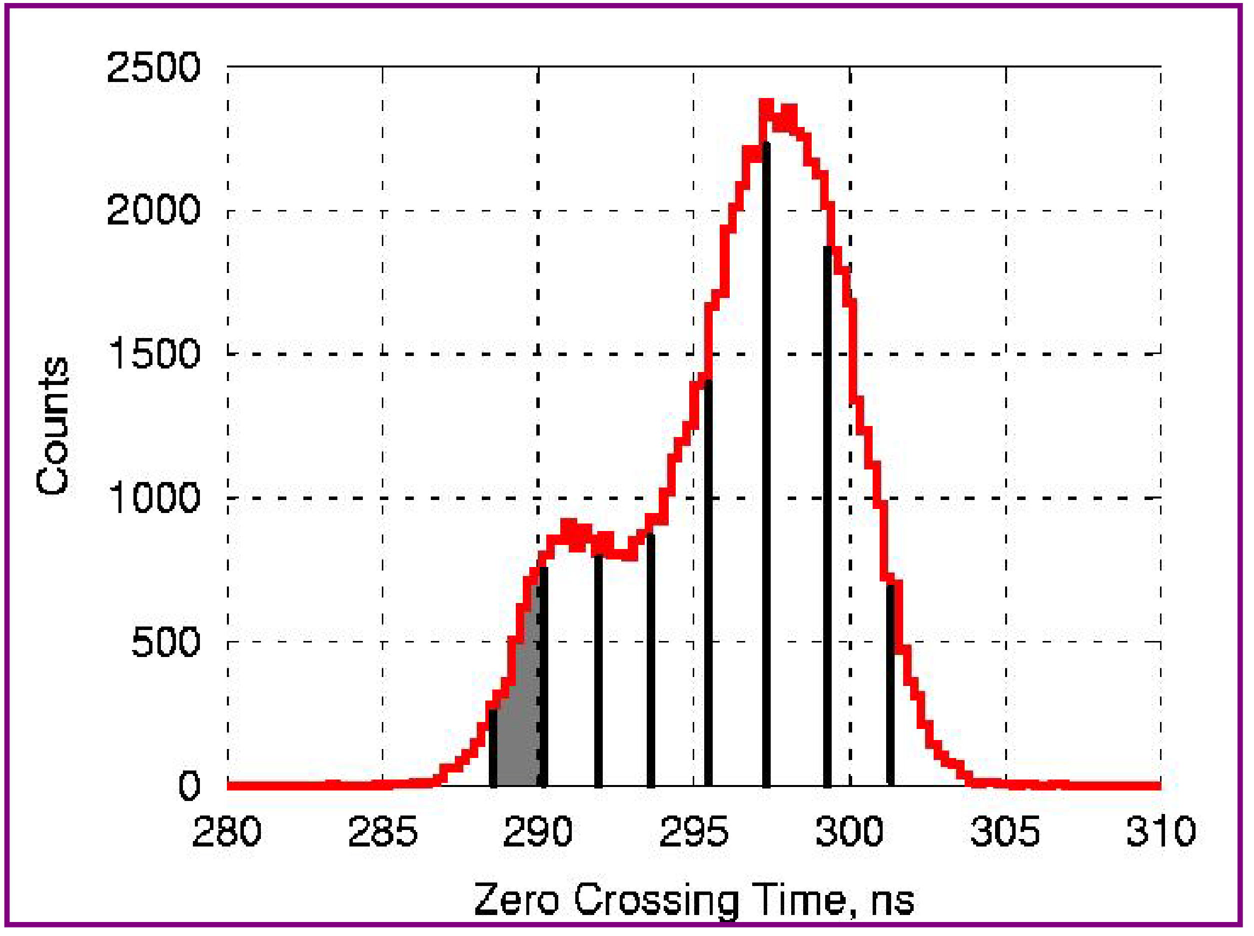

n⁺ region

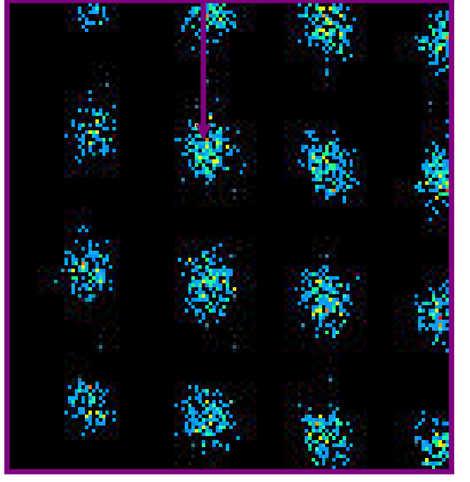

Results: Zero Crossing Time Maps

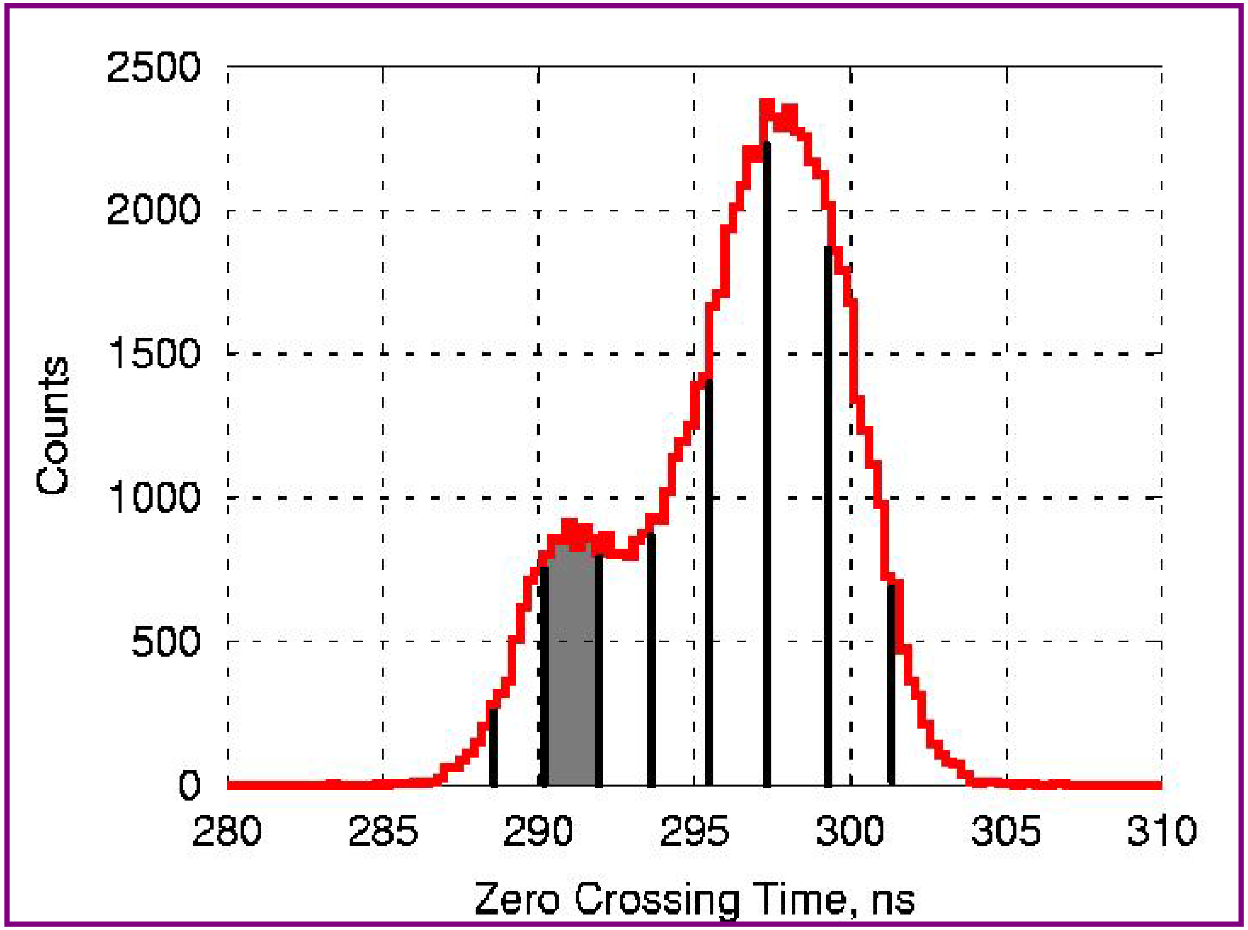

n^+ region

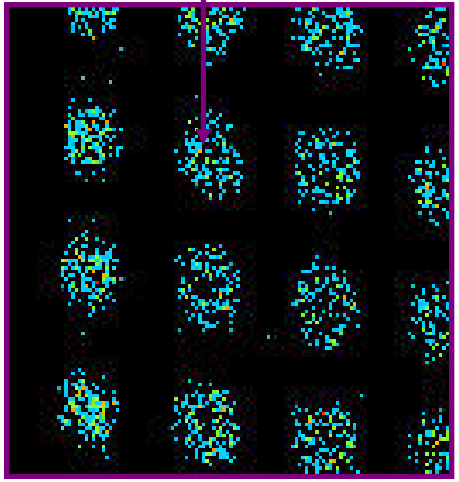

Results: Zero Crossing Time Maps

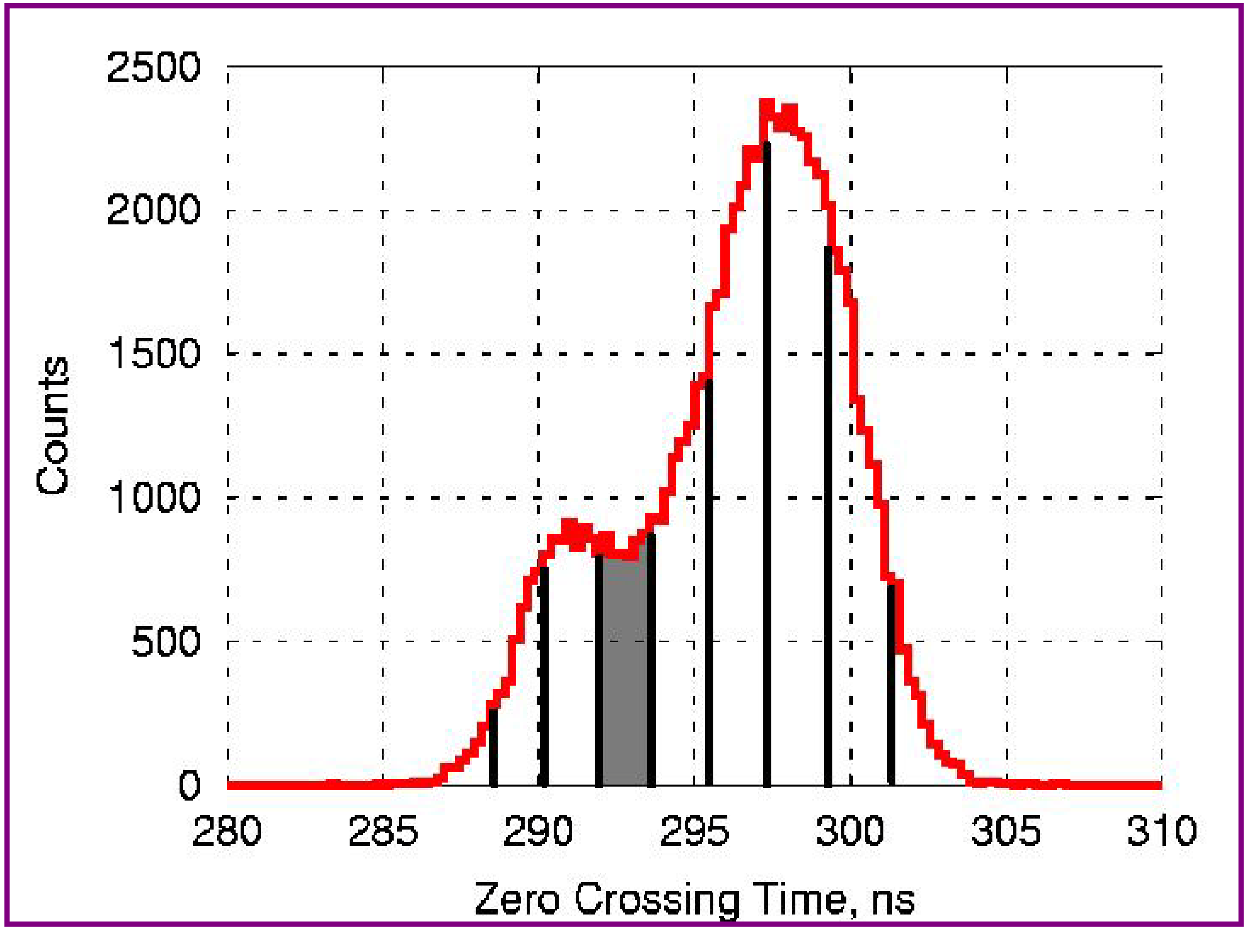

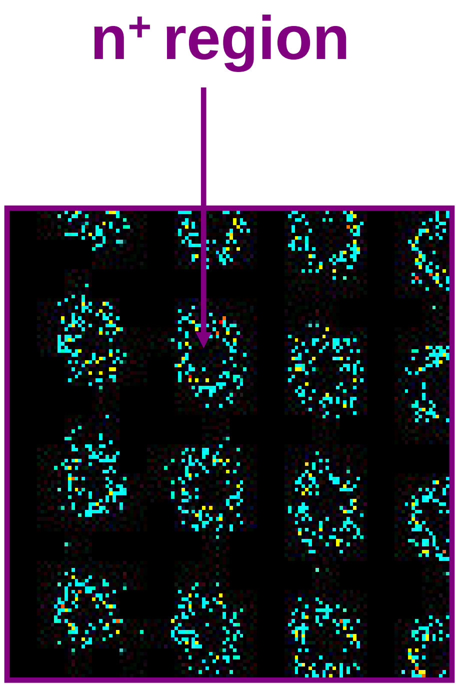

Results: Zero Crossing Time Maps

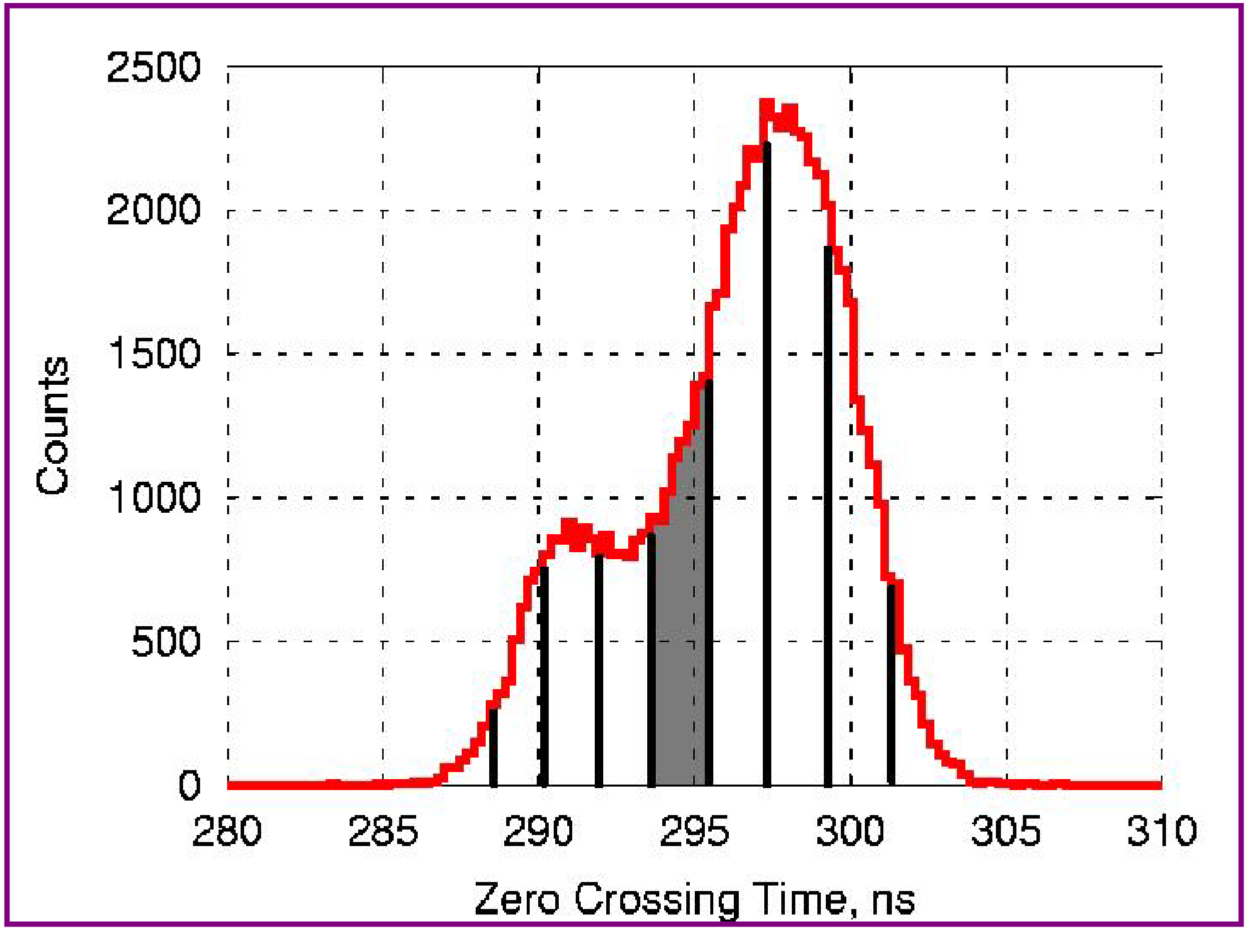

n+ region

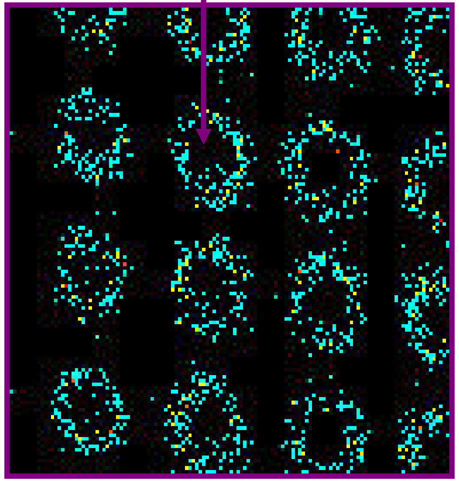

Results: Zero Crossing Time Maps

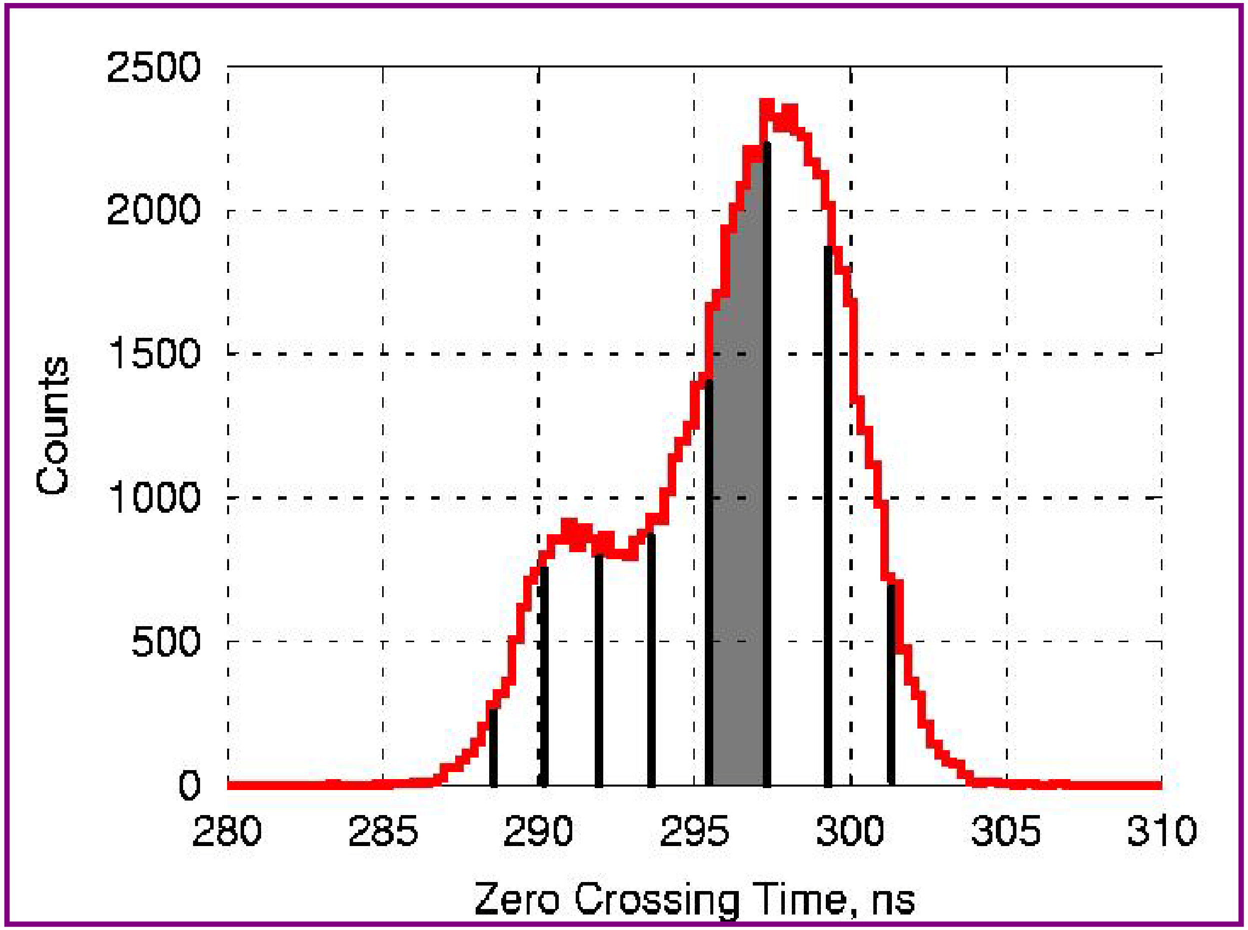

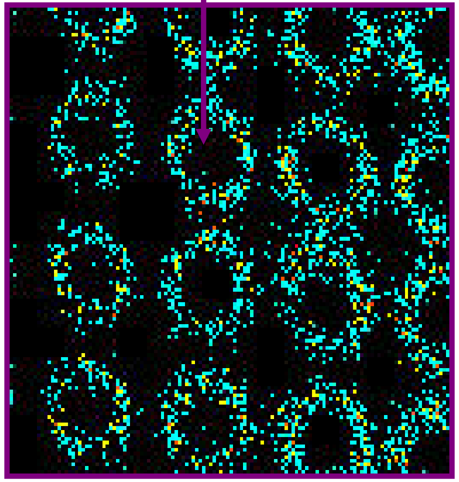

Results: Zero Crossing Time Maps

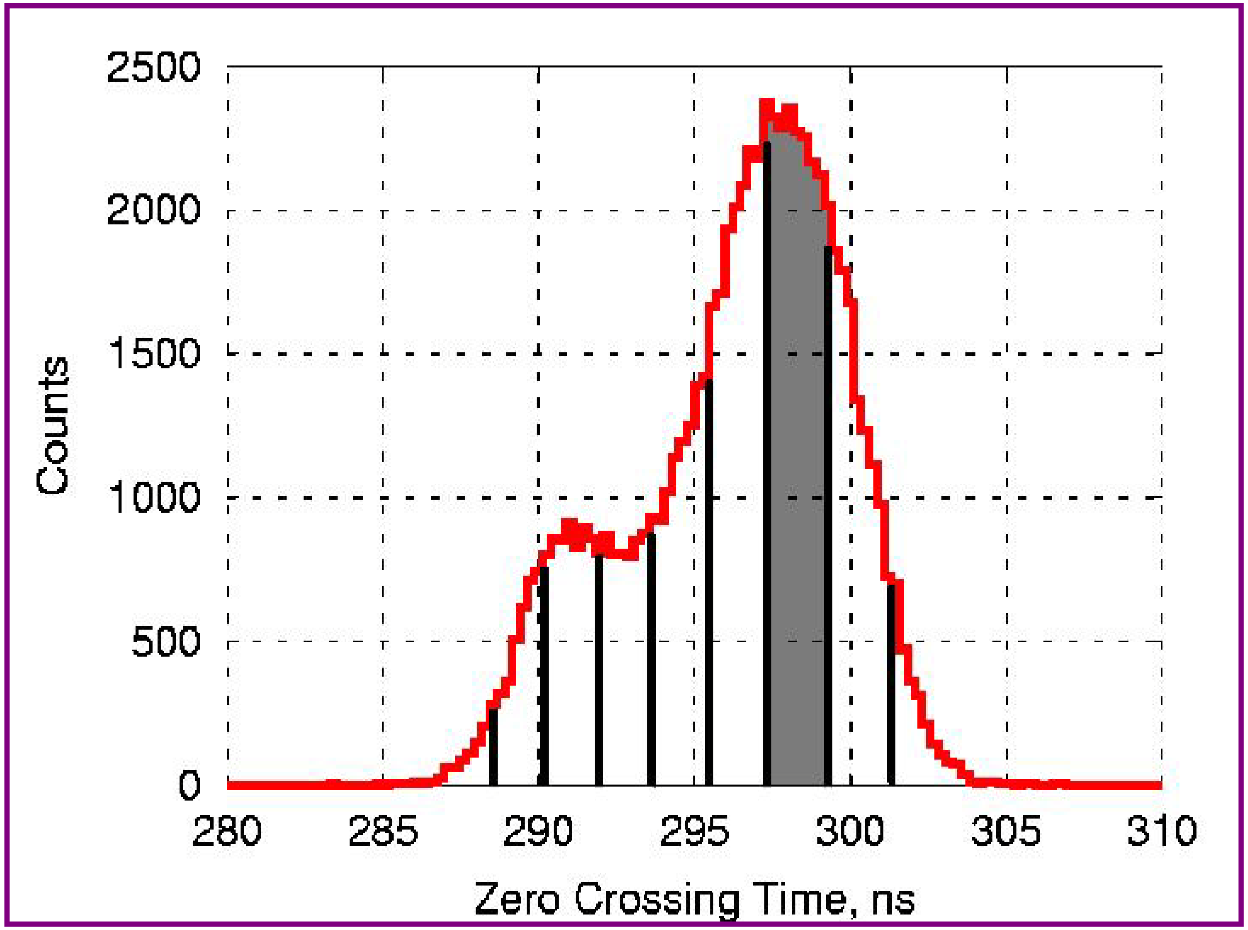

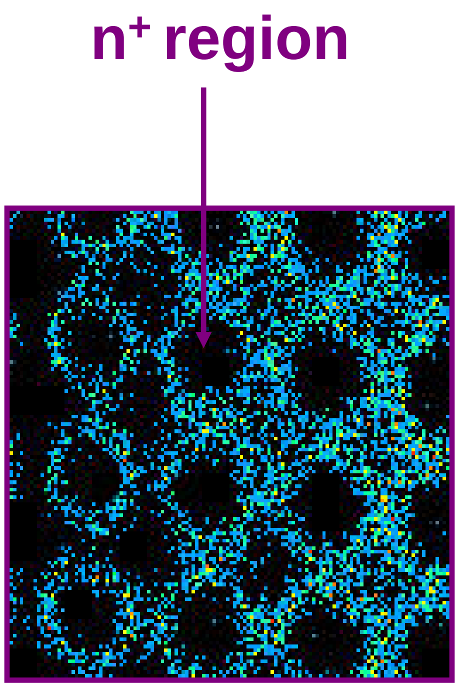

Results: Zero Crossing Time Maps

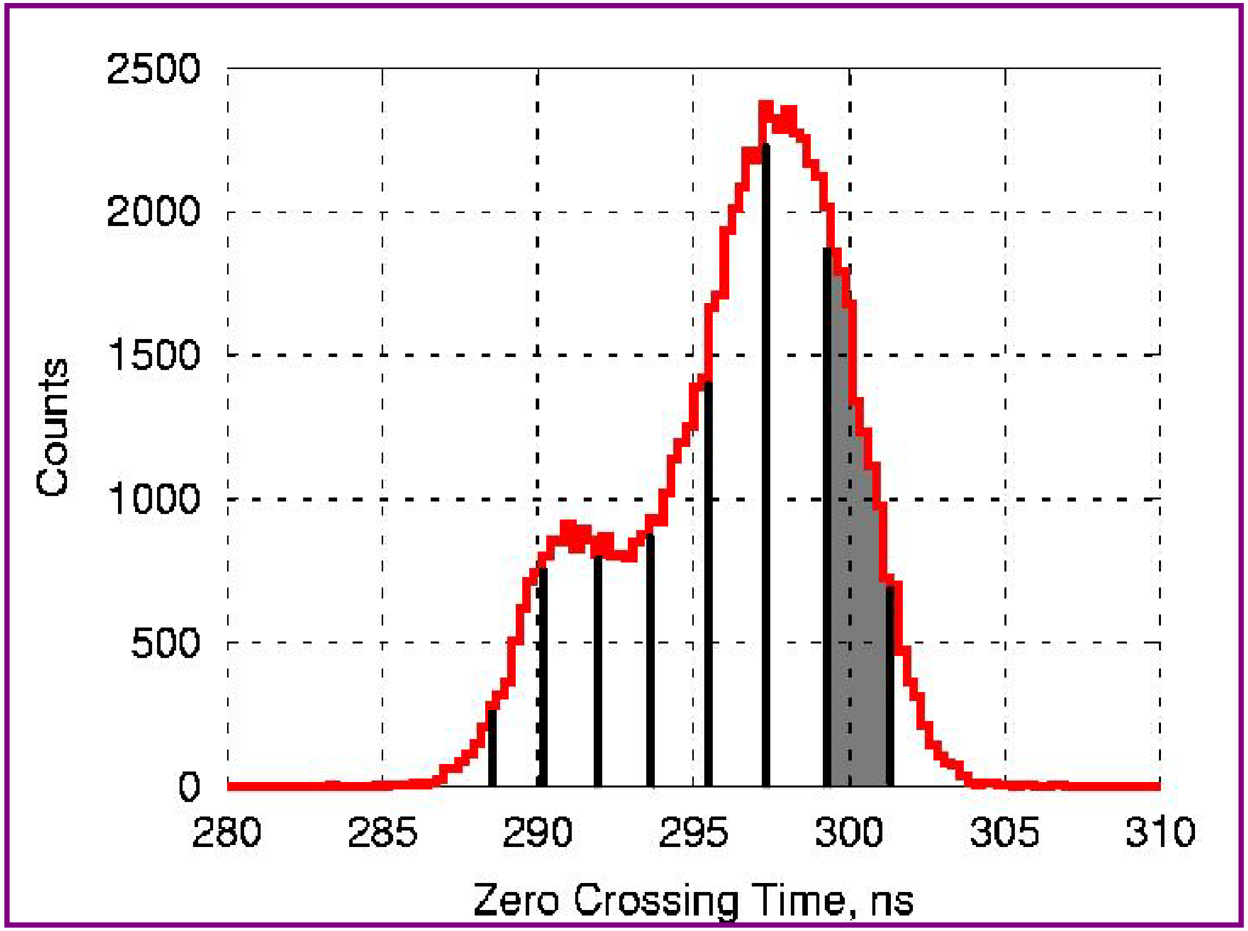

n$^+$ region

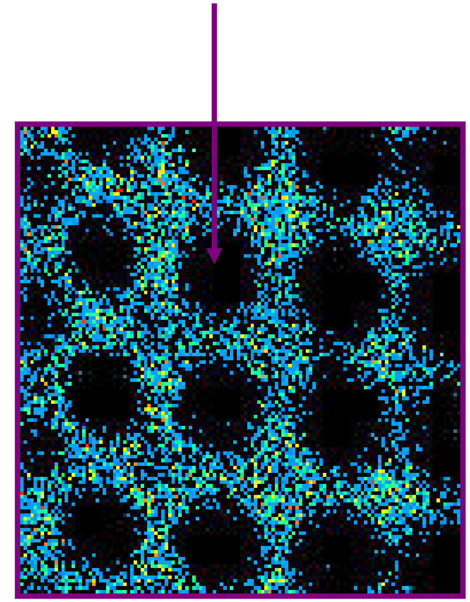

Improvement of Sensitive Volume and Spectral Response with PSD technique

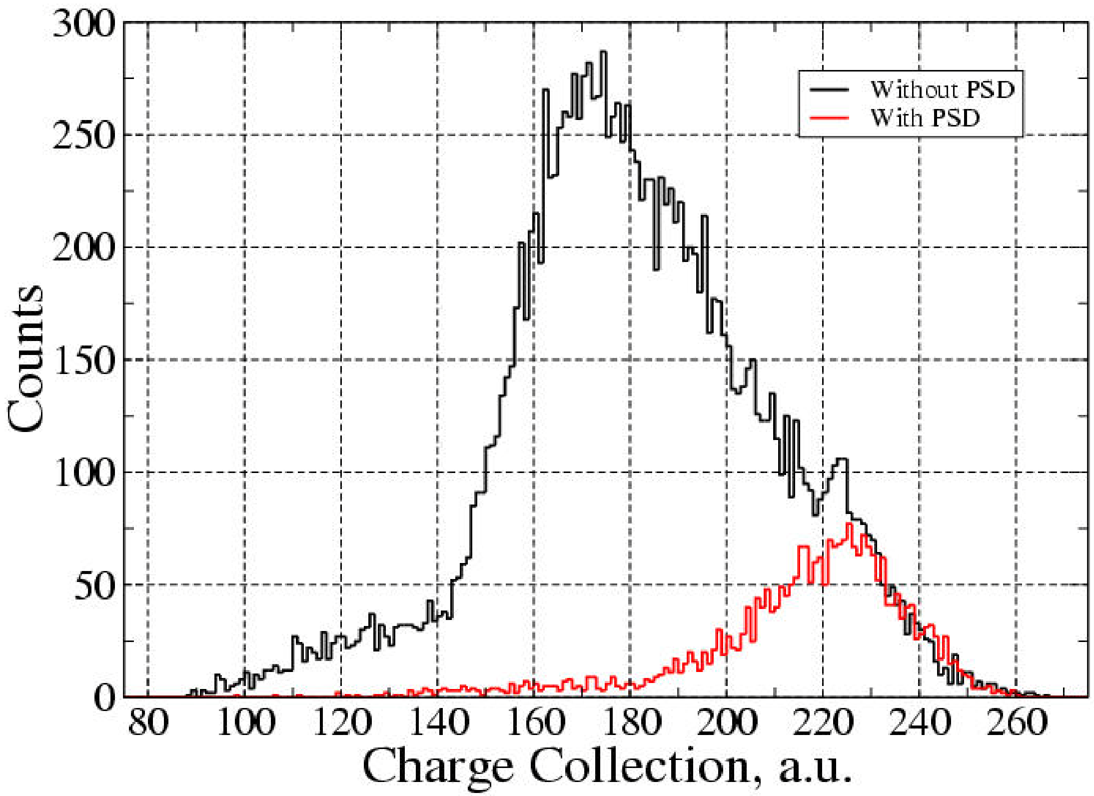

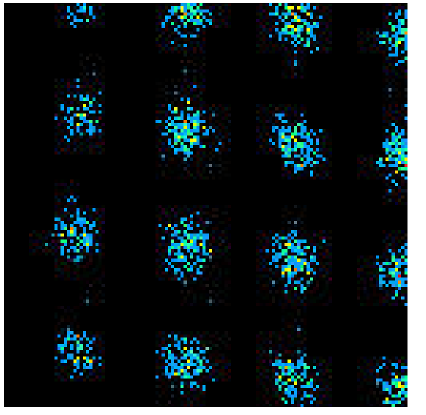

- Ion strikes outside the n^+ region are ignored
- Sensitive Volume 10x10x10 μm

- **Charge collection spectrum for 20 MeV C-12 source.**

SOI Microdosimetry-2 in neutron therapy : Harper hospital

ARDENT
Advanced Radiation Dosimetry European Network Training

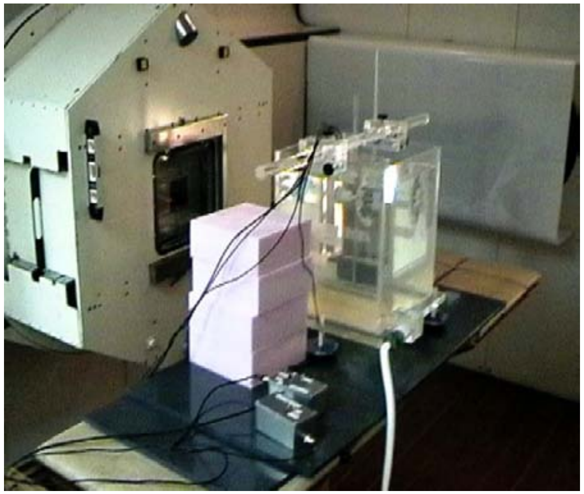

Neutron beam production:
- Superconducting cyclotron 40 μA
- Target: Be(d48.5)
- Average energy of neutrons:20MeV

- Good agreement with TEPC
- TEPC has an advantage in low LET region

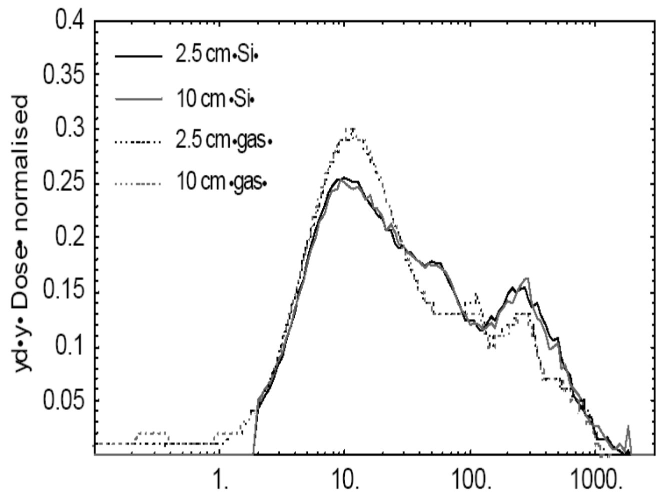

Central axis, different depth. Field 10x10 cm2

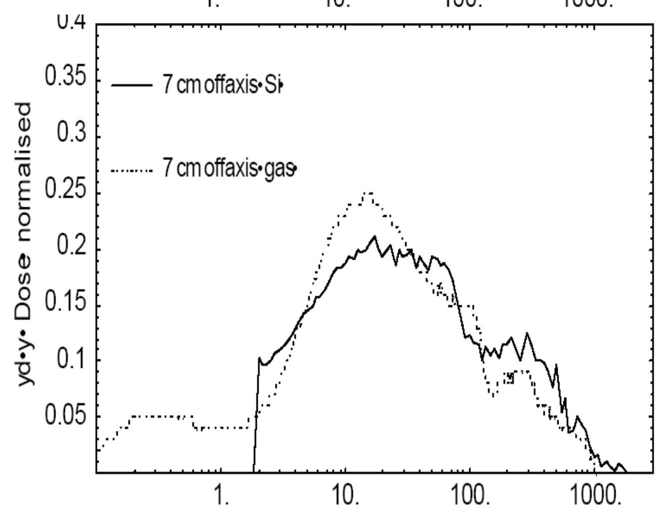

Lateral 7cm out of field at depth 10 cm

GEANT4 Simulation : Event Tallying in FNT

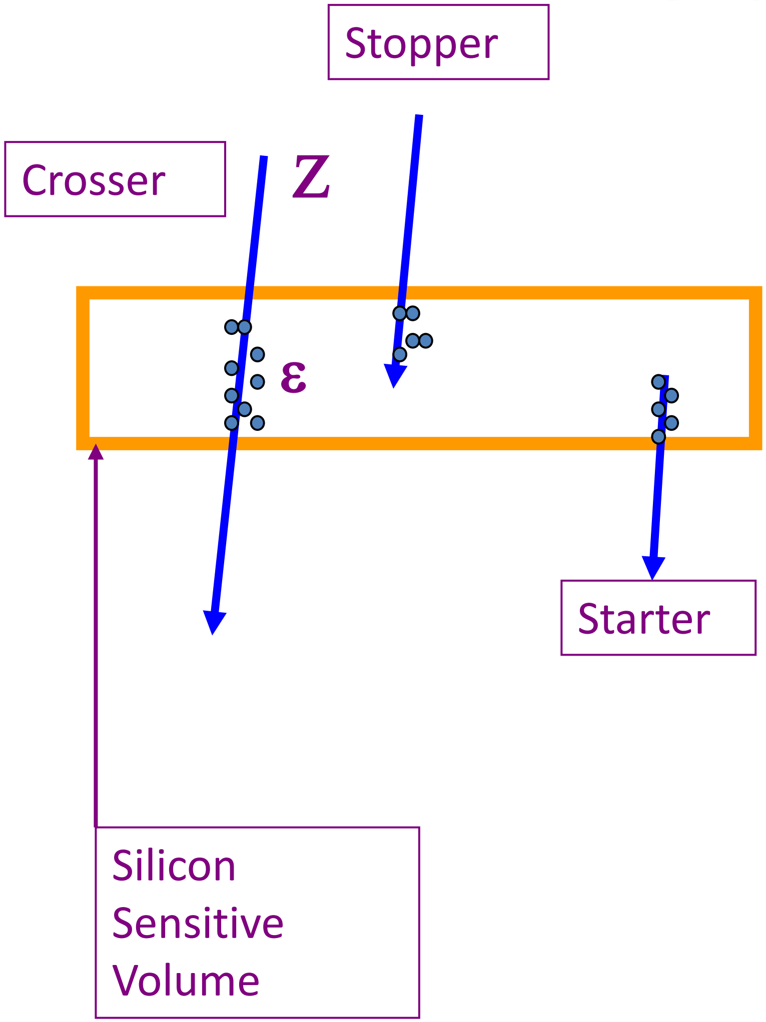

- For each event:
- Calculate ionisation energy loss, ε, in silicon sensitive volume and hence lineal energy event, y
- Record particle atomic number, Z
- Record whether particle crossed, started, or stopped in sensitive volume

Results and Discussion
Experiment vs. Simulation

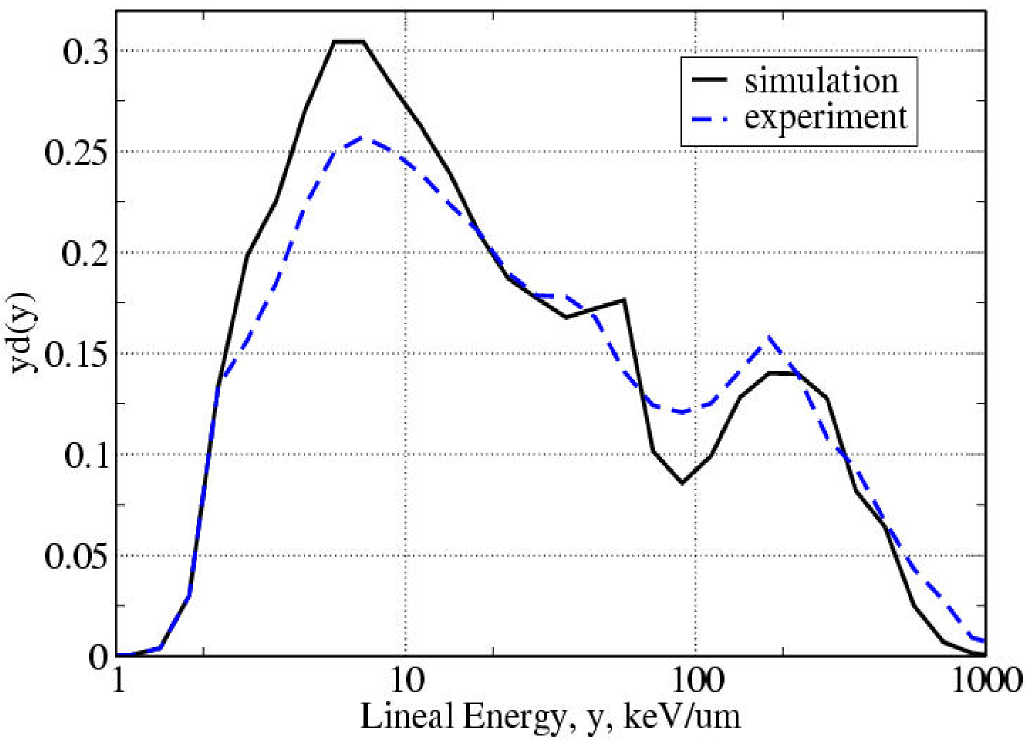

- Spectra share similar features
- Peak in region 1-100 keV/µm
- “shoulder” at ~70keV/ µm
- Peak in region 100-1000 keV/µm
- Spectra for each particle type to determine relative contribution

I. Cornelius , A.Rosenfeld , *IEEE Trans. on Nucl. Sci* , **51**, N3, 873-877, 2004

Results and Discussion: Z Components

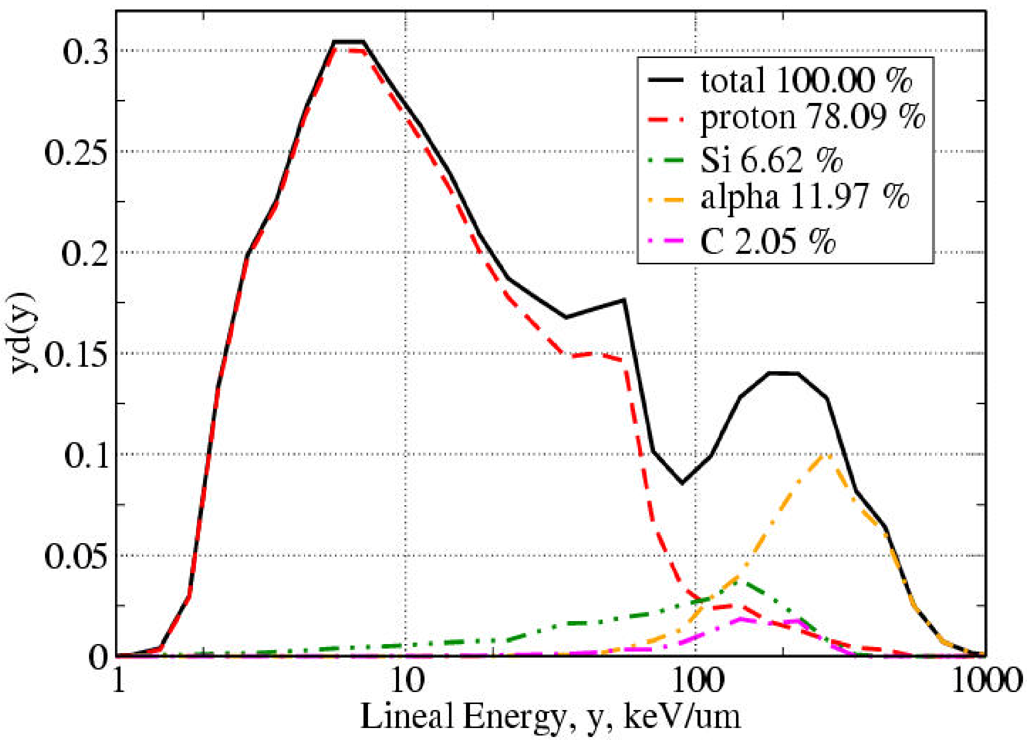

- Protons (elastic + inelastic) dominate 1-100 keV/μm peak
- 100-1000 keV/μm peak dominated by alphas
- Significant contribution by Si recoils
- Small contribution by Carbon
- Create spectra for starting, stopping, and crossing particles

Results and Discussion
Starters, Stoppers and Crossers

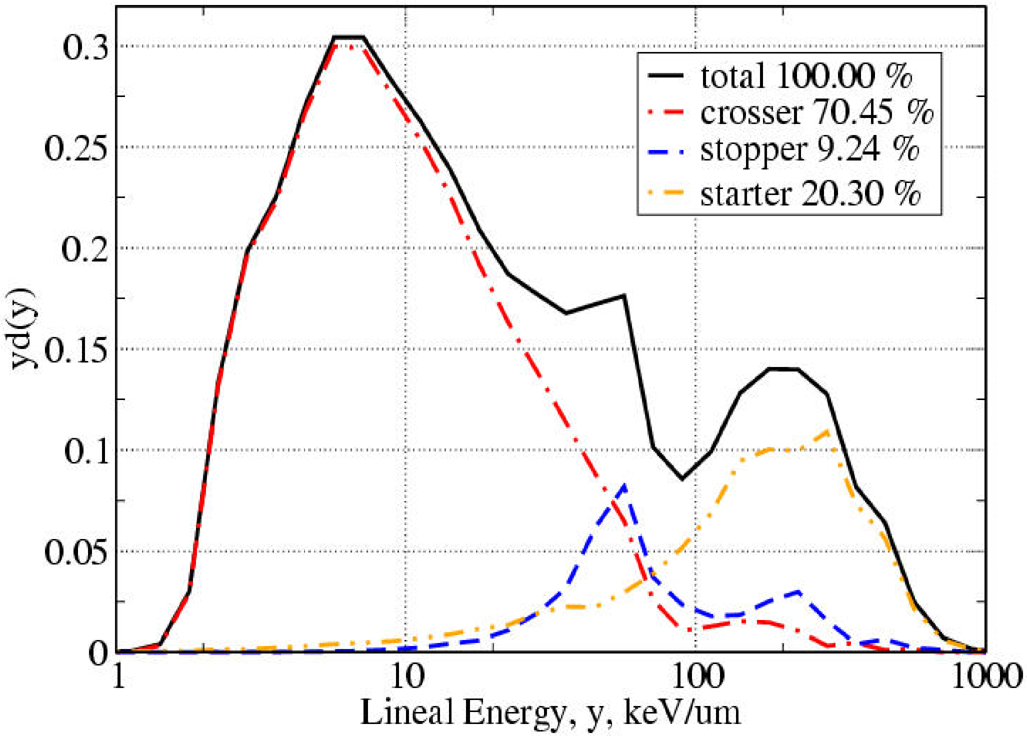

- Crossers dominate spectrum
- Stopping proton contribution significant. Source of “shoulder” at ~70keV/μm
- Starters (Si, Alphas) dominate 100-1000 keV/μm peak and contribute to approximately 20% of total dose

Microdosimertry on 100 MeV Proton Therapy

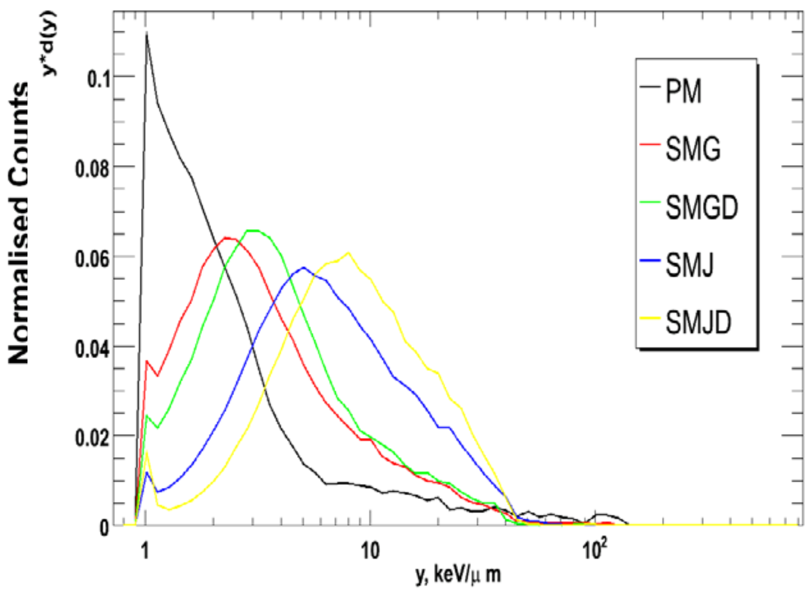

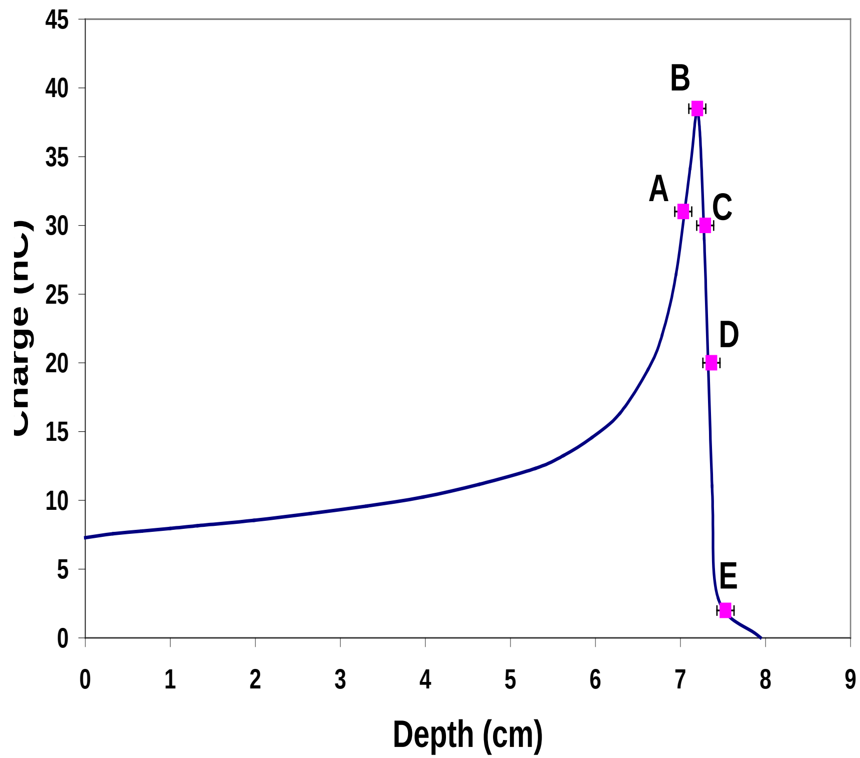

- Microdosimetric spectra from 10 mm SOI micro at consecutive positions in a Bragg Peak
- Possibility to estimate Q of the beam

For more details see: A Rosenfeld "Electronic Dosimetry in Radiotherapy", Rad. Meas., 41, 134-153, 2007

SOI Dose Equivalent Studies

- Determine the neutron field in free air as a function of distance from the treatment field edge.
- Assess the change in neutron dose as a function of depth within a polystyrene phantom.
- Assess the change in neutron dose as a function of distance from the treatment field edge at depth within a phantom.
- Assess the neutron dose along the central axis past the Bragg Peak

Experimental Setup

- The microdosimeter was moved parallel to the central beam axis 5cm from the field edge.
- The device was centred to the height of the central axis
- Incident protons of 225MeV were used.

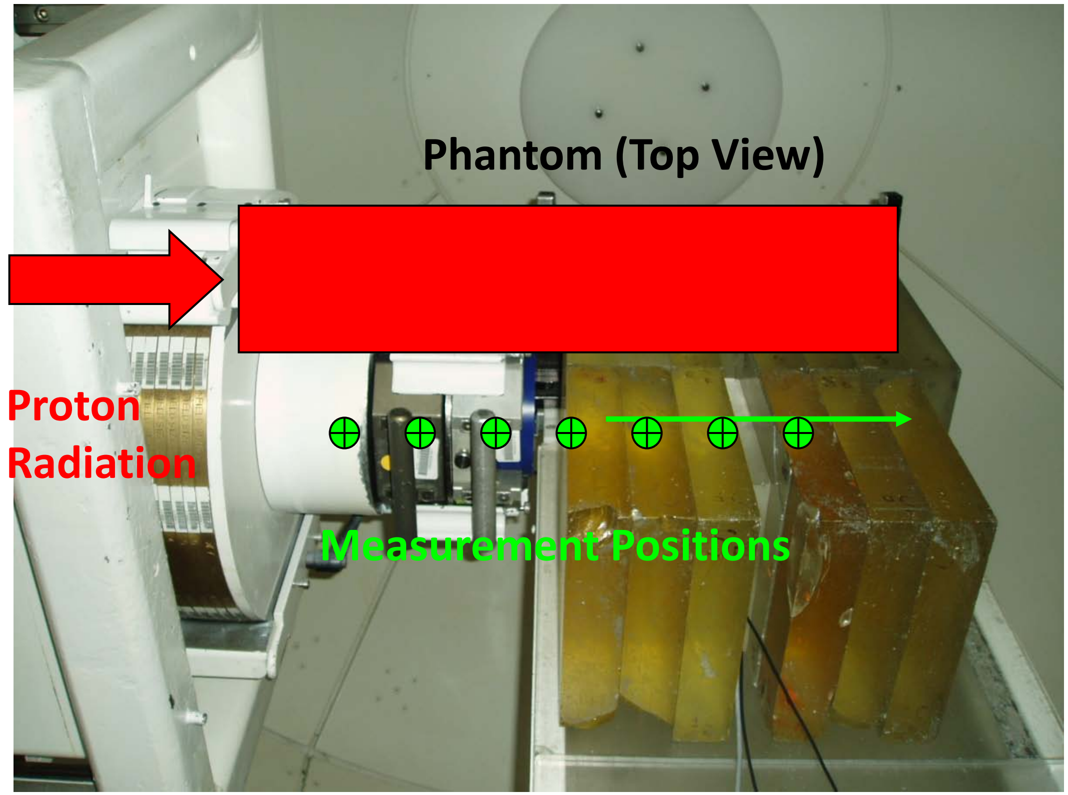

Results LLUMC

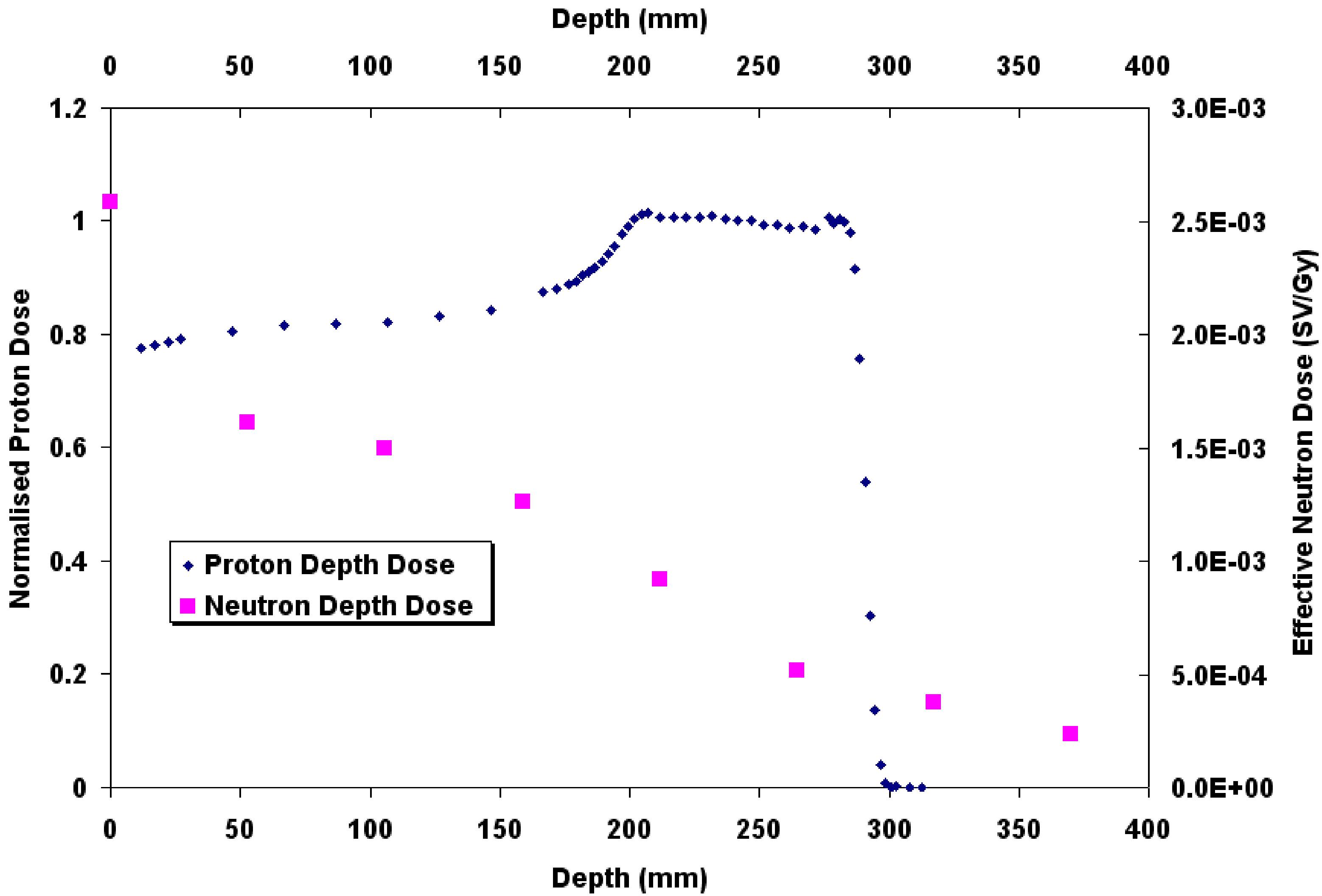

A. Wroe et al. *Med. Physics*, **34**(9), 3449-3455, 2007

Out of Field:Experimental Setup

- The microdosimeter was moved parallel to the central beam axis 5cm from the field edge.

- The device was centred to the height of the central axis
- Incident protons 28.5cm range in water were used.
- Modulation SOBP 10.4cm

Prostate field, double scattering technique, MGH

- Proton energy= 28.78 cm , modulation =10.38 cm
- Patient specific brass aperture 40 cm2, 7.5x7.0 cm2,
- Modification devices: lead foils fixed scatterer followed by a rotating wheel modulator , variable collimating jaws, lead second scatterer and patient aperture

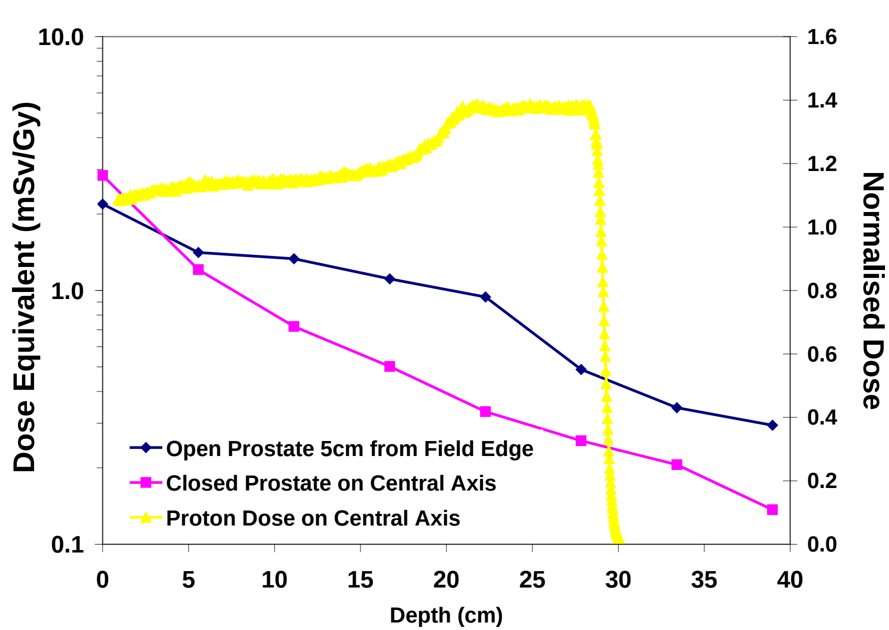

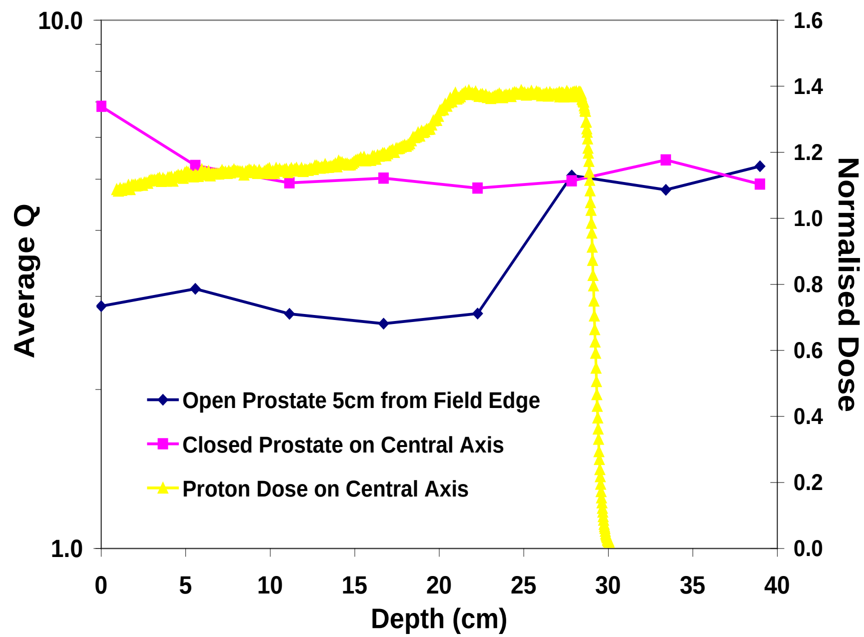

A.Wroe et al. *IJOROPB, 73, 306-313, 2009*

CENTRE FOR MEDICAL RADIATION PHYSICS
UNIVERSITY OF WOLLONGONG

Results:Dose Equivalent and Q

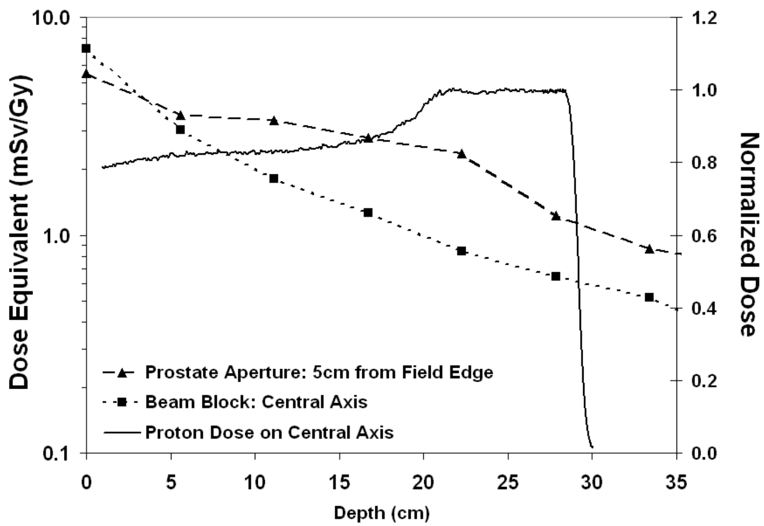

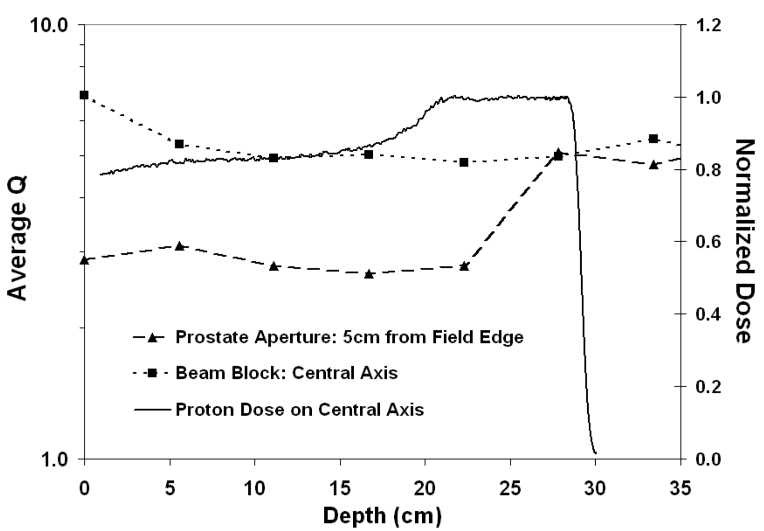

Scanning parallel to the beam at 5cm offset

- 0.9 mSv/Gy < $H_{aperture}$ < 5.5 mSv/Gy
- 0.5 mSv/Gy < H_{block} < 7.1 mSv/Gy
- $H_{aperture}$ has a different dependence on depth than H_{block}
- Scattered primary protons affects H and the determination of Q up to 22.3 cm depth
- Downstream of the Bragg peak, difference in H is due to neutron generated in the phantom

Heidelberg Heavy Ion Therapy facility

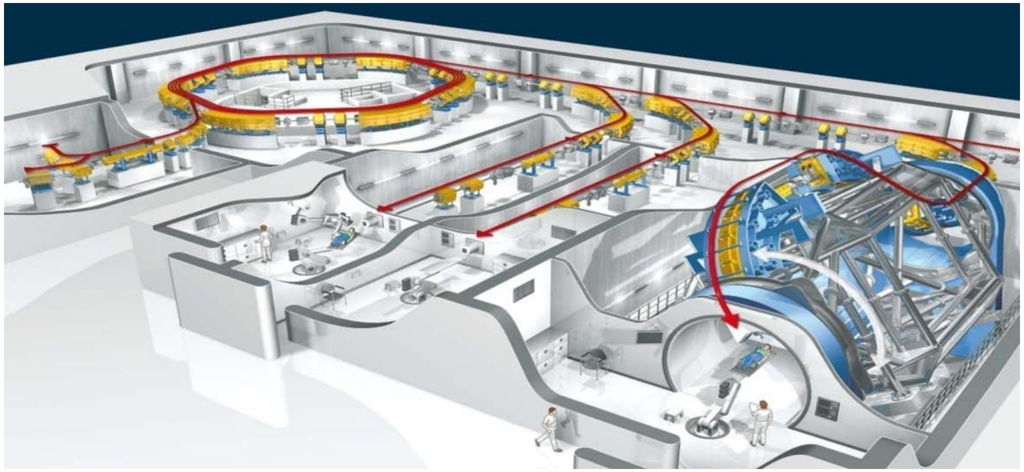

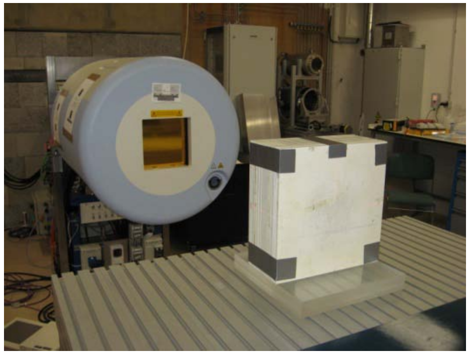

- Scanned carbon/proton with range in water
- Range 2-30 cm in 1 mm steps
- The beam can be delivered in 10 intensity steps
- Scanned field in the isocenter is 20 x 20 cm2
  FWHM of PSB 10mm

CMRP Collaboration with Heidelberg (Dr Maria Martisikova *et al*
and Milano Politechnik (Prof S. Agosteo ,Prof A. Fazzi *et al*)

Heidelberg HIT Experiment

- Two treatment plans were used
  - **5 x 5 x 5 cm2 cubic irradiation using a Spread Out Bragg Peak (SOBP)**
    - Energy range from 124.25 MeV/u to 202.95 MeV/u in 18 energy steps or slices (4.32 MeV/u steps in energy)
    - Pencil beam profile of 6.7 mm FWHM in diameter
  - **Actual brain tumour treatment plan**
    - Energy range from 142.09 MeV/u to 266.08 MeV/u for brain treatment

- Both treatment plans calibrated for dose in water
  - 1.2 cm diameter ionisation chambers used for verification of dose plan in a water phantom

- PMMA phantom used for the experiment
  - $\rho_{PMMA} = 1.17\ g/cm^3$
  - $\rho_{Water} = 1\ g/cm^3$
  - Therefore range in PMMA ~85.47% that of range in water

^{12}C Cubic SOBP Experimental Setup

- Cubic shaped dose profile
- Proximal edge (E_{min} =124.25 MeV/u) depth in water = 36.8 mm
- Distal edge (E_{max}=202.95 MeV/u) depth in water = 86.8 mm
- 5 x 5 x 5 cm^3 SOBP painted with PSB, FWHM 10mm
- Delivery of SOBP with constant dose in SOBP region
- y_D - Dose mean lineal energy (RBE) simulated based on measured microdosimetric spectra with SOI microdosimeters

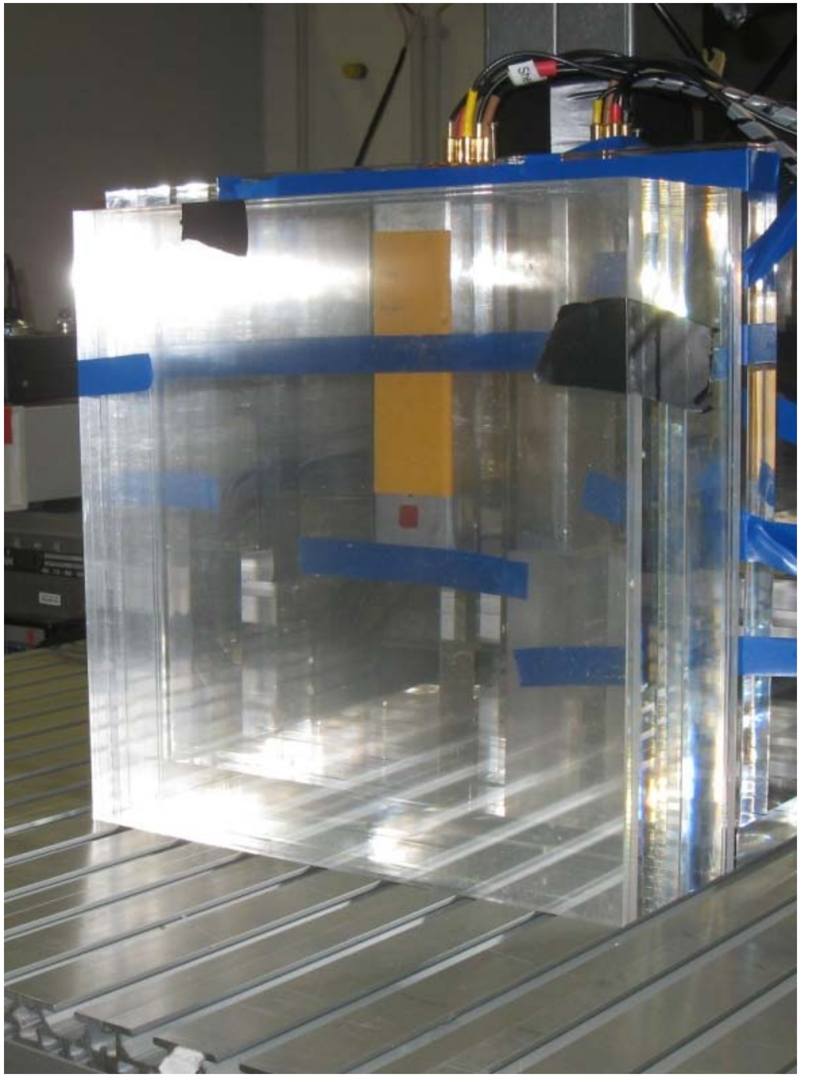

LEM treatment planning-dose cube

Parameters of LEM:

- Assumption that chordoma cells for the tumour (cube 5x5x5 cm3)

- Rest of phantom volume are brain cells

- Voxel size in TPS 1x1x1 mm3

- α and β parameters of LQM for both cells type were the same: α=0.1Gy-1 and β=0.05 Gy-2

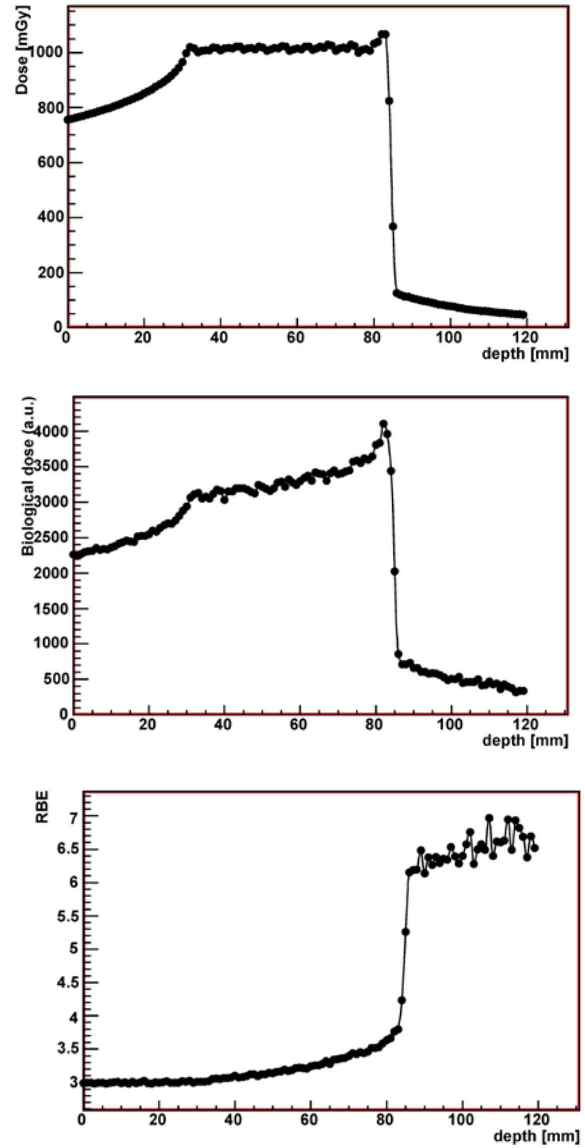

C -12 SPB :5 x 5 x 5 cm dose cube

Emin=142 MeV/u

Emax=266 MeV/u

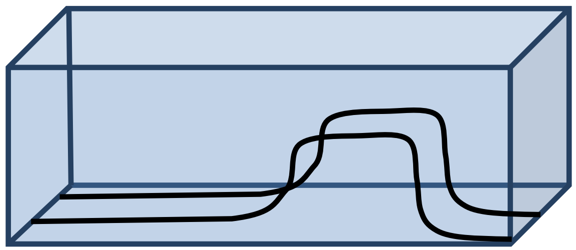

$\bar{y}_F$

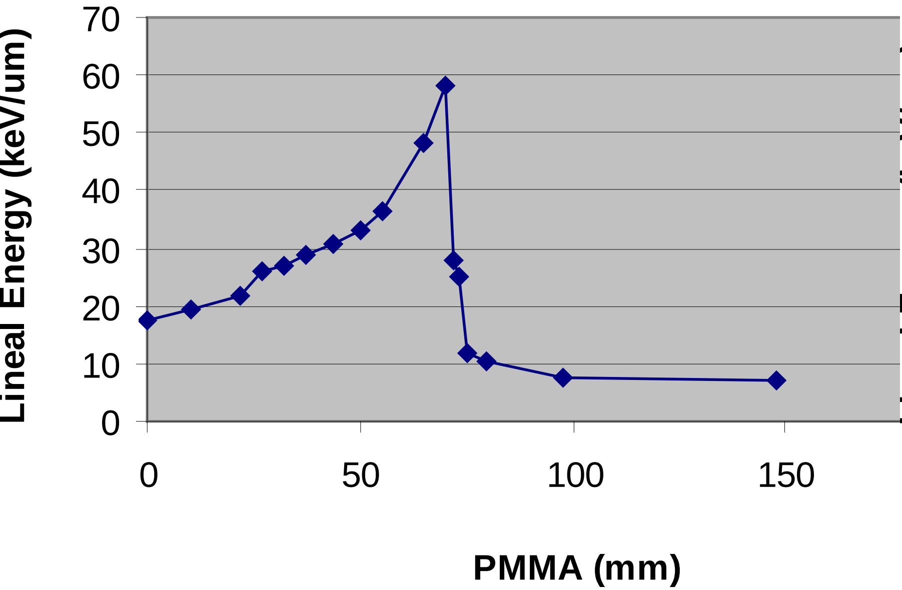

$\bar{y}_D$

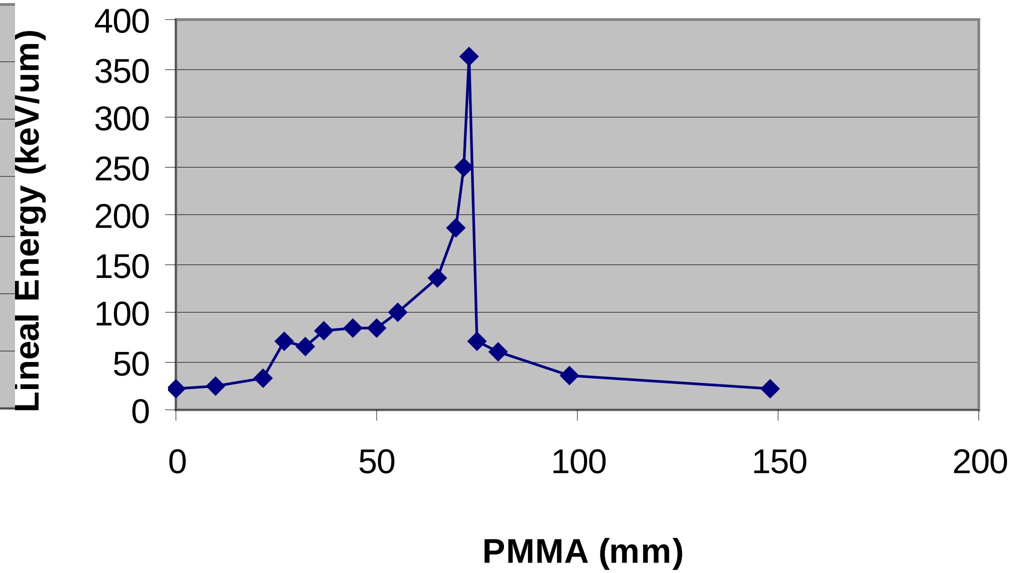

- •5x5x5 cm3 SOBP painted with PSB, FWHM 10mm
- •Delivery of SOBP of constant RBE in SOBP region (non constant absorbed dose)
- •Yf-frequency average lineal energy
- •Yd-dose average lineal energy (RBE)

C -12 SPB :5 x 5 x 5 cm dose cube

Microdosimetric spectra was collected along the Spread Out Bragg Peak.

Modification of SOI microdosimetric spectra with depth

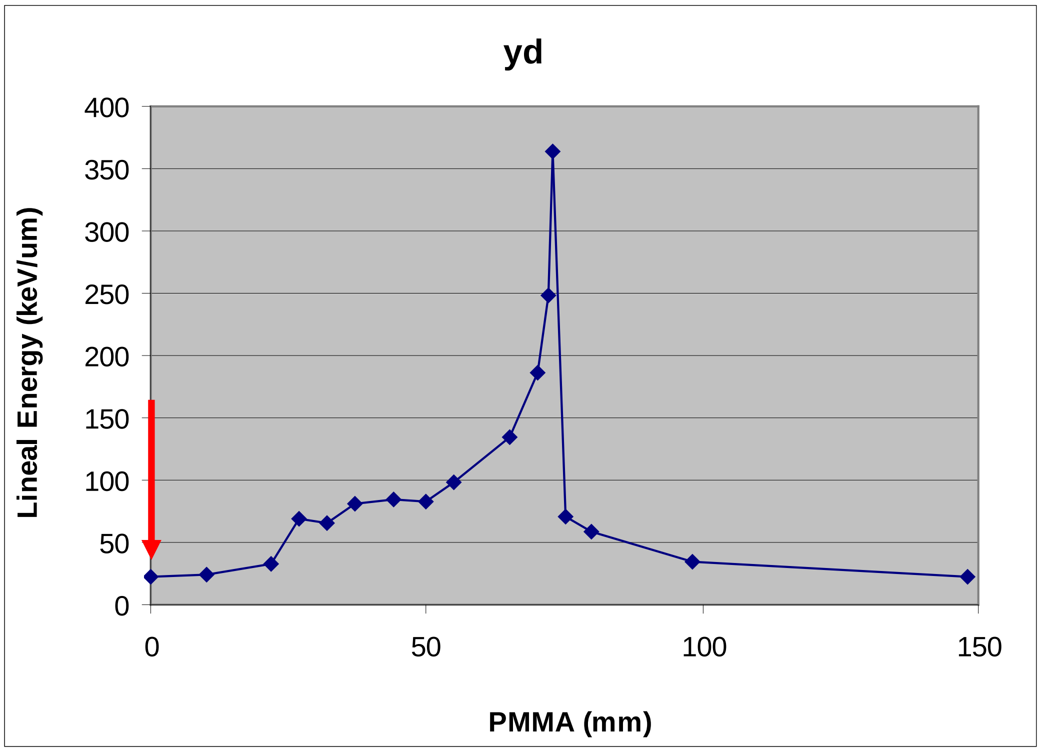

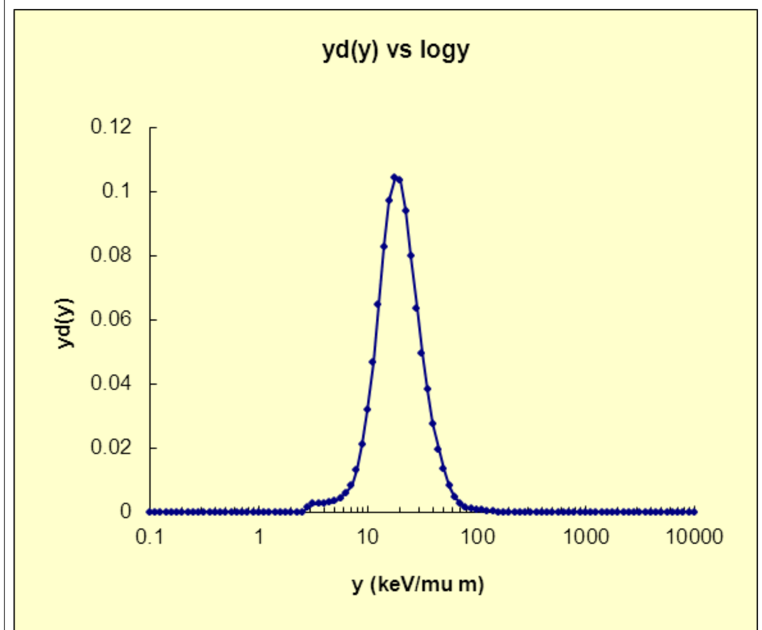

C -12 SPB :5 x 5 x 5 cm3 dose cube

Modification of SOI microdosimetric spectra with depth

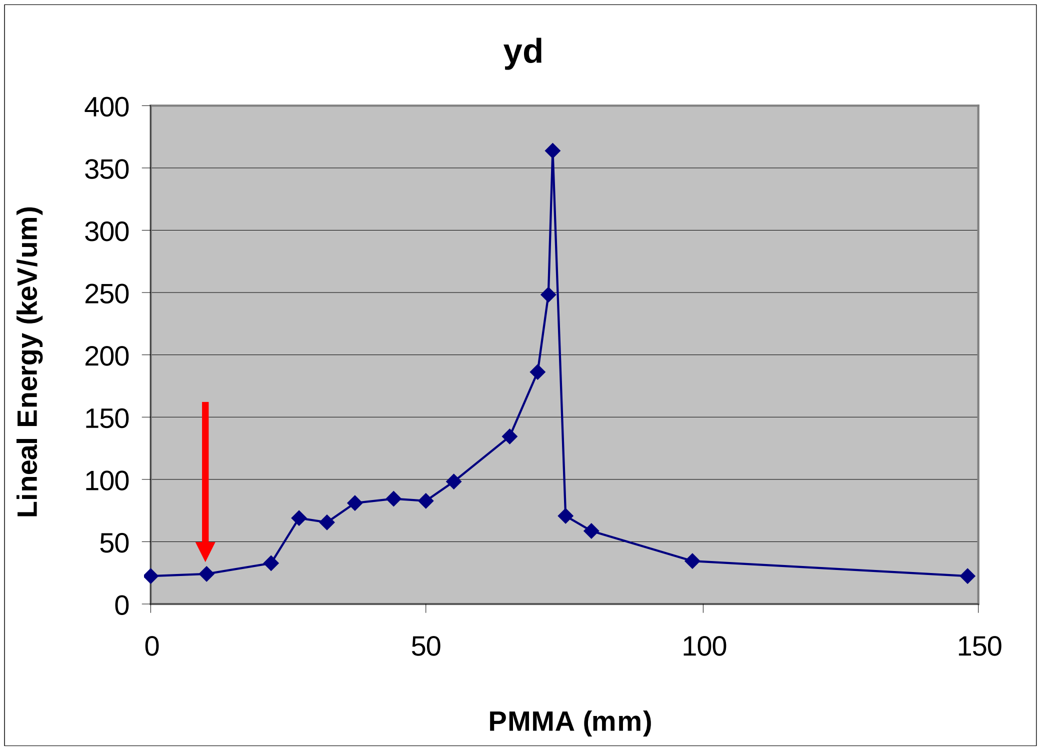

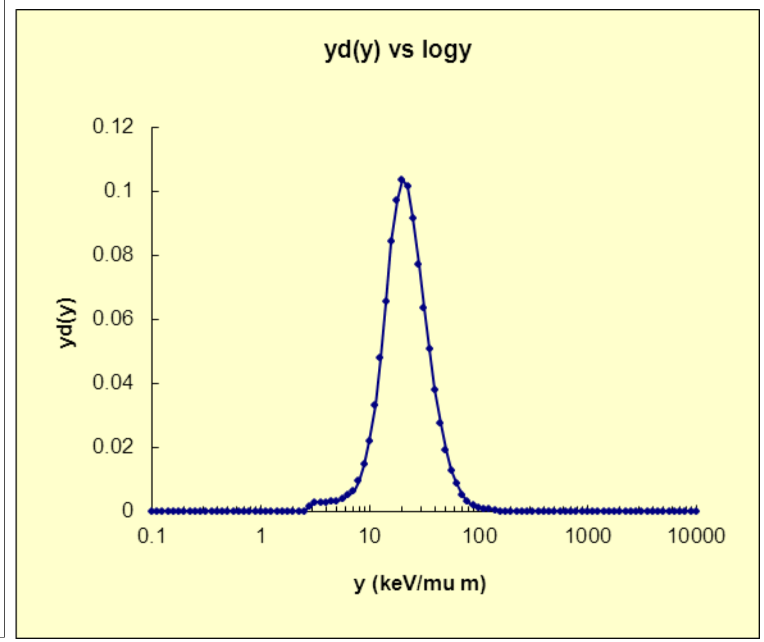

C -12 SPB :5 x 5 x 5 cm3 dose cube

Modification of SOI microdosimetric spectra with depth

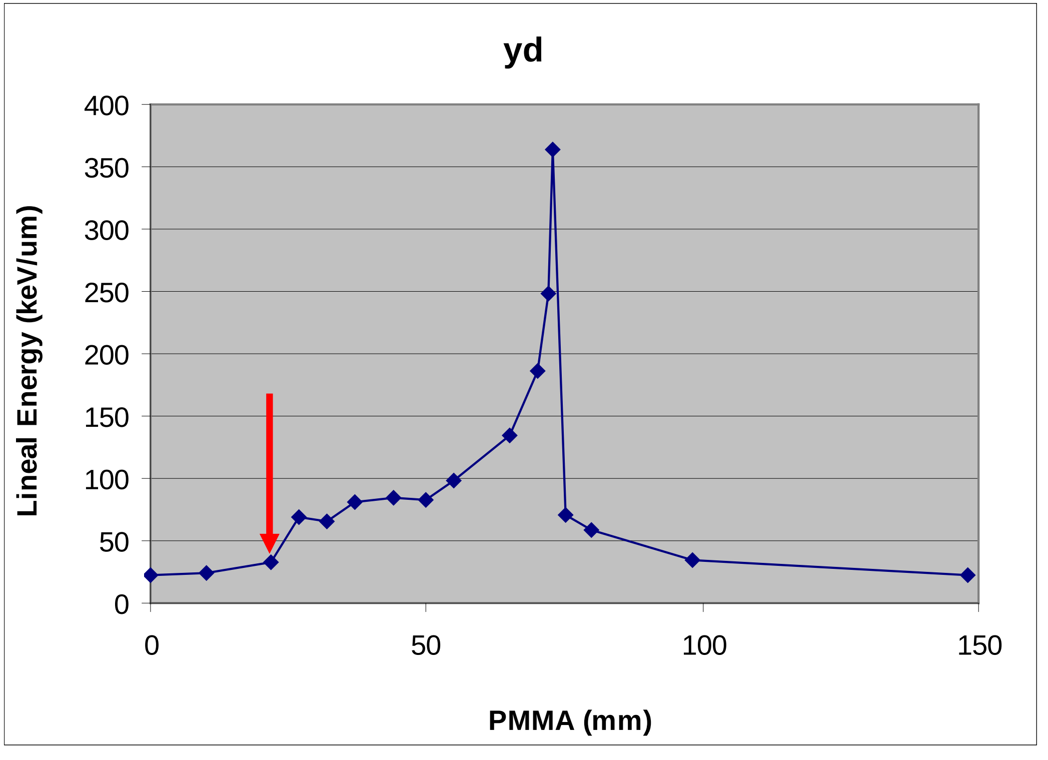

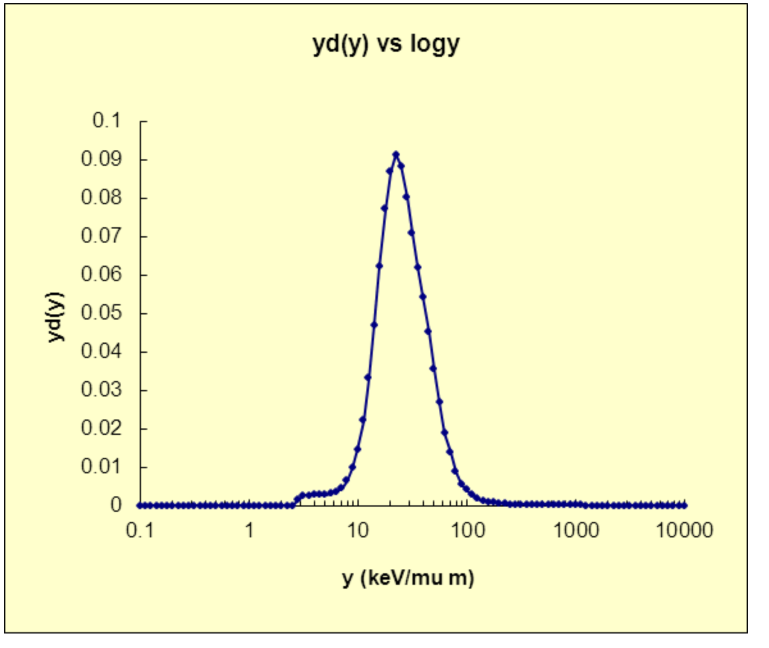

C -12 SPB :5 x 5 x 5 cm3 dose cube

Modification of SOI microdosimetric spectra with depth

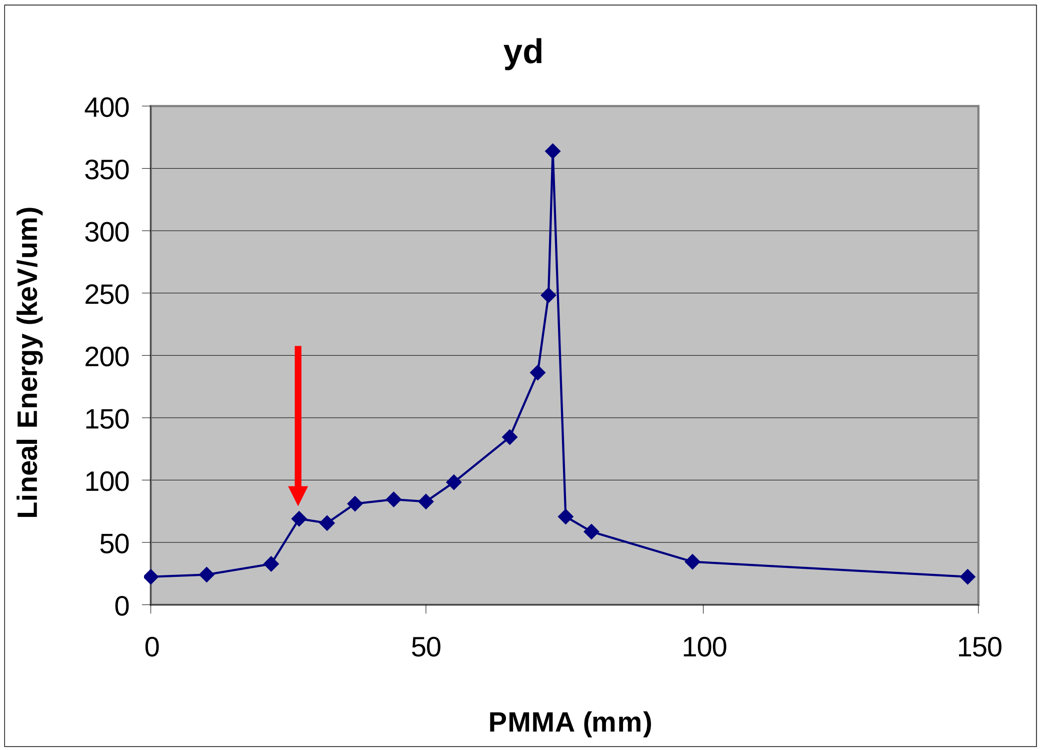

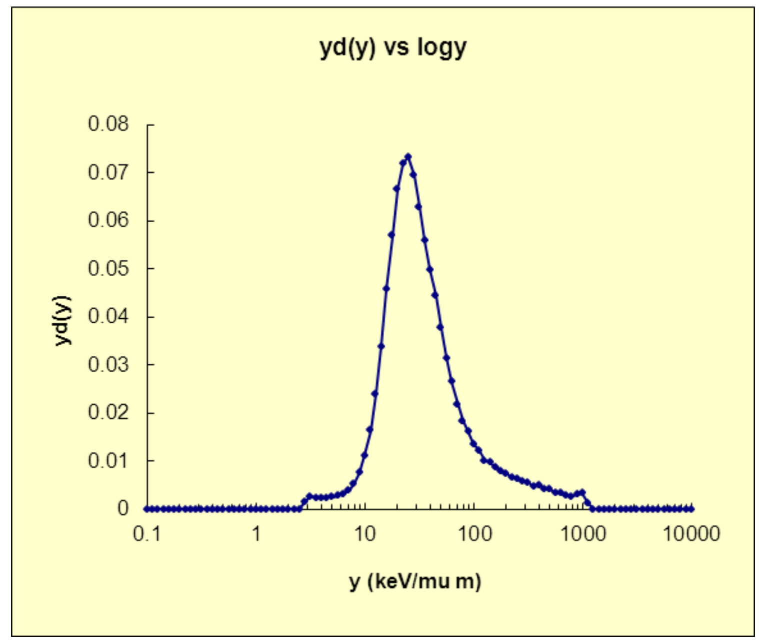

C -12 SPB :5 x 5 x 5 cm3 dose cube

Modification of SOI microdosimetric spectra with depth

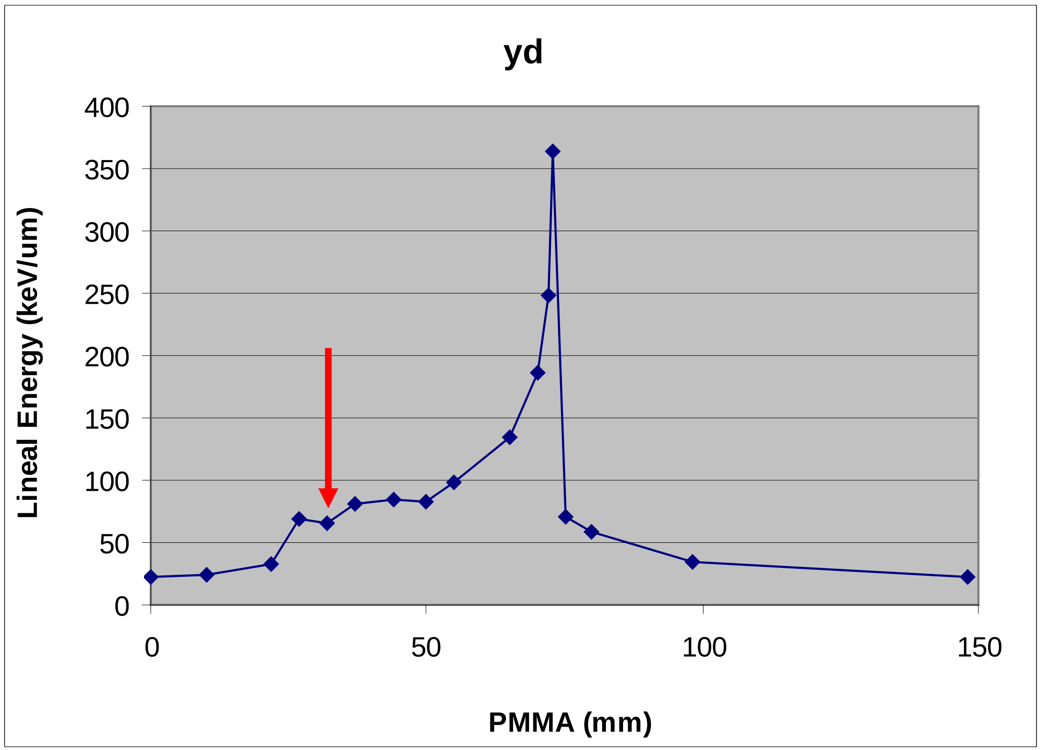

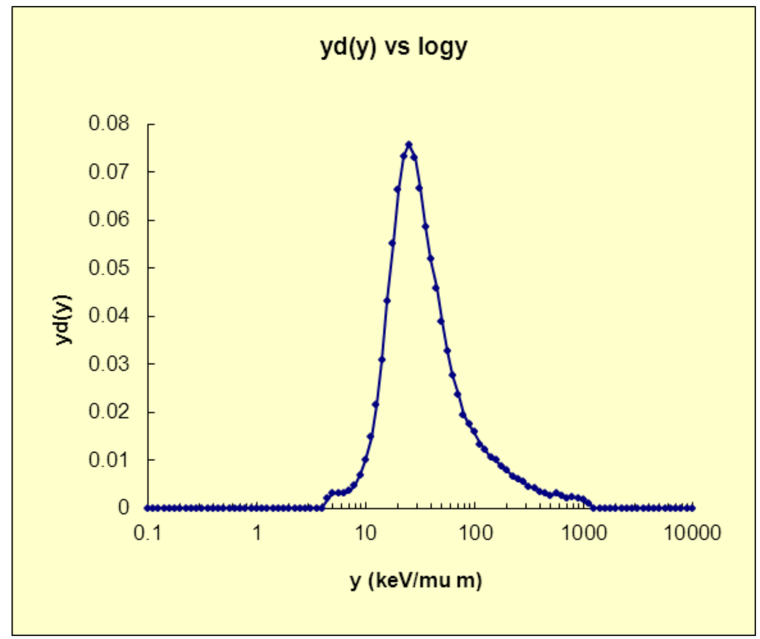

C -12 SPB :5 x 5 x 5 cm3 dose cube

Modification of SOI microdosimetric spectra with depth

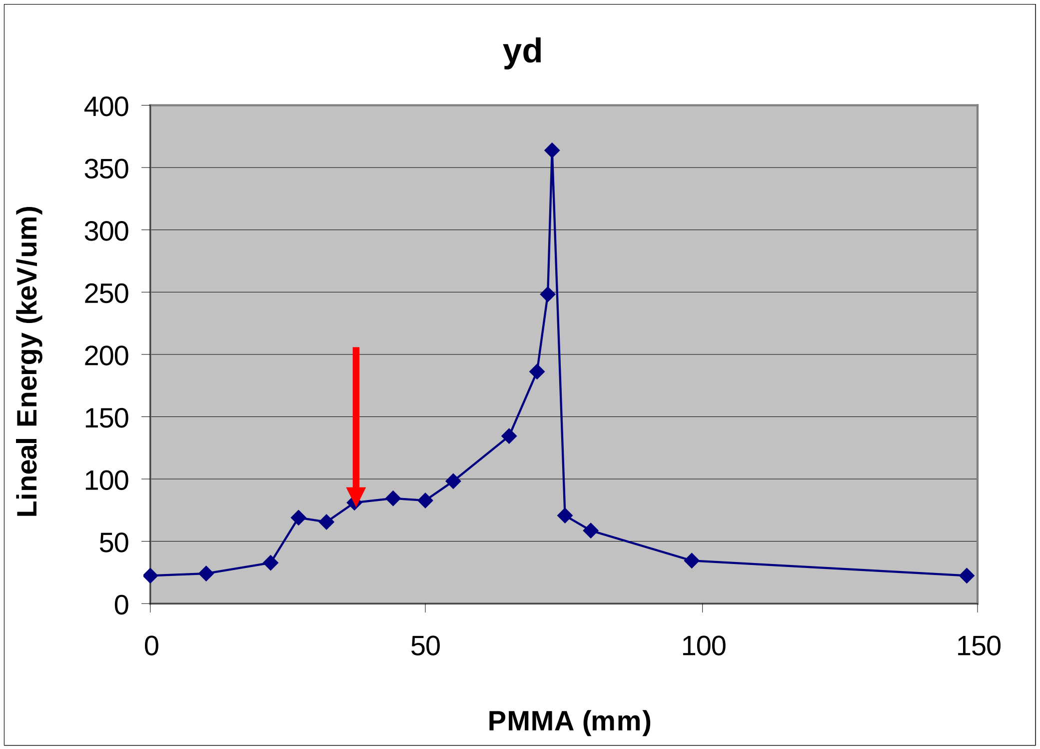

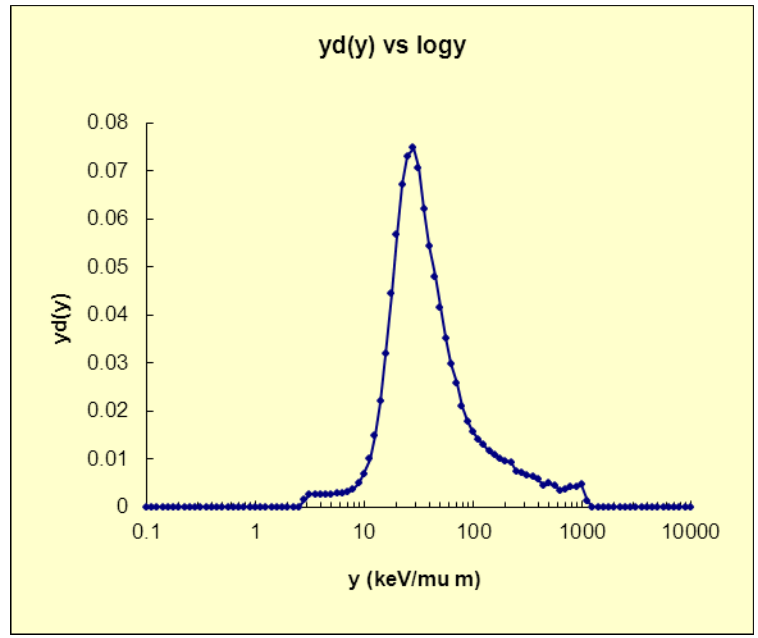

C -12 SPB :5 x 5 x 5 cm3 dose cube

Modification of SOI microdosimetric spectra with depth

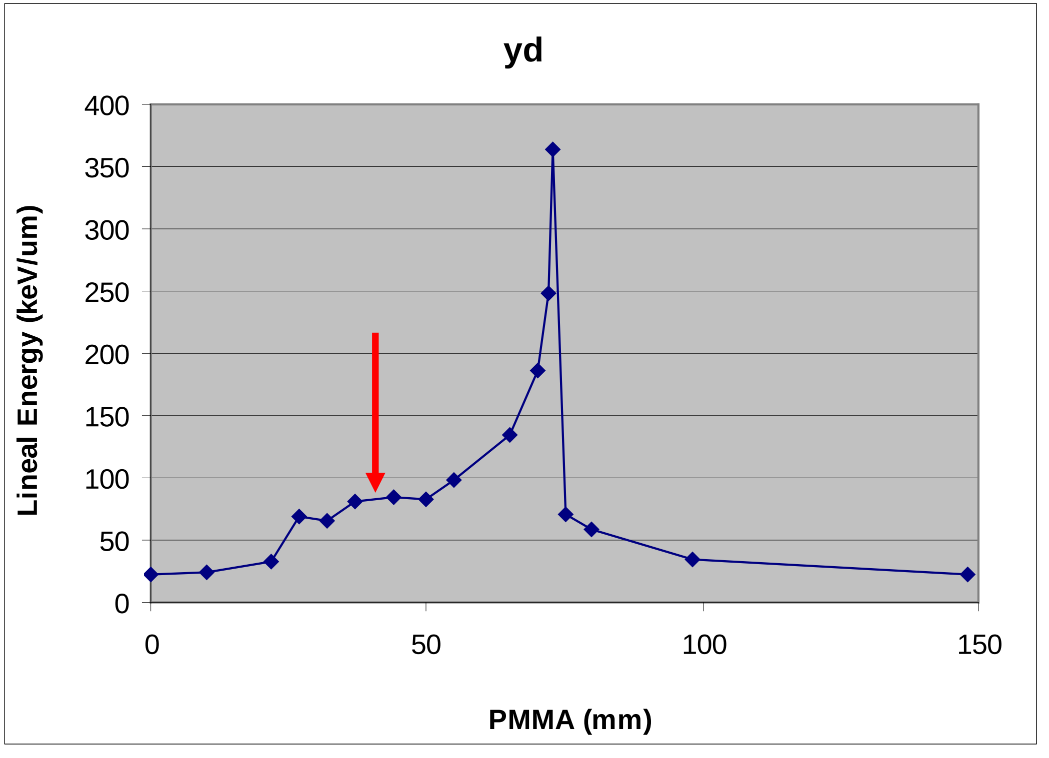

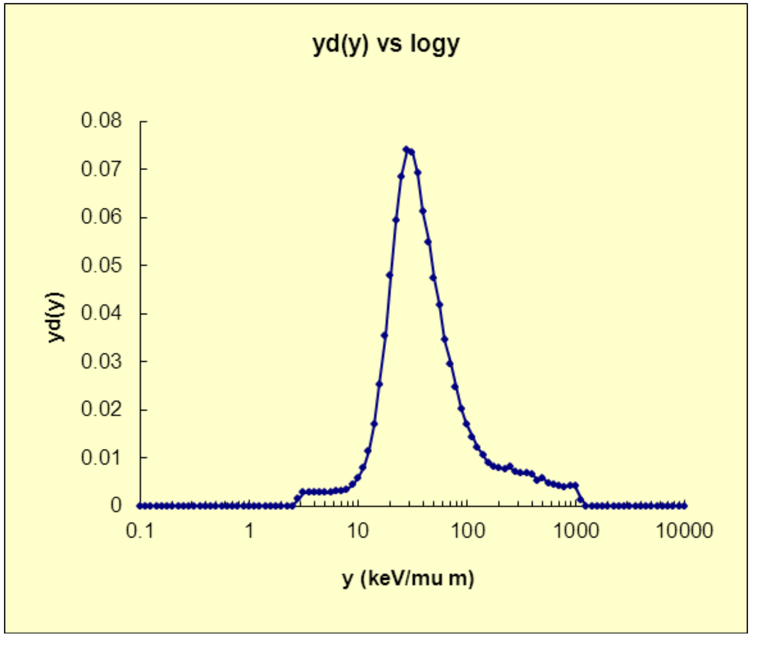

C -12 SPB :5 x 5 x 5 cm3 dose cube

Modification of SOI microdosimetric spectra with depth

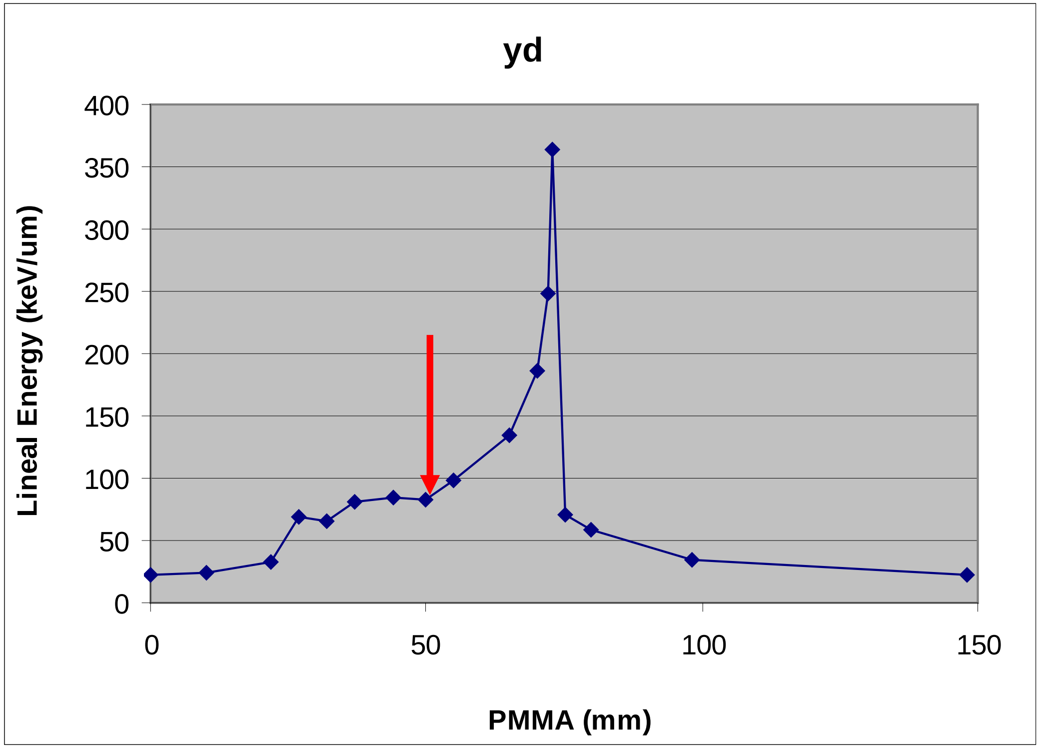

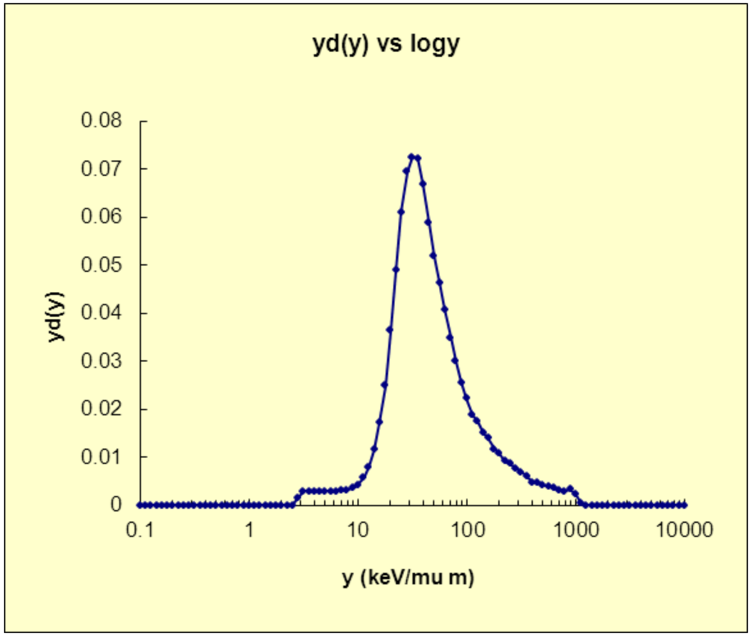

C -12 SPB :5 x 5 x 5 cm3 dose cube

Modification of SOI microdosimetric spectra with depth

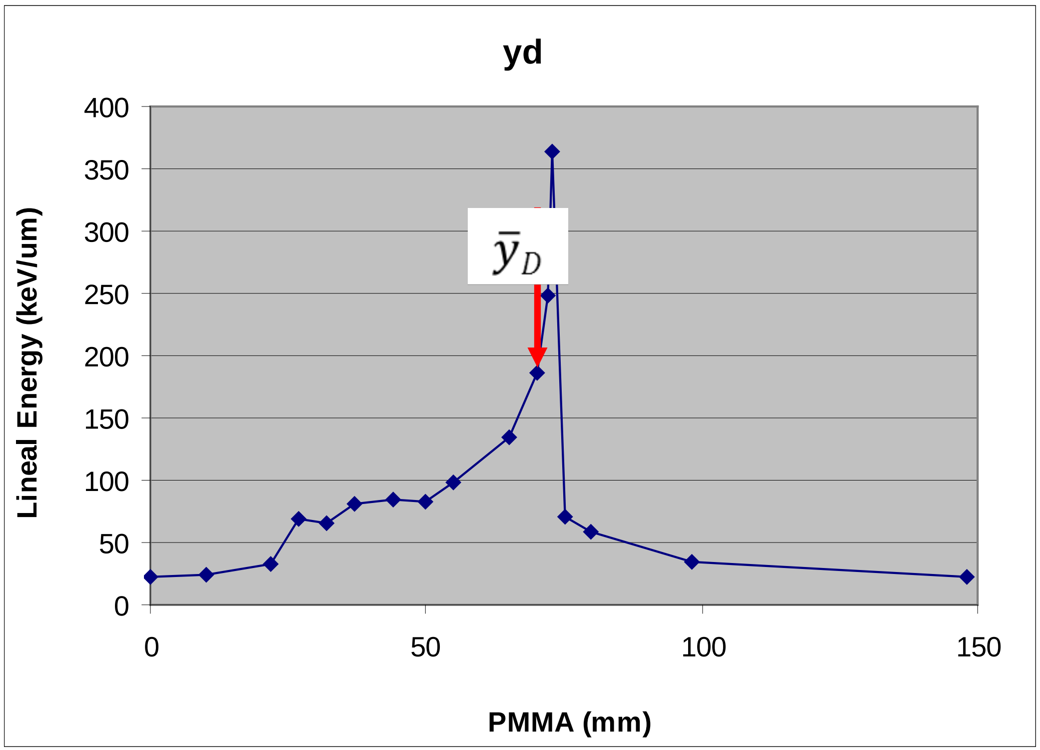

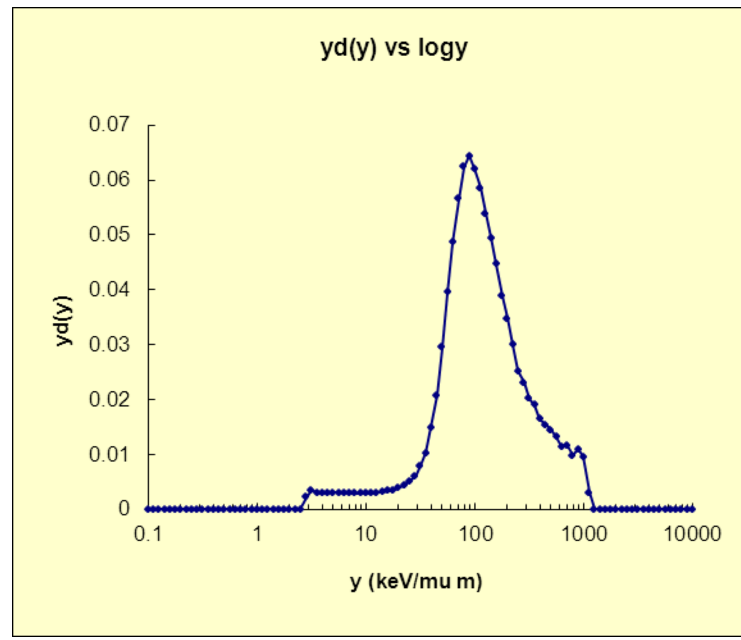

C -12 SPB :5 x 5 x 5 cm3 dose cube

Modification of SOI microdosimetric spectra with depth

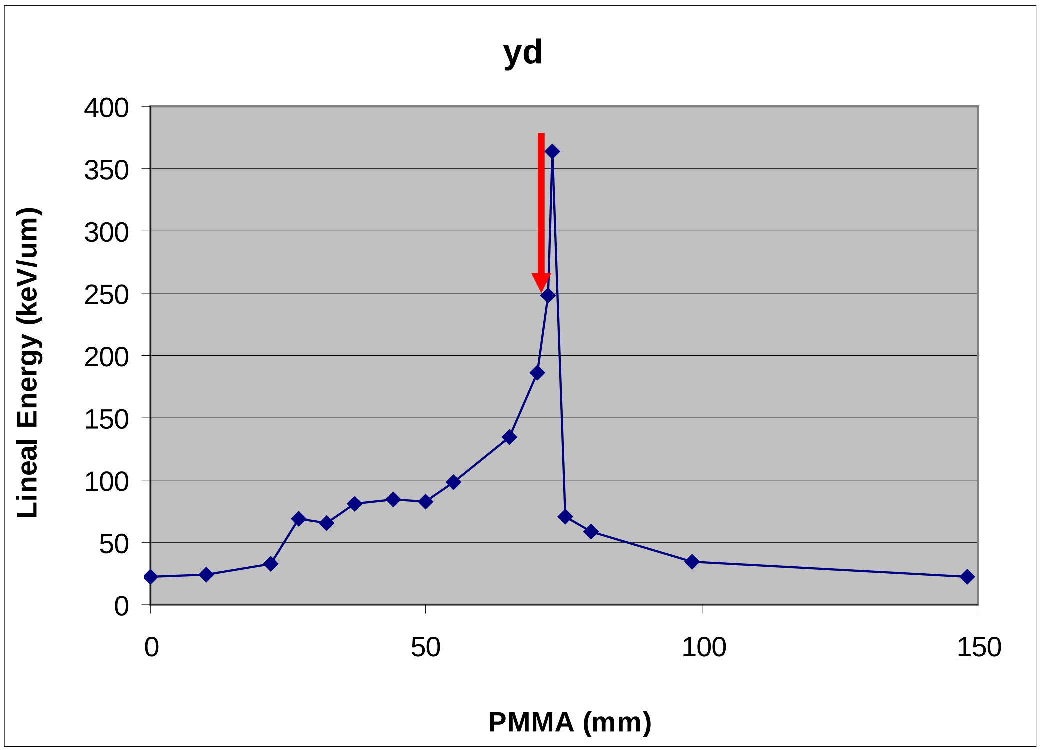

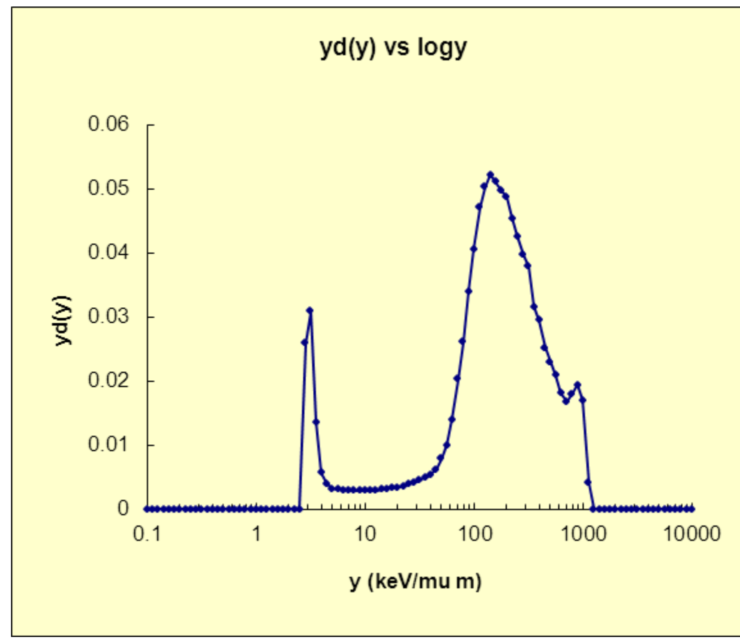

C -12 SPB :5 x 5 x 5 cm3 dose cube

Modification of SOI microdosimetric spectra with depth

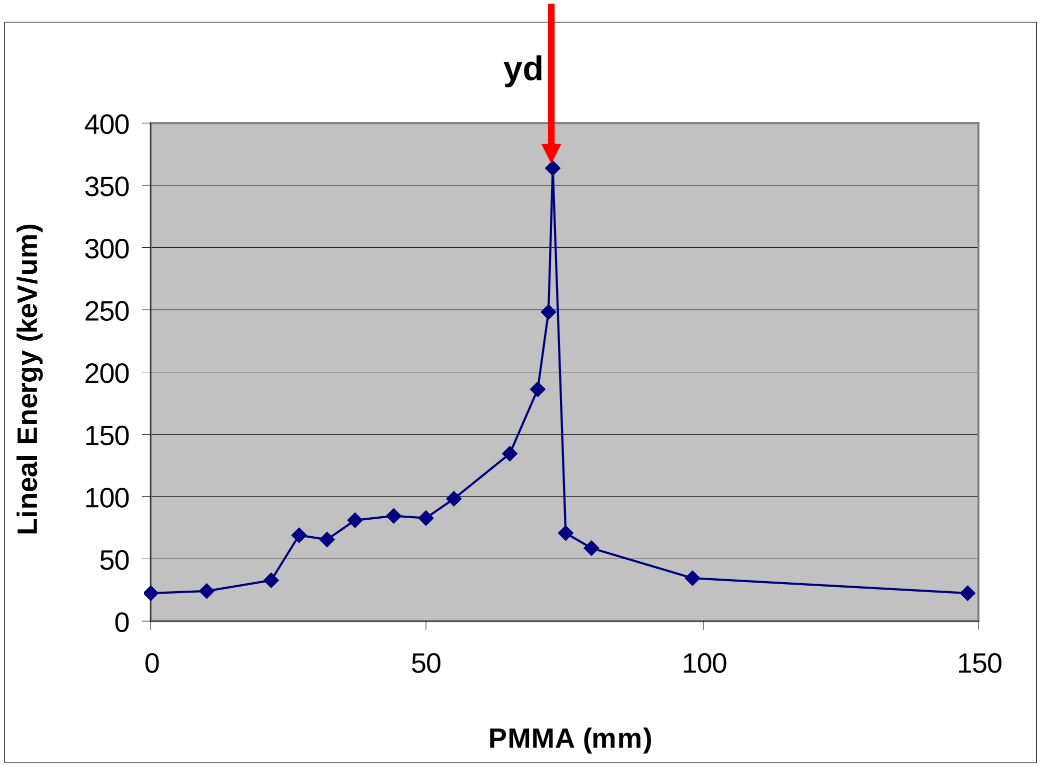

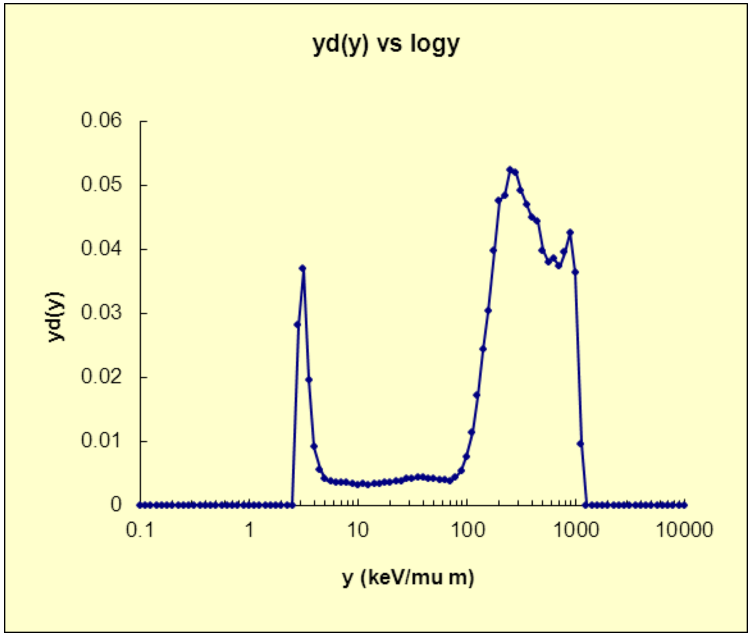

C -12 SPB :5 x 5 x 5 cm3 dose cube

Modification of SOI microdosimetric spectra with depth

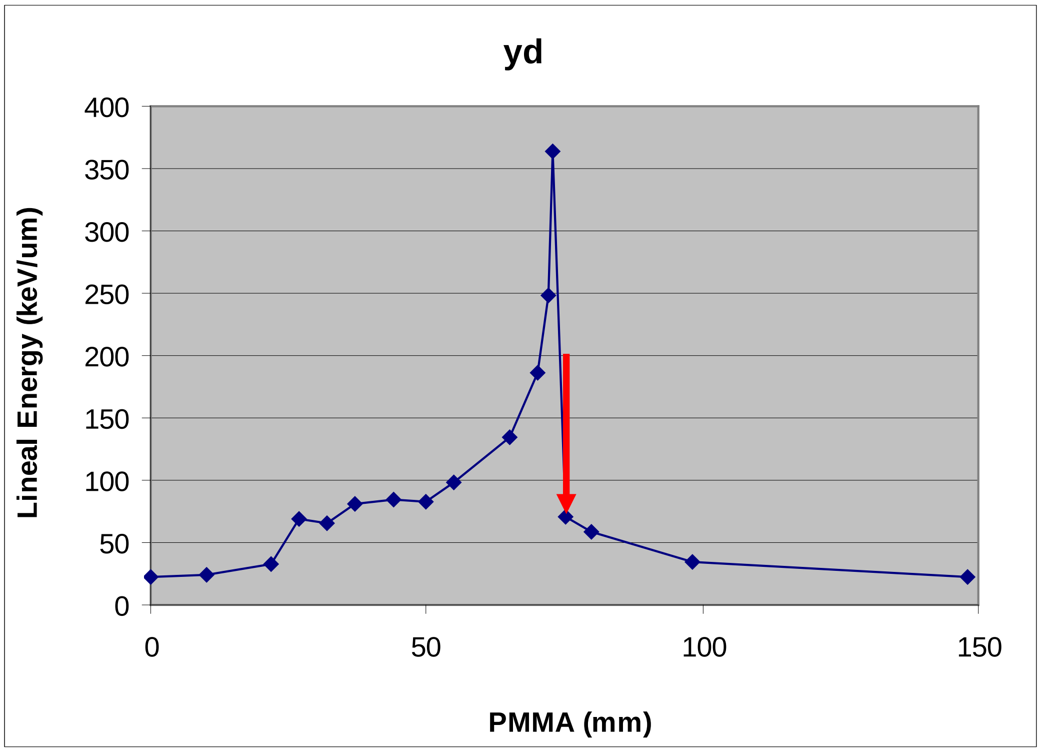

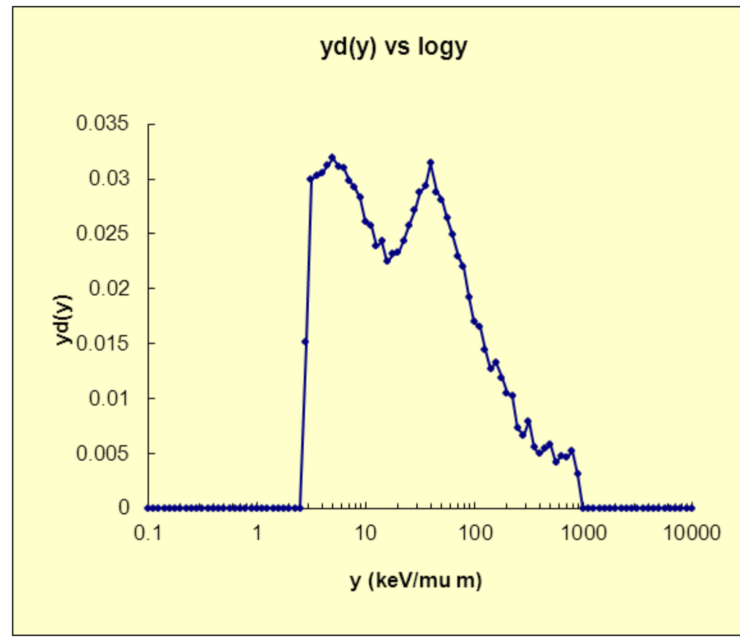

C -12 SPB :5 x 5 x 5 cm3 dose cube

Modification of SOI microdosimetric spectra with depth

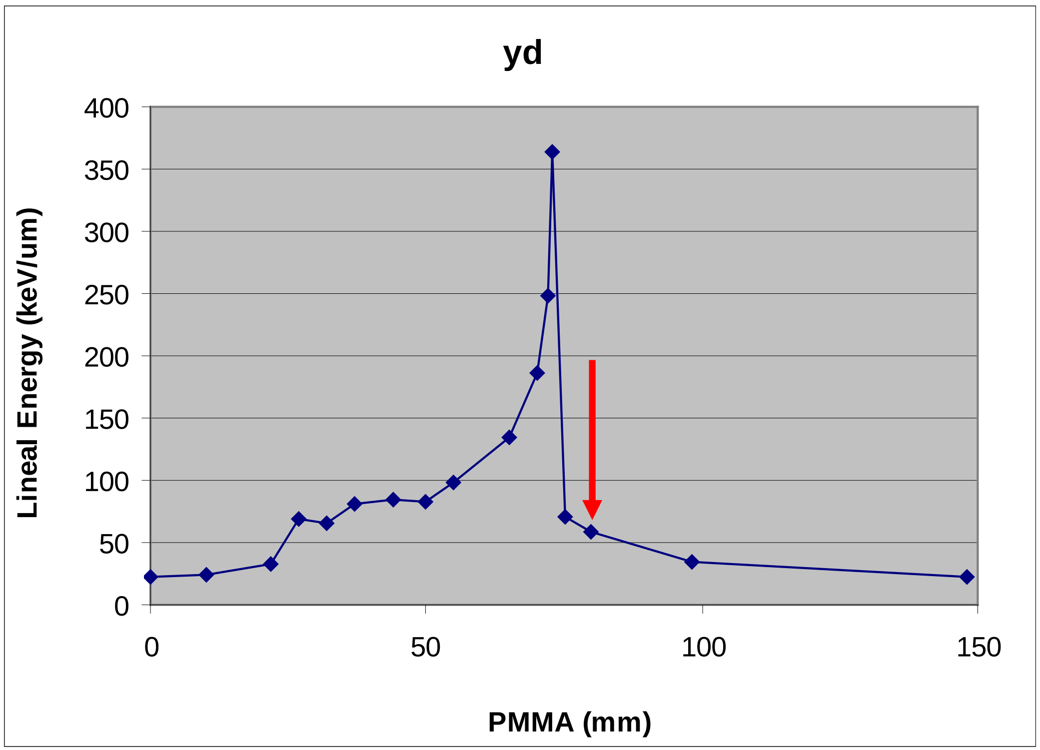

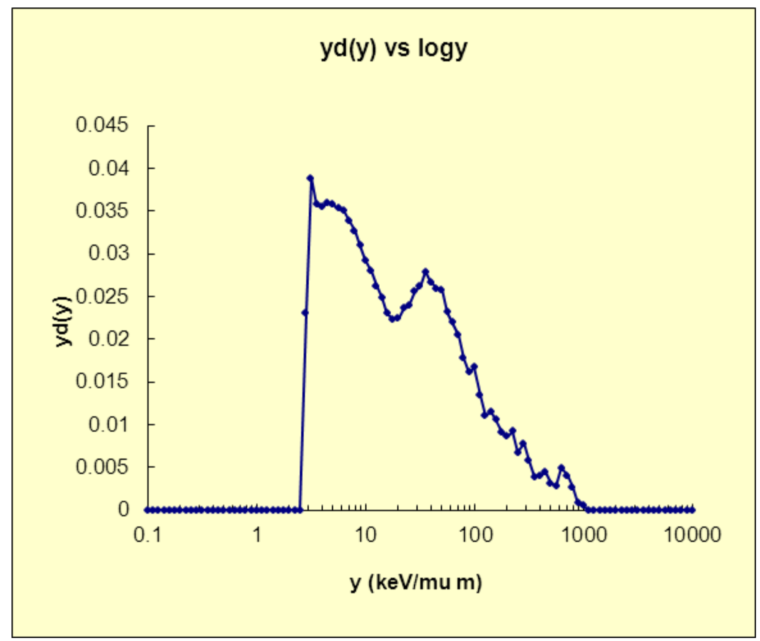

CENTRE FOR MEDICAL RADIATION PHYSICS
UNIVERSITY OF WOLLONGONG

C -12 SPB :5 x 5 x 5 cm3 dose cube

Modification of SOI microdosimetric spectra with depth

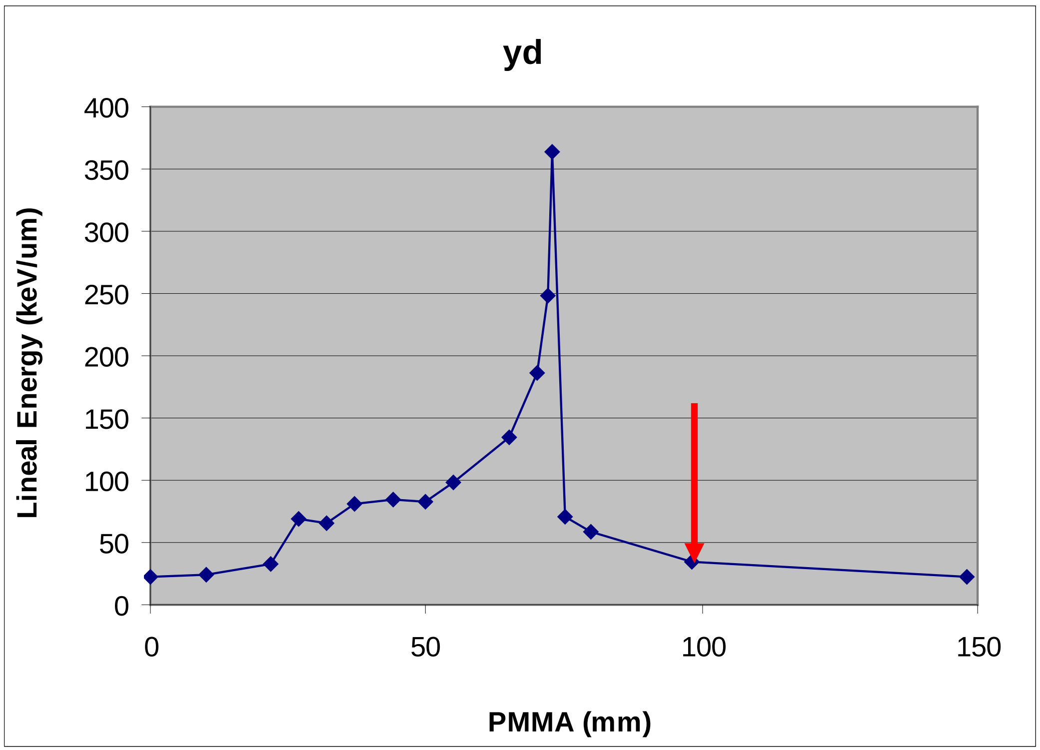

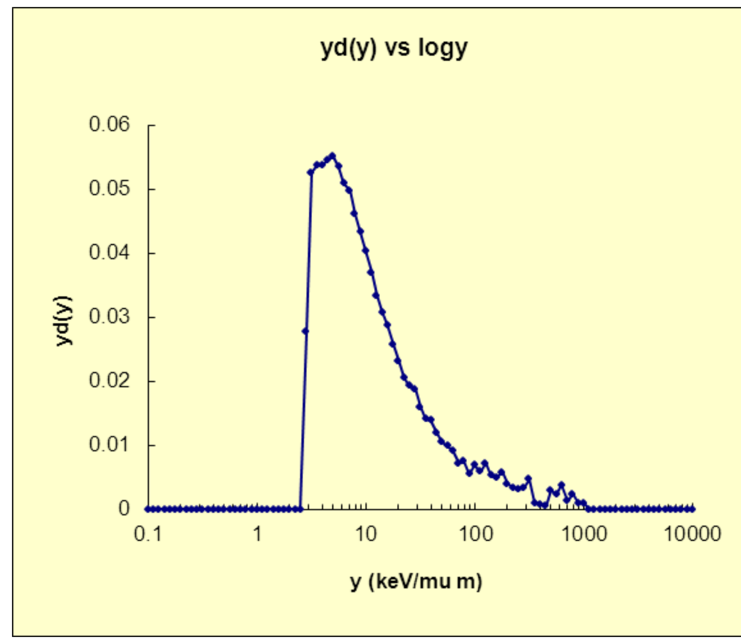

C -12 SPB :5 x 5 x 5 cm3 dose cube

Modification of SOI microdosimetric spectra with depth

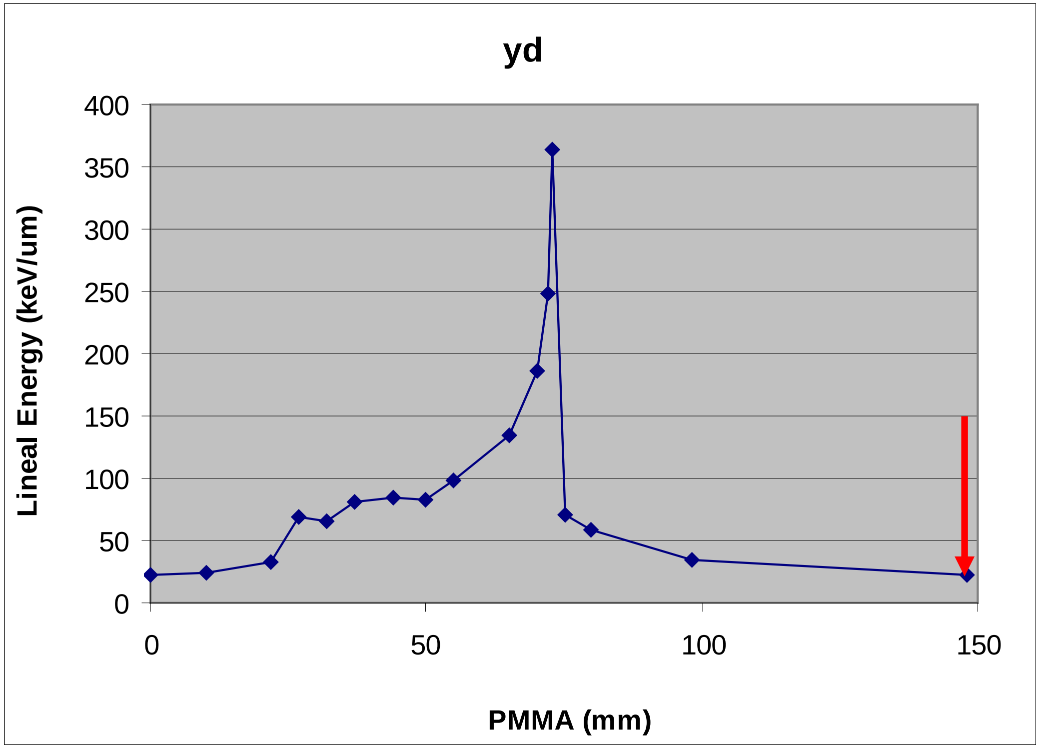

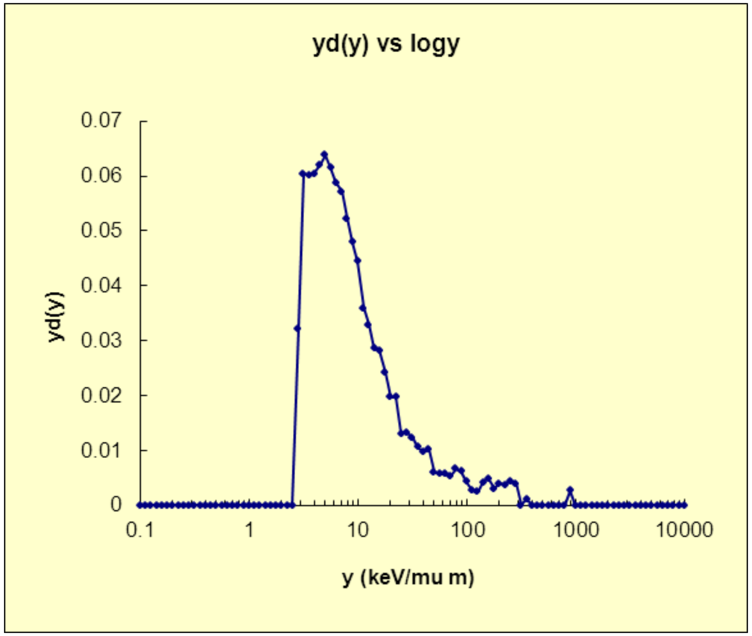

SOBP: SOI Microdosimetry summary

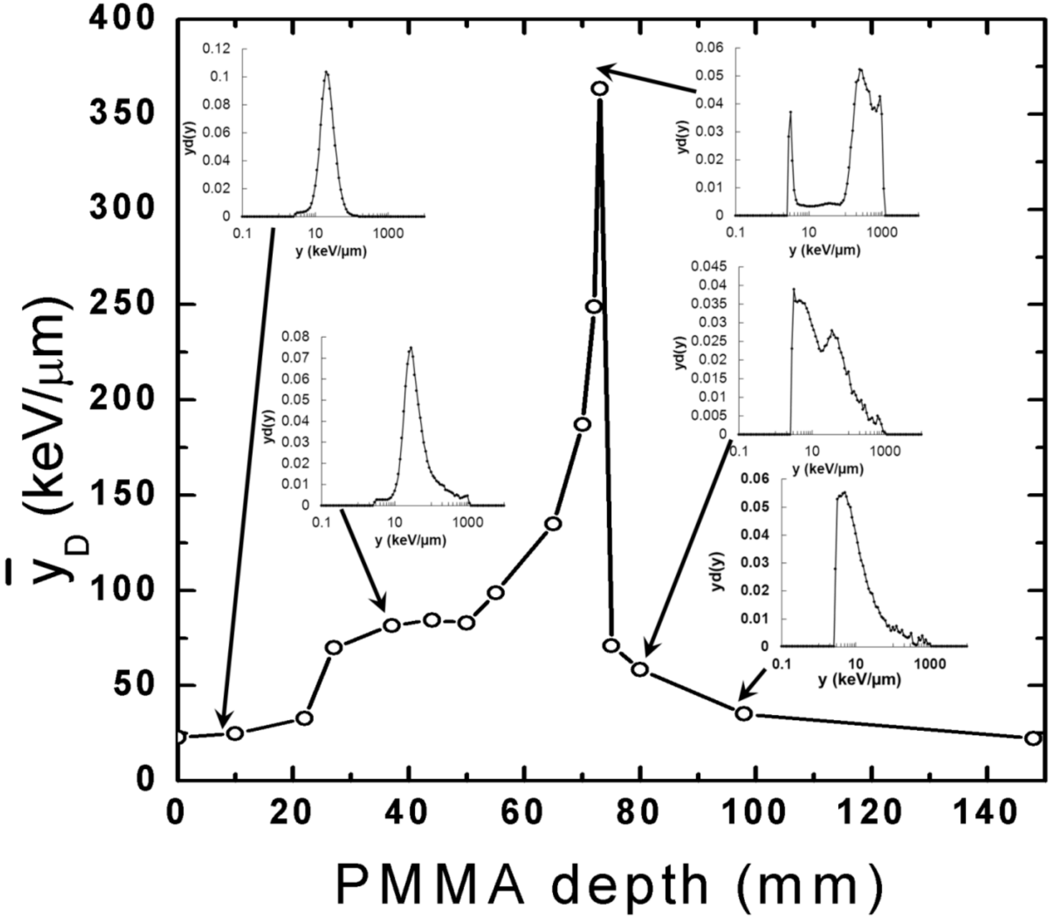

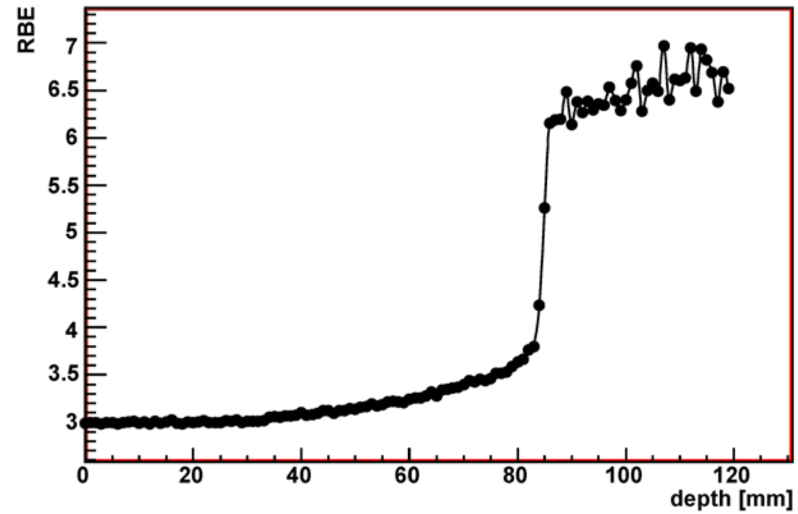

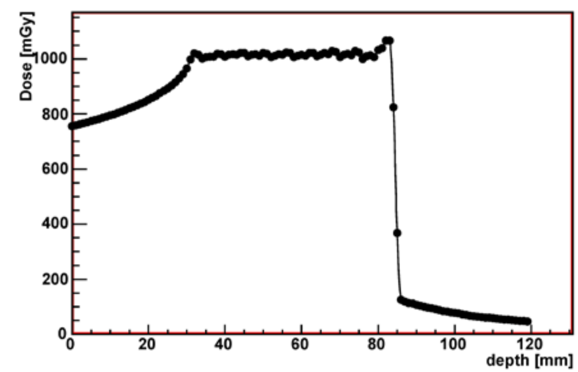

SOI microdosimetry spectra provides specific signatures of the field composition while LEM is integrated

Common features between LEM RBE and Yd

- SOI microdosimetry Yd: 3.5 increasing
- LEM RBE: 2.5 increasing
- Similar behavior downstream of SOBP
- Scaling in depth is required

Cubic SOBP: Lateral Measurements

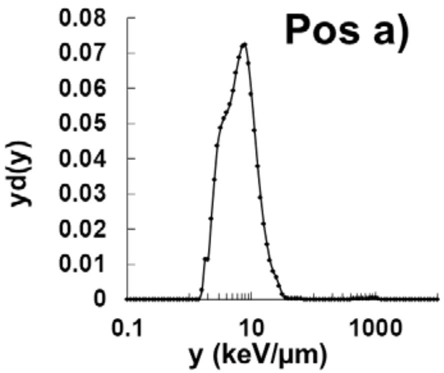

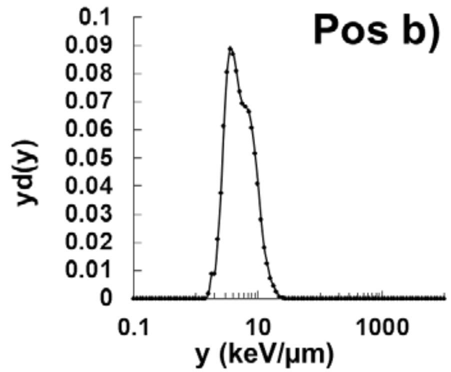

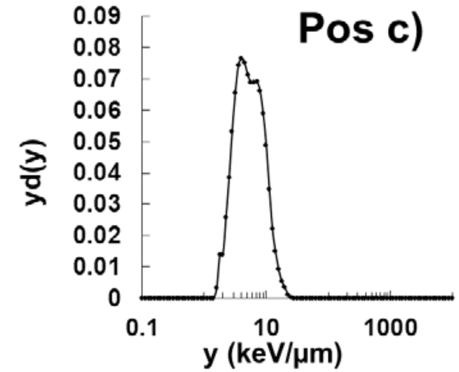

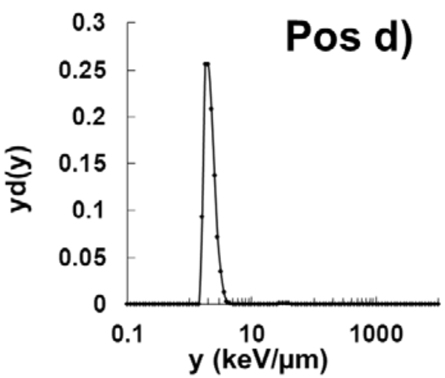

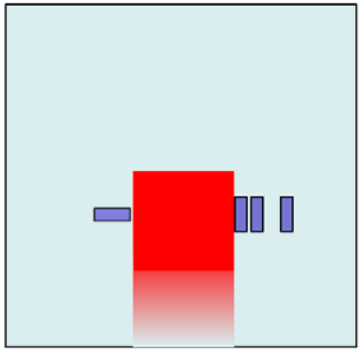

Pos a) 25 mm from beam isocentre
Pos b) 28 mm from beam isocentre
Pos c) 48 mm from beam isocentre
Pos d) Same position as Pos a) but rotated 90° towards upstream direction. Shown on opposite side for figure clarity

HIMAC, July ,2013 Experimental Setup,

Joint CMRP -Polimi ARDENT experiments

2nd Generation SOI Microdosimeter

1st Generation SOI Microdosimeter

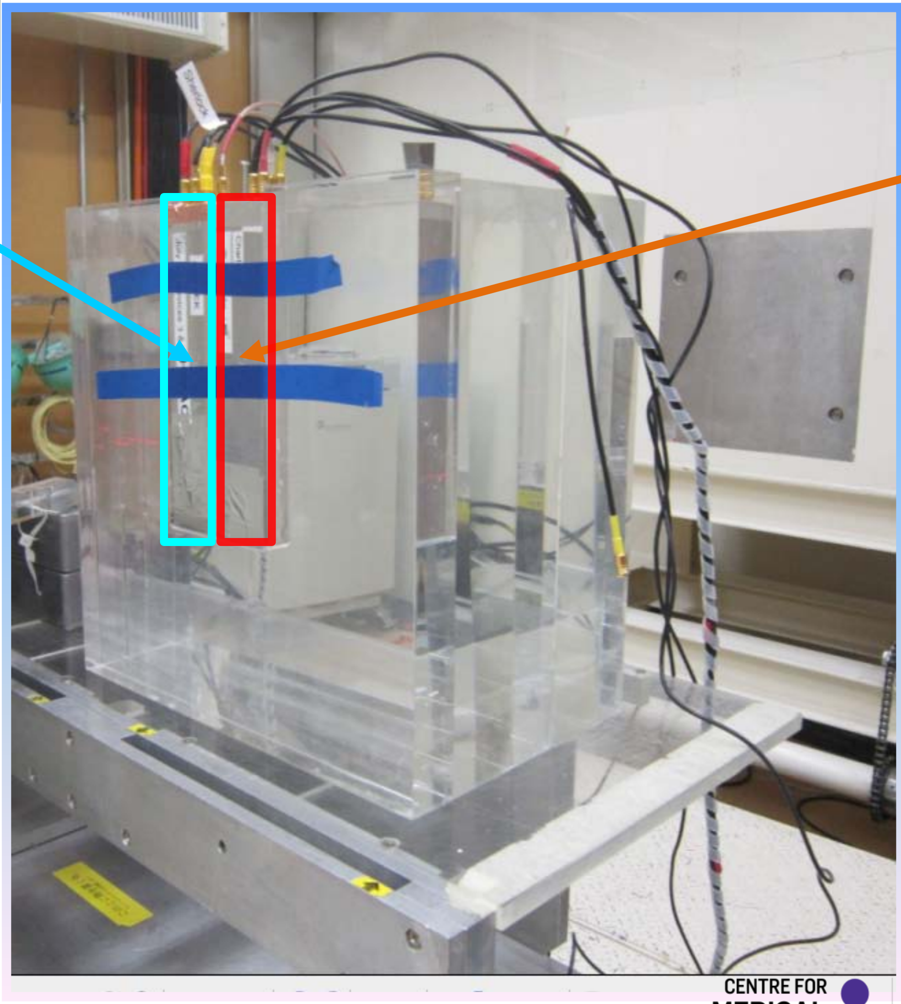

- Passive 290 MeV/u C-12 beam
- Pristine and SOBP delivery
- SOI and ΔE-E microdosimetry
- In field and out of field microdosimetry

C^{12} SOBP, 2nd generation SOI microdosimeter

High spatial resolution of SOI microdosimetry can't be bitten by TEPC

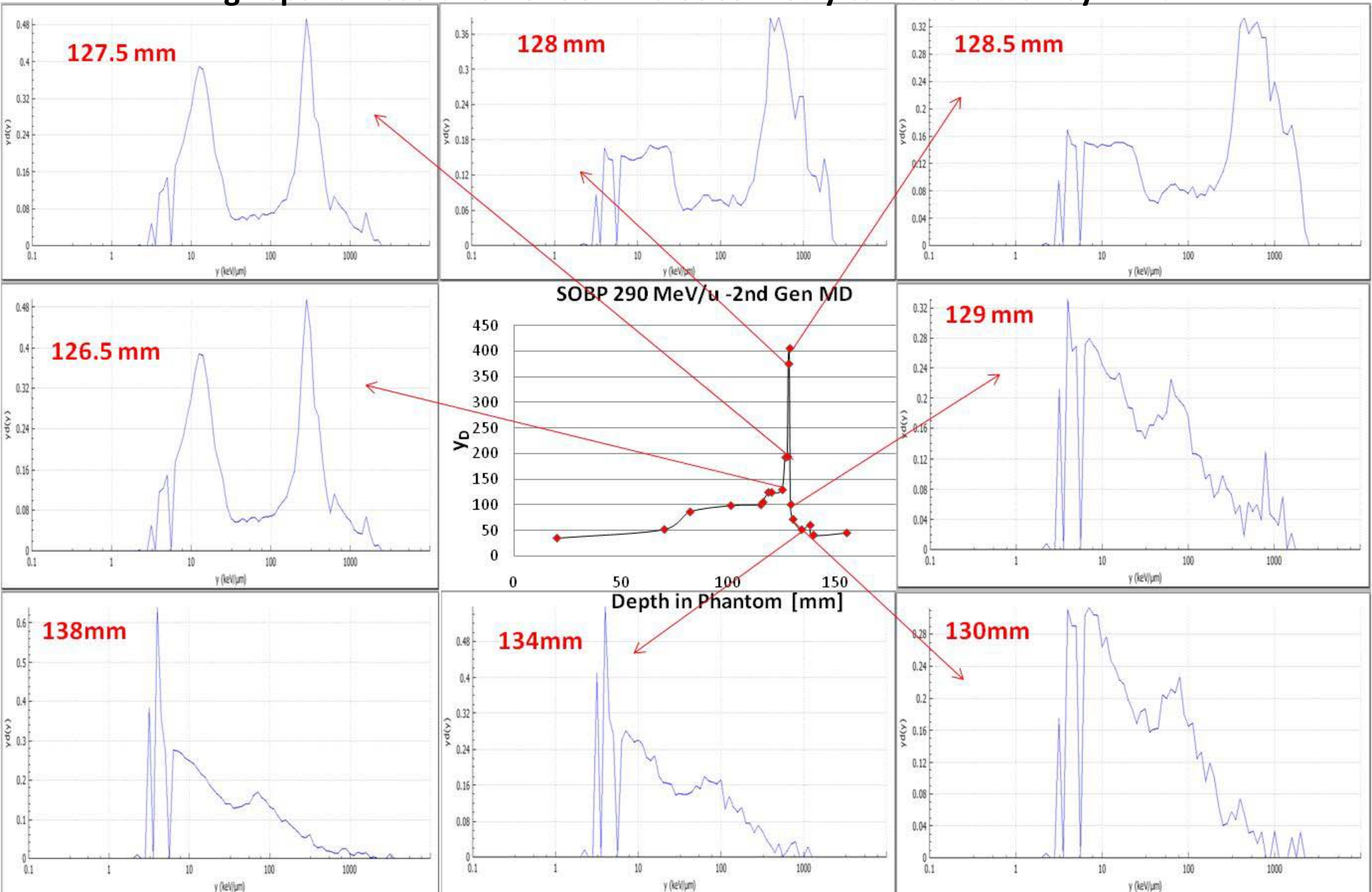

Experiment at HIMAC, Japan, July 2013

TEPC and MKM model calculation

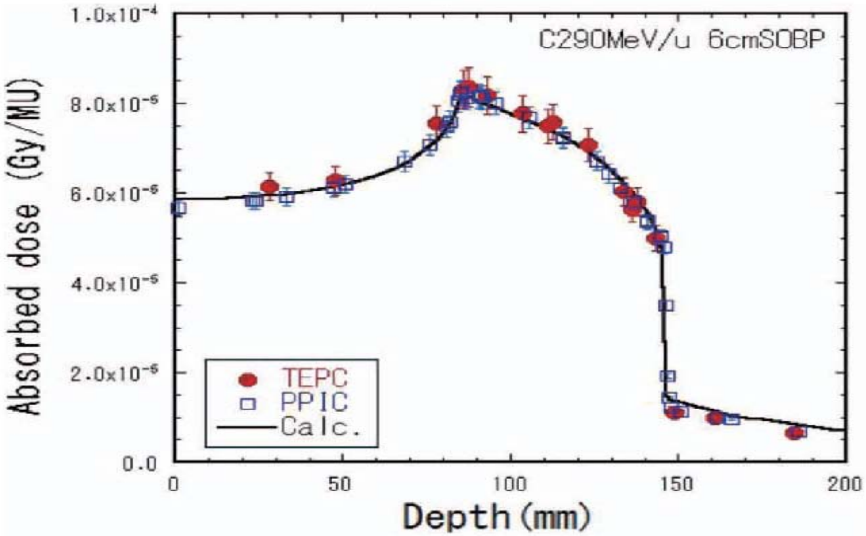

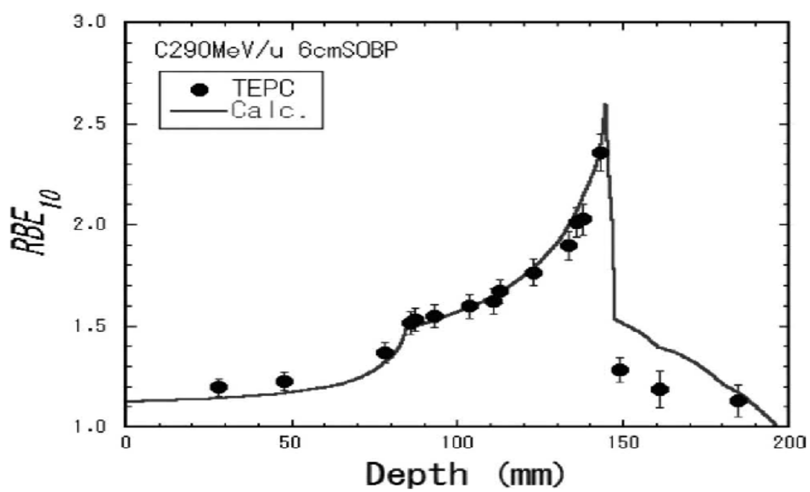

NIRS, N.Matsufuji et al.

Measured by CMRP microdosimeters

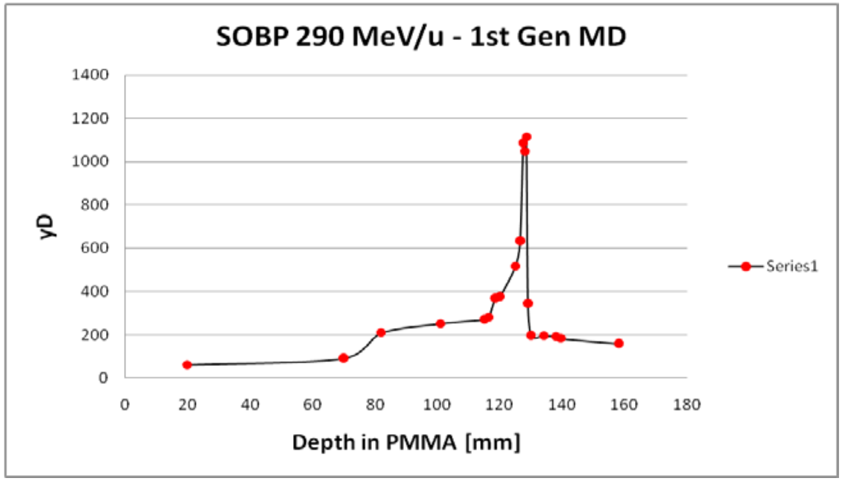

correction:

$$\bar{y}_F = \int_0^\infty y f(y)\,dy$$

$$\bar{y}_D = \int_0^\infty y d(y)\,dy = \frac{1}{\bar{y}_F}\int_0^\infty y^2 f(y)\,dy$$

Saturation

$$y^* = \frac{\int_0^\infty y_{sat}\, y f(y)\,dy}{\int_0^\infty y\, f(y)\,dy}$$

where the saturation co

is:

$$y_{sat} = \frac{y_0^2}{y}\left(1 - e^{-(y/y_0)^2}\right)$$

NEW PROPOSED DESIGN 3D MICRODOSIMETERS DEVELOPED BY CMRP

[S. Parker et al, 1995
C. Kenney et al, 1997]

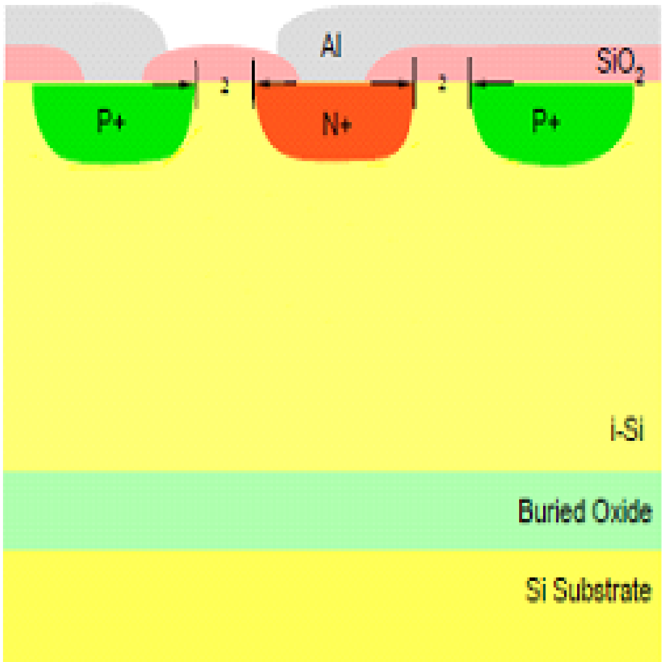

A. Cross Sectional Schematic of the Microdosimeter
(a)

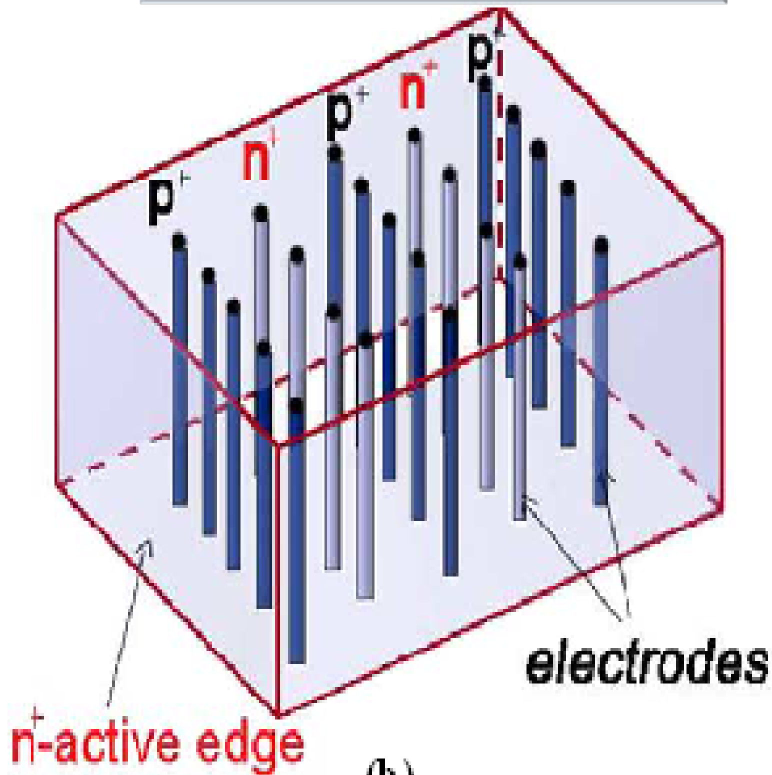

(b)

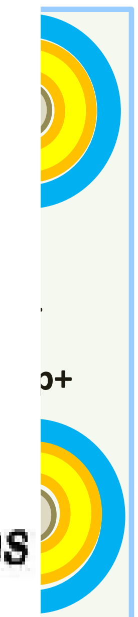

[S. Parker et al, 1995
C. Kenney et al, 1997]

- PMMA medium is filled around the sensitive volumes to produce tissue equivalent medium in order to avoid generation of secondary particles from Si lateral to SV.

3D "Mushrooms" microdosimeter design: 3D MiMiC collaboration CMRP-SINTEF-ESRF

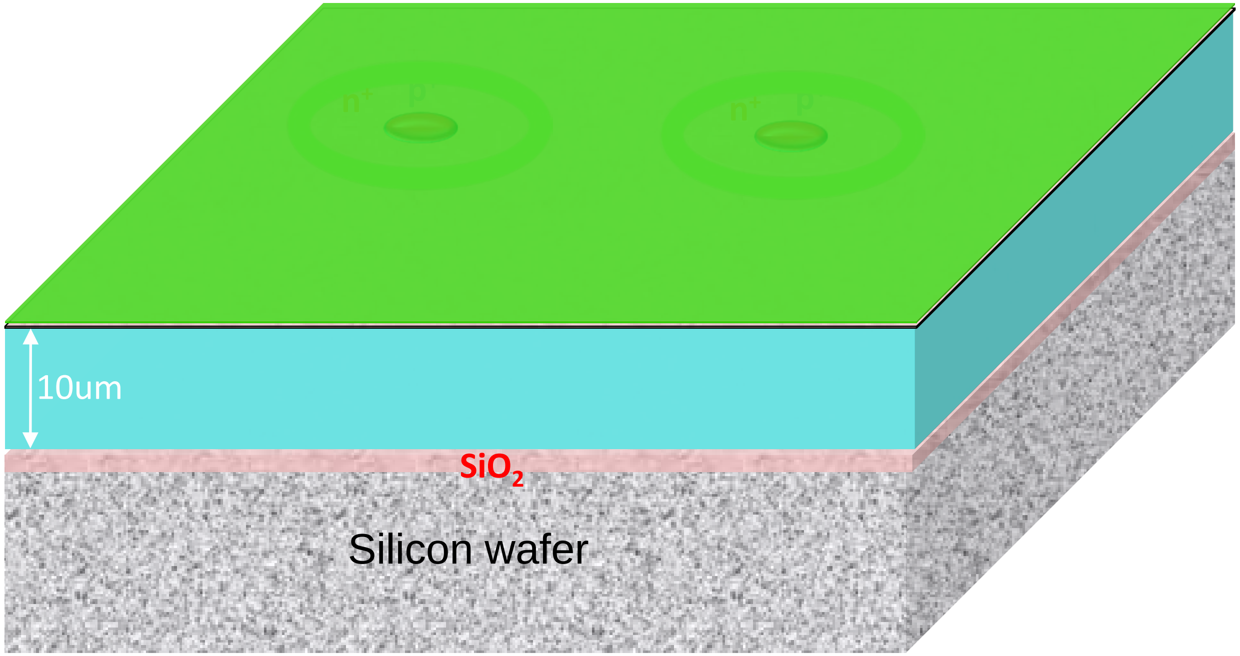

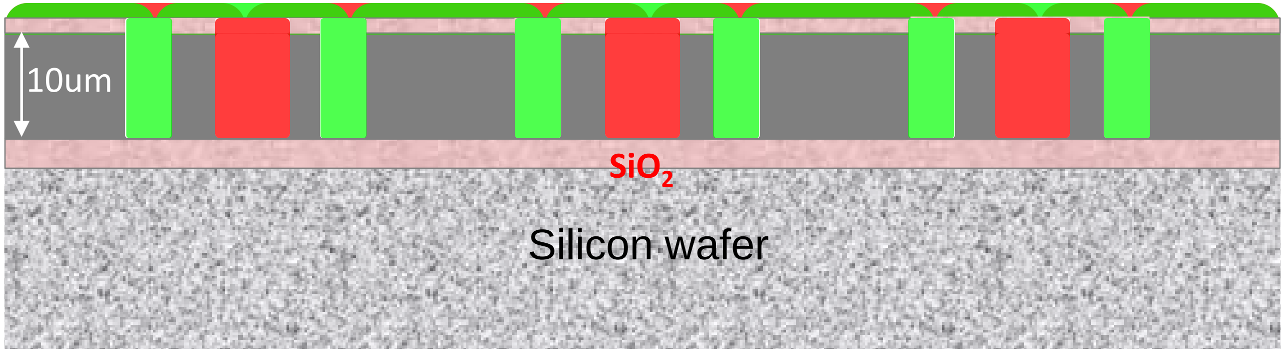

- **Drilling hole in Si wafer using DRIE**
- **The holes are filled with polysilicon**
- **The trench is etched and then doped using gas doping and filled with polysilicon**
- **Finally the silicon surrounding the SVs is etched away**
- **Deposition of PMMA**

Substrate thinning

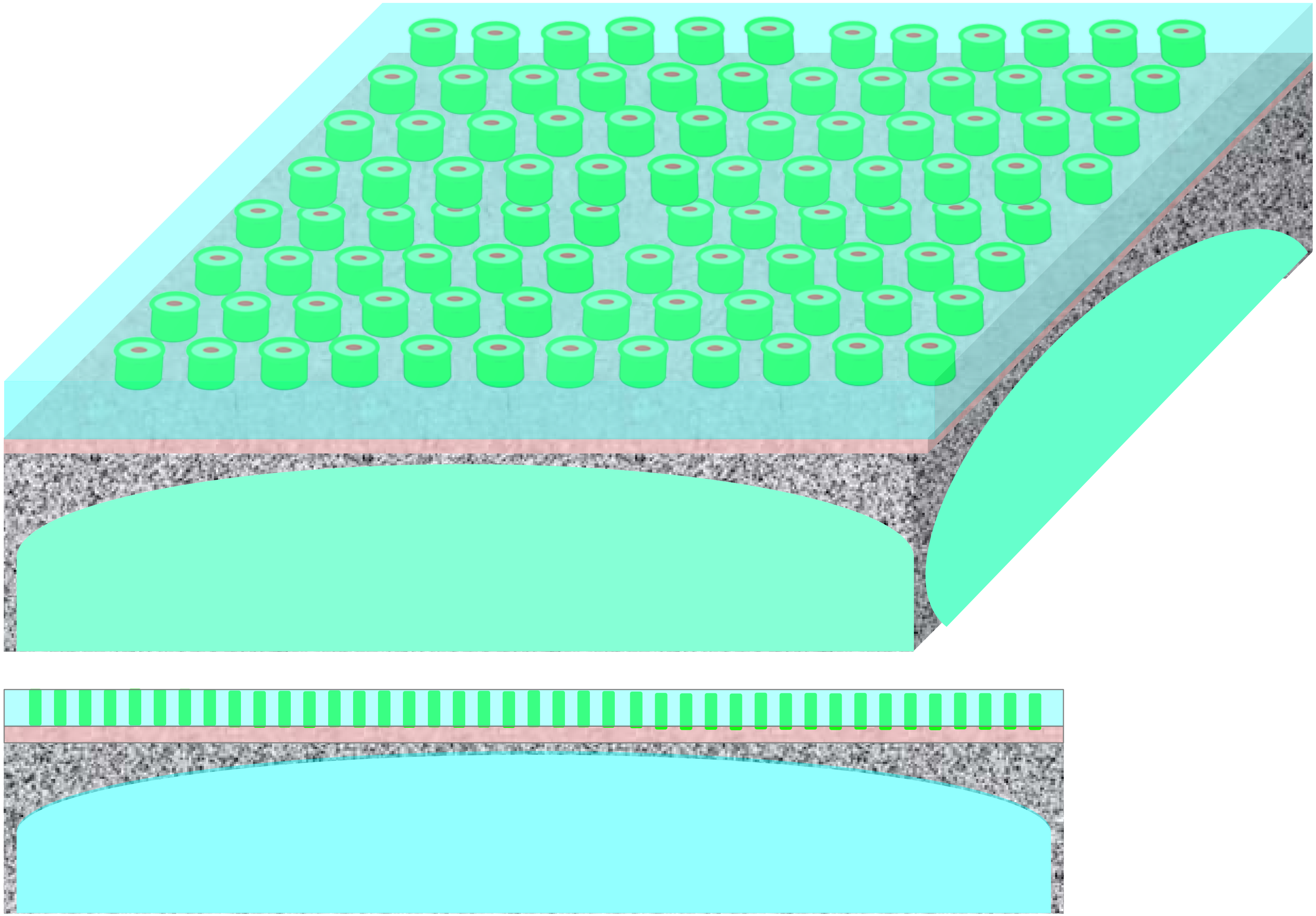

GEANT4 SIMULATION FOR 3D MICRODOSIMETER EMBEDDED IN PMMA

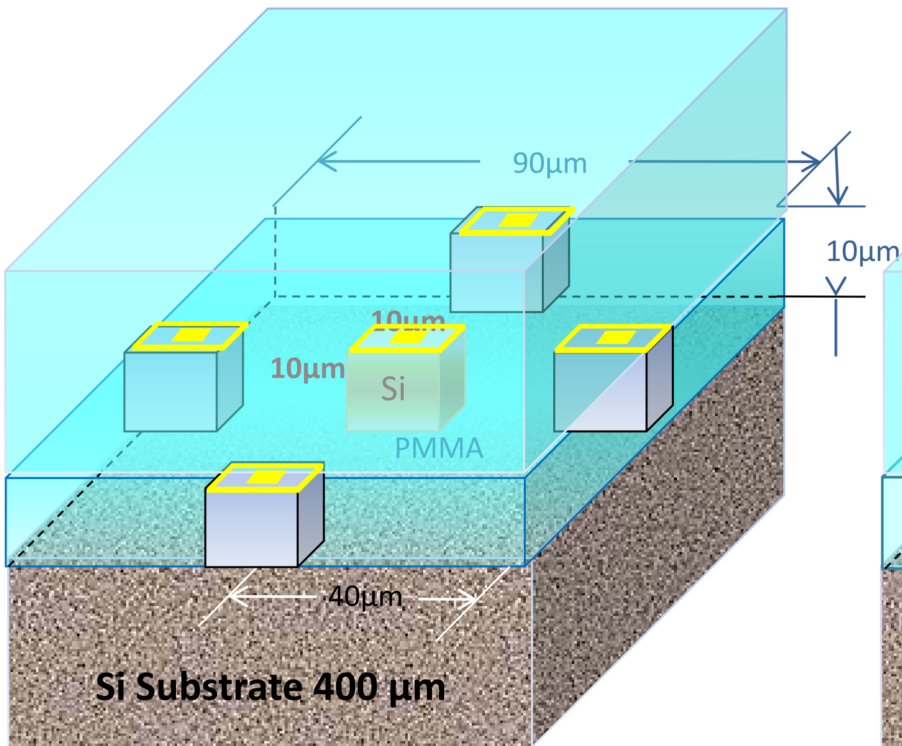

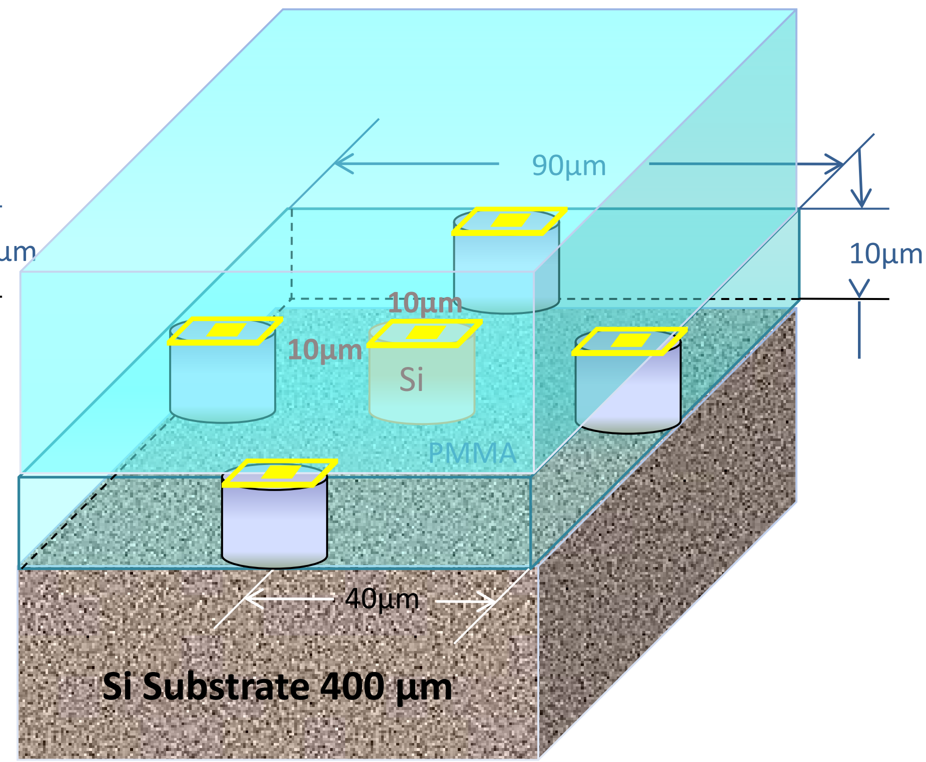

- Silicon Wafer: 90 x 90 x 400 µm^3
- PMMA Slab: 90 x 90 x 10 µm^3
- SiO_2 RPP: 0.145 µm thick
- Al contacts: 2 x 2 x 1 µm^3 *(central region)* and 10 x 1 x 1 µm^3 strip *(edge regions)*

- Cubic SV: 10x10x10 µm^3
- Cylindrical: SV 10 µm diameter and 10µm height.

Tissue equivalent conversion for silicon mushroom microdosimeter in response to avionic isotropic neutron field.

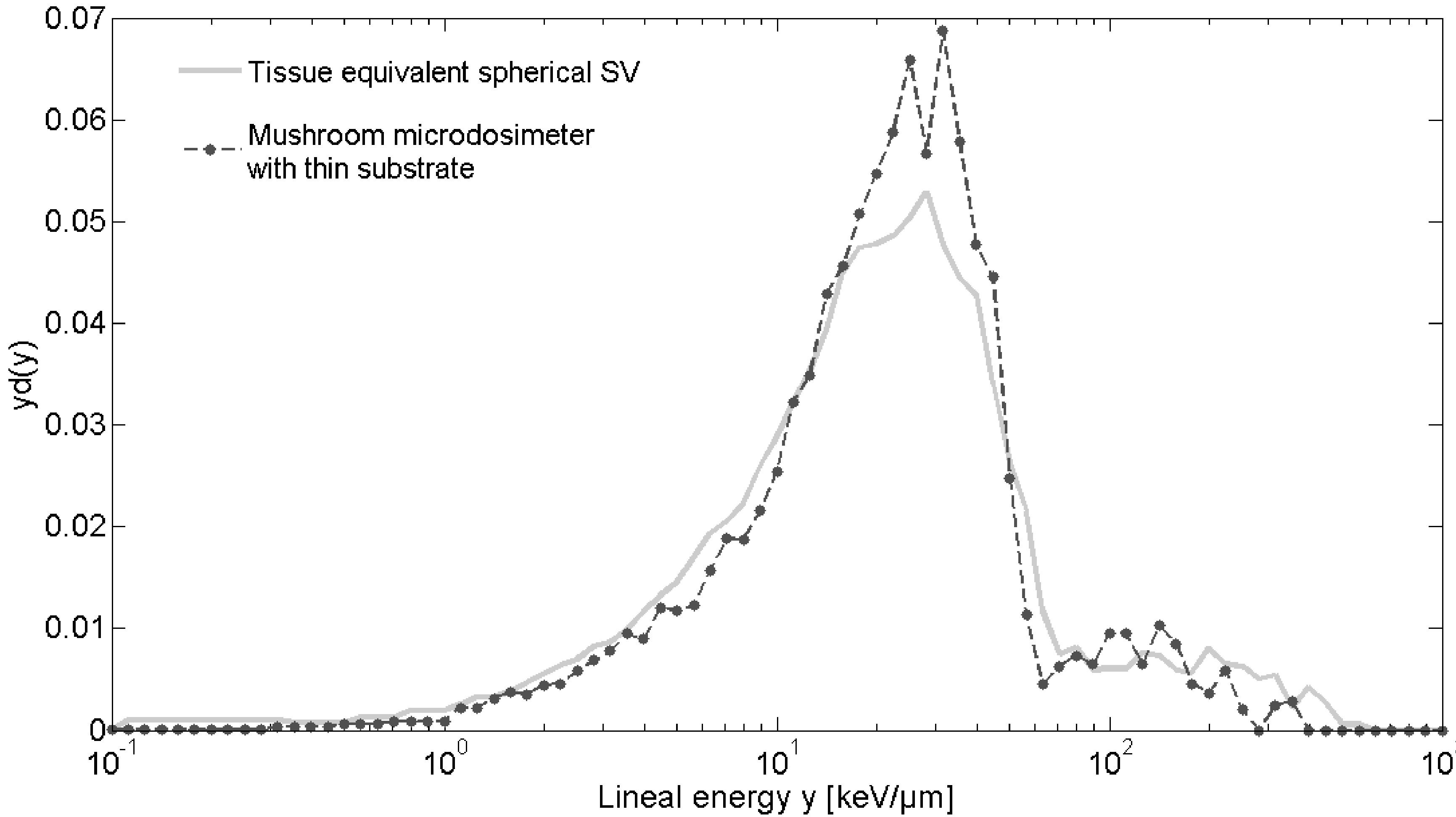

Summary of SOI microdosimetry systems

For more information on Silicon Microdosimetry look at :

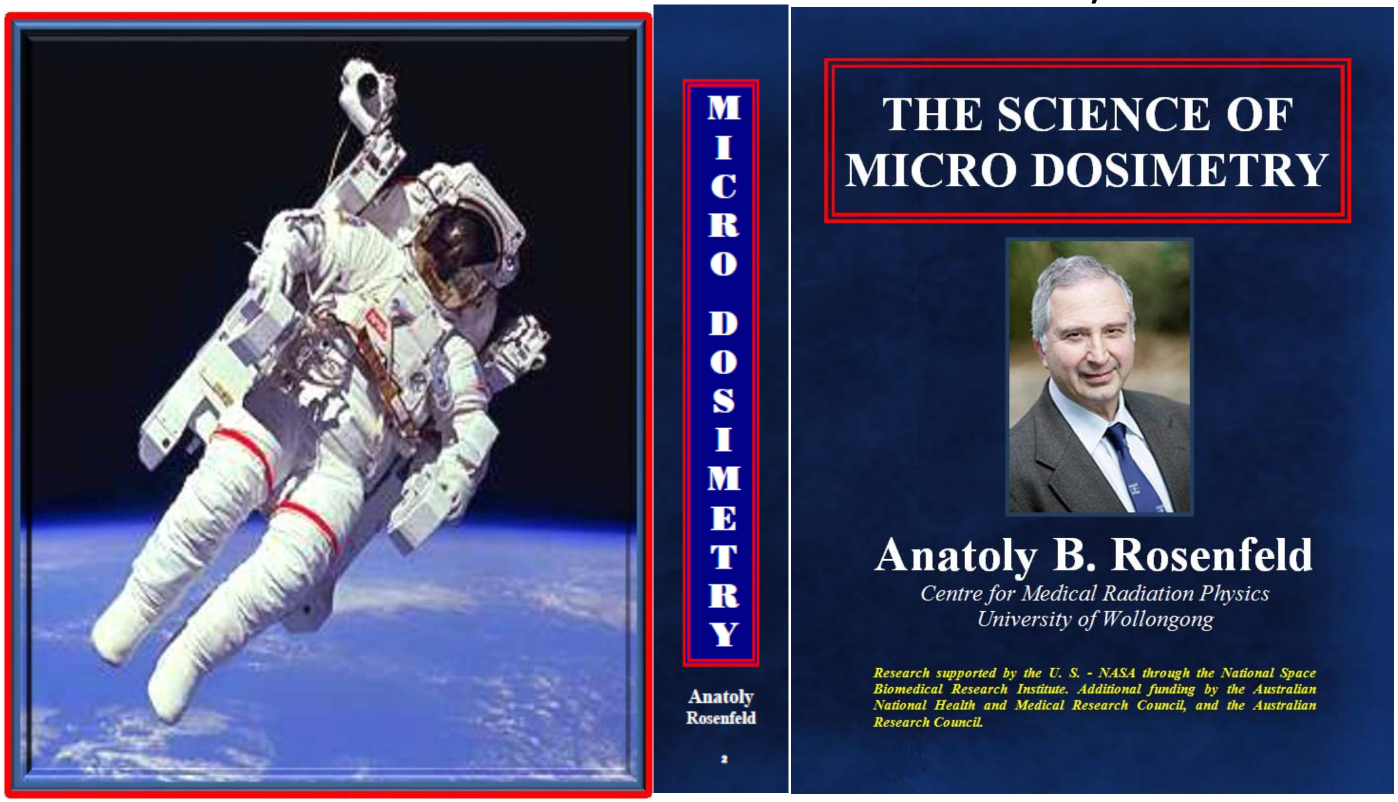

New book has been published recently by USNA/NSBRI- summarizing our findings during the projects supported by NSBRI, ARC and NHMRC grants. Collection of more than 40 papers and reports on silicon microdosimetry and its applications. Can be useful for ARDENT students.

Thanks to Prof Jim Ziegler, USNA

Entrepreneurial Physics Students is reality of CMRP and future of Australia and ARDENT is a step to the FUTURE of Radiation Detection Science

- Students given opportunities to undertake training in research commercialisation training schemes
  - Ash Cullen
  - Michael Weaver
  - Jeremy Davis
  - Kevin Loo

Conclusion

- Silicon SOI microdosimetry has been proven as useful
- Option for characterization of mixed radiation fields
- High spatial resolution (better then 0.5mm) SOI microdosimeters is useful in RBE studies of distal part of SOBP in proton and HI therapies that impossible with TEPC
- Important design issue is a high definition of SV and isolation of them from Si matrix to reduce contribution of inelastic reactions in Si
- 3D detector technology is a step forward to advanced SOI microdosimeter.
- Next step is integration of 3D SOI microdosimeter sensor with readout electronics on the same chip.

Acknowledgement

- CMRP current and former PhD students and wide national and international microdosimetry collaboration.
- Australian collaborators: ANSTO, UNSW
- International collaborators: LLUMC, MGH , Gershenson Cancer Centre, MSKCC, USNA, NSBRI-USA, Politechnic Milano-Italy, SINTEF –Norway, Heidelberg HIT, PTB –Germany, NIRS-Japan

PARTNERSHIPS with Industry

ansto

SPA-BIT

Semiconductors

AMCRYS-H

Scintillators

AMCRYS-H

PARTNERSHIPS Proton Therapy / μ-dosimetry

MSKCC - Memorial Sloan-Kettering Cancer Center

Memorial Sloan-Kettering Cancer Center

LOMA LINDA UNIVERSITY MEDICAL CENTER

LLUMC – Loma Linda University Medical Center

F.H. Burr Proton Therapy Center – MGH

MGH 1811 MASSACHUSETTS GENERAL HOSPITAL

UNITED STATES NAVAL ACADEMY HONOR... COURAGE... COMMITMENT

United States Naval Academy

CERN

NATIONAL SPACE BIOMEDICAL RESEARCH INSTITUTE

NSBRI

PARTNERSHIPS in Research

Wisconsin Institutes for Medical Research - University of Wisconsin

University of Wisconsin SCHOOL OF MEDICINE AND PUBLIC HEALTH

NSW HEALTH

Illawarra Cancer Care Centre, Wollongong Hospital

ESRF

The Prince of Wales Hospital, Sydney

New South Wales Government

NSW Health Department

South Eastern Sydney & Illawarra Area Health Service

European Synchrotron Radiation Facility, Grenoble

Liverpool Hospital

St George Hospital and Community Health Services

SINTEF

PTB

Physikalisch-Technishce Bundesanstalt

POLITECNICO DI MILANO

VTT

Technical Research Centre of Finland

ARDENT
Advanced Radiation Dosimetry European Network Training